



UNIVERSITÀ DEGLI STUDI DI SALERNO
Via Giovanni Paolo II, 132
84084 Fisciano (SA)
Tel. 089 96 4029 Fax 96 4343
www.unisa.it



UNIVERSITÀ DEGLI STUDI
DI SALERNO
Dipartimento di
Ingegneria Civile

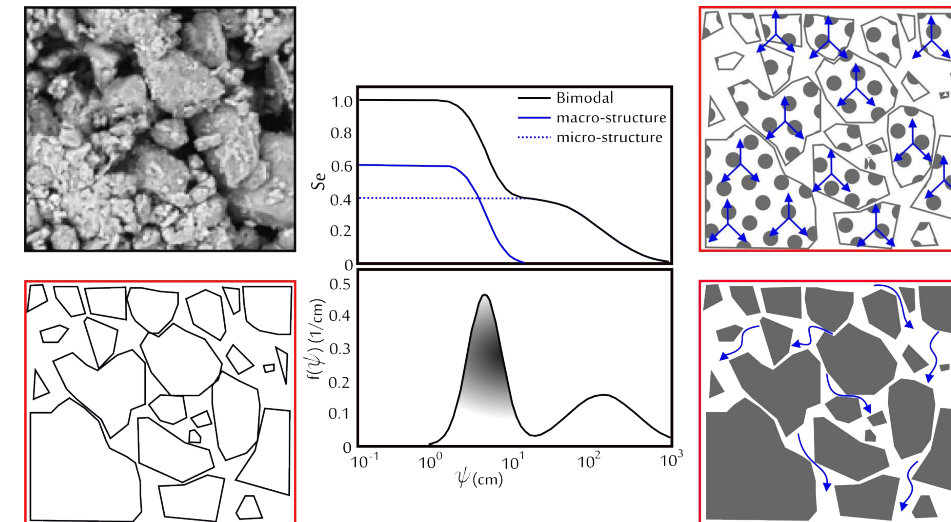


CORSO DI
DOTTORATO DI RICERCA IN
Ingegneria Civile per
l'Ambiente ed il Territorio

Tesi di Dottorato

MODELING HYDROLOGICAL RESPONSE OF STRUCTURED SOILS

ing. Fabio Ciervo



Correlatori
prof. Riccardo RIGON
prof. ing. Vicente MEDINA

Relatore
prof. ing. Maria Nicolina PAPA



**DOTTORATO DI RICERCA IN INGEGNERIA CIVILE PER
L'AMBIENTE ED IL TERRITORIO**
XIII Ciclo - Nuova Serie (2012-2014)
DIPARTIMENTO DI INGEGNERIA CIVILE, UNIVERSITÀ DEGLI STUDI DI SALERNO

MODELING HYDROLOGICAL RESPONSE OF STRUCTURED SOILS

**MODELLAZIONE DELLA RISPOSTA IDROLOGICA DI
TERRENI STRUTTURATI**

ING. FABIO CIERVO

Relatore:

PROF. ING. MARIA NICOLINA PAPA

Coordinatore

PROF. ING. VINCENZO BELGIORNO

Correlatori:

PROF. ING. RICCARDO RIGON

PROF. ING. VICENTE MEDINA

In copertina: Immagini parzialmente originali. I grafici si rifanno alle figure 1a e 1b di Romano et al., 2011. La fotografia è stata estratta dalla figura 11 di Casini et al., 2012.

TITOLO DELLA TESI DI DOTTORATO

Copyright © 2005 Università degli Studi di Salerno – via Ponte don Melillo, 1 – 84084 Fisciano (SA), Italy – web: www.unisa.it

Proprietà letteraria, tutti i diritti riservati. La struttura ed il contenuto del presente volume non possono essere riprodotti, neppure parzialmente, salvo espressa autorizzazione. Non ne è altresì consentita la memorizzazione su qualsiasi supporto (magnetico, magnetico-ottico, ottico, cartaceo, etc.).

Benché l'autore abbia curato con la massima attenzione la preparazione del presente volume, Egli declina ogni responsabilità per possibili errori ed omissioni, nonché per eventuali danni dall'uso delle informazioni ivi contenute.

Finito di stampare il 30/12/2014.

TABLE OF CONTENTS

TABLE OF CONTENTS	i
List of Figures	iii
List of Tables	vi
SOMMARIO	vii
ABSTRACT	ix
RINGRAZIAMENTI	xi
About the author	xii
1 Introduction	15
1.1 About the problem	15
1.2 Research line and objectives	17
1.3 Thesis layout	19
2 Literature review	21
2.1 Soil properties	21
2.1.1 Soil texture and structure	21
2.1.2 Pore size distribution and significance to soil hydraulic behavior	25
2.2 Soil water flow	29
2.2.1 Darcy's law	31
2.2.2 The Richards' model	32
2.2.3 Constitutive hydraulic functions	34
2.3 Shear strength behavior	39
2.3.1 Stress state variables	39
2.3.1 Soil shear strength	42
2.4 Infinite slope stability analysis	47
3 Bimodality effects of the hydraulic properties on shear strength of unsaturated soils	51
3.1 Extending the suction stress theory	54
3.2 Bimodal unsaturated suction stress equation	55
3.3 Validation	56
3.4 Numerical maxima exploration and sensitivity analysis	66
3.5 Final remarks	71
4 Modeling transient water and slope stability in dual-structure soils	73
4.1 Infiltration model	74

4.1.1	Unimodal and bimodal hydraulic functions	75
4.2	Infinite slope stability model.....	77
4.2.1	“Saturated” and “unsaturated” approaches to assess FoS.....	77
4.3	Numerical implementation.....	79
4.4	Validation.....	83
5	Comparing uni- and bimodal water infiltration and slope stability modeling results.....	85
5.1	Simulation scenarios.....	86
5.1.1	Soil properties	86
5.1.2	Rainfall scenarios.....	90
5.2	Results and discussions.....	91
5.2.1	Transient ψ and S_e profiles (Soil 1).....	92
5.2.2	Transient σ^s and FoS profiles (Soil 1).....	98
5.2.3	Transient ψ and S_e profiles (Soil 2).....	103
5.2.4	Transient σ^s and FoS profiles (Soil 2).....	111
5.3	Final remarks.....	122
	CONCLUSIONS.....	125
	REFERENCES.....	129

LIST OF FIGURES

Figure 2.1 Three representative granular-type structured soils with different grade of macrostructure (increasing from a to c) (Zhao et al., 2013).....	24
Figure 2.2 A typical soil water characteristic curve showing desaturation Stage (Kayadelen et al., 2007).....	36
Figure 2.3 Bimodal (a) effective saturation and (b) PSD $f(h)$ for an hypothetical soil. (Romano et al., 2011).....	37
Figure 2.4 A typical bimodal soil water characteristic curve showing desaturation Stage (Zhao et al., 2013).....	38
Figure 3.1 BWRC - soils A and B.....	60
Figure 3.2 Comparison σ_H^s/ψ with σ_M^s - soils A and B.....	60
Figure 3.3 Comparison σ_H^s/Se with σ_M^s - soils A and B.....	61
Figure 3.4 σ^s versus σ_M^s - soils A and B.....	61
Figure 3.5 BWRC - soils C and D.....	63
Figure 3.6 Comparison σ_H^s/ψ with σ_M^s - soils C and D.....	63
Figure 3.7 Comparison σ_H^s/Se with σ_M^s - soils C and D.....	64
Figure 3.8 σ^s versus σ_M^s - soils C and D.....	64
Figure 3.9 BWRC - soils E and F.....	65
Figure 3.10 Comparison σ_H^s/ψ with σ_M^s - soils E and F.....	65
Figure 3.11 Comparison σ_H^s/Se with σ_M^s - soils E and F.....	66
Figure 3.12 σ^s versus σ_M^s - soils E and F.....	66
Figure 3.13 . Numerical exploration of maximum suction stress.....	67
Figure 3.14 RCS versus suction head respect to ψ_{macro}	70
Figure 3.15 RCS versus suction head respect to σ_{macro}	70
Figure 4.1 Comparisons in terms of suction (a) and volumetric water content (b).....	84
Figure 5.1 Unimodal and bimodal hydraulic functions of soil 1: a) water retention curve; b) relative hydraulic conductivity curves.....	87
Figure 5.2 Unimodal and bimodal hydraulic functions of soil 2: a) water retention curve; b) relative hydraulic conductivity curves.....	88
Figure 5.3 Suction stress characteristic curves $\sigma^s-\psi$	89
Figure 5.4 Suction stress characteristic curves σ^s-S_e	90
Figure 5.5 Simulated suction profiles for soil 1, Simulation Id1.....	94

Figure 5.6 Simulated water content profiles for soil 1, Simulation Id1 ...	95
Figure 5.7 Simulated suction profiles for soil 1, Simulation Id2	96
Figure 5.8 Simulated water content profiles for soil 1, Simulation Id2...	97
Figure 5.9 Simulated suction and suction stress at two different depths for soil 1, Simulation Id1	100
Figure 5.10 Simulated FoS at two different depths for soil 1, Simulation Id1.....	100
Figure 5.11 Simulated FoS profiles for soil 1, Simulation Id1.....	101
Figure 5.12 Simulated suction and suction stress at two different depth for soil 1, Simulation Id2.....	102
Figure 5.13 Simulated FoS at two different depths for soil 1, Simulation Id2.....	102
Figure 5.14 Simulated FoS profiles for soil 1, Simulation Id2.....	103
Figure 5.15 Simulated suction profiles for soil 2, Simulation Id3	106
Figure 5.16 Simulated water content profiles for soil 2, Simulation Id3	107
Figure 5.17 Simulated suction profiles for soil 2 – Simulation Id4.....	108
Figure 5.18 Simulated water content profiles for soil 2, Simulation Id4	108
Figure 5.19 Simulated suction profiles for soil 2, Simulation Id5	109
Figure 5.20 Simulated water content profiles for soil 2, Simulation Id5	110
Figure 5.21 Simulated suction and suction stress at two different depths for soil 2, Simulation Id3.....	114
Figure 5.22 Simulated FoS at two different depths for soil 2, Simulation Id3.....	114
Figure 5.23 Simulated FoS profiles for soil 2, Simulation Id3.....	115
Figure 5.24 Simulated suction and suction stress at two different depths for soil 2, Simulation Id4.....	116
Figure 5.25 Simulated FoS at two different depths for soil 2, Simulation Id4.....	116
Figure 5.26 Simulated FoS profiles for soil 2, Simulation Id4.....	117
Figure 5.27 Simulated suction and suction stress at two different depths for soil 2, Simulation Id5.....	118
Figure 5.28 Simulated FoS at two different depths for soil 2, Simulation Id5.....	118
Figure 5.29 Simulated FoS profiles for soil 2, Simulation Id5.....	119
Figure 5.30 Simulated suction and suction stress at two different depths for soil 2, Simulation Id5bis.....	120

Figure 5.31 Simulated FoS at two different depths for soil 2, Simulation Id5bis.....	120
Figure 5.32 Simulated FoS profiles for soil 2, Simulation Id5bis.....	121

LIST OF TABLES

Table 2.1 Summary of some unimodal water retention functions.....	35
Table 3.1 Data used.....	57
Table 3.2 Optimal bWRC-fitting parameters.....	58
Table 3.3 Idealized bWRC parameters.....	70
Table 5.1 Optimal fitting parameters for soil 1 (Durner, 1994)	86
Table 5.2 Optimal fitting parameters for soil 2	86
Table 5.3 Configuration performed simulations.....	90
Table 5.4 Unsteady rainfall.....	91

SOMMARIO

L'intento della ricerca contenuta in questo lavoro è di esplorare gli effetti indotti dall'utilizzo di modelli di ritenzione idraulica bimodale sulla rappresentazione modellistica dei fenomeni idraulici in terreni strutturati e contestualmente della stabilità degli stessi. I processi che caratterizzano il movimento dell'acqua nel suolo variano in dipendenza della configurazione e della distribuzione dei vuoti nel sistema poroso. I suoli naturali sono sovente caratterizzati dalla presenza di eterogeneità di varia natura e tipologia le quali incidendo direttamente sulla distribuzione e l'assetto del sistema dei vuoti possono comportare effetti anche significativi sulla risposta idraulica del suolo e a cascata su quella meccanica che da essa ne deriva. In letteratura è stato ampiamente dimostrato che un'ampia classe di suoli naturali "eterogenei" può essere adeguatamente rappresentata da modelli definiti a doppia-struttura (o doppia porosità, o ancora doppia permeabilità). I suddetti modelli si basano sul concetto secondo il quale il sistema poroso caratteristico del suolo è costituito da due distinti ma interagenti domini porosi ai quali è possibile attribuire due diversi comportamenti idraulici. Nei mezzi porosi strutturati, il moto viene frequentemente descritto come combinazione del flusso matriciale, o di microstruttura, che ha luogo nei micropori interposti tra le particelle primarie del suolo, e del flusso nei macropori, detto di macrostruttura, generalmente più rapido rispetto al primo. Assunto che la scala di dimensione dei macropori sia comparabile con quella di Darcy, e che pertanto i processi idraulici possano adeguatamente essere descritti dall'equazione di Richards, un approccio di analisi è quello di considerare il suolo strutturato come un mezzo continuo in cui la complessa eterogeneità del sistema poroso e della relativa risposta idraulica possano essere descritti da modelli di distribuzione dei pori (e di ritenzione) bimodali.

Una prima parte del lavoro è focalizzata sulla descrizione di una nuova metodologia analitica sviluppata per l'analisi degli effetti indotti dalla bimodalità idraulica sulla resistenza meccanica di suoli strutturati parzialmente saturi. Il modello proposto consiste in una ricontestualizzazione del principio degli sforzi efficaci basato sulla teoria

delle suction stress in un contesto di risposta idraulica bimodale del suolo. Per la rappresentazione matematica di quest'ultima ci si è avvalsi di un modello di ritenzione idraulica bimodale di tipo lognormale. I risultati del modello proposto risultano in buon accordo con i dati sperimentali di letteratura. In funzione del tipo di suolo e del range di suzioni in cui i processi sono indagati, la micro o la macrostruttura prevarrebbe incidendo sul comportamento meccanico del suolo.

La seconda parte del lavoro è dedicata ad un'indagine dinamica dei processi idraulici e di stabilità che interessano i suoli strutturati. A tal fine un codice di calcolo originale (Ri.D1) per la risoluzione numerica di un modello monodimensionale di infiltrazione verticale alla Richards è stato sviluppato in linguaggio JAVA. Ri.D1 implementa funzioni idrauliche bimodali di tipo lognormale. Per l'analisi dinamica transitoria di stabilità il codice implementa un modello di resistenza esteso al parzialmente saturo basato sulla teoria delle suction stress. Dal confronto dei risultati di infiltrazione (suzione e contenuto) ottenuti dall'utilizzo di un modello unimodale (van Genuchten) e bimodale su due diversi suoli strutturati, sono state analizzate le differenze emerse. Analogamente si è proceduto per l'analisi di stabilità (fattore di sicurezza), confrontando i risultati di un modello di pendio indefinito saturo unimodale (convenzionale) con uno parzialmente-saturo basato sulla teoria delle suction stress estesa al contesto bimodale della risposta idraulica. L'intento della ricerca è stato di valutare, previa scelta di un predefinito modello idraulico e di stabilità, le differenze ottenute dai due modelli nella riproduzione del transitorio.

ABSTRACT

The hydraulic processes that control the water movements through the soil strictly depend on the configuration and distribution of the soil pores. Natural soils are often characterized by the presence of heterogeneities of various kinds which directly impacts on the distribution and structure of the pore network system; this may result in significant consequences on the hydraulic response of the soil and indirectly on the mechanical behavior. In literature it has been shown that a wide class of "heterogeneous" soils should be adequately represented by commonly defined "dual-porosity" models (or dual structure, dual permeability or still). These models conceptually consider the whole soil pore system as constituted by two distinct but interacting porous sub-domains to which it is possible to assign two different hydraulic behaviors.

In dual-structure soils the water movement is frequently described as a combination of the flow matrix (or microstructural flow), that affects the micropores between the primary particles of the soil, and the flow in macropores (or macrostructural flow) that is generally faster than the previous. Assuming that the size scale of heterogeneities is comparable with Darcy scale (therefore the hydraulic processes can be adequately described by the Richards' equation), an analysis approach is to consider dual-structure soil as a continuous medium in which the complex heterogeneity of the porous system and its related hydrological response can be described by bimodal models.

This work explores the influence of dual-structure on the stress-strain behavior of unsaturated terrain and proposes a new analytical method to assess the effects of the hydraulic properties on soil shear integrating a bimodal lognormal function to describe water retention behavior within the suction stress theory framework. Hydraulic properties affect the shear strength of unsaturated soils in terms of suction, predicted as a function of water volume in the pores. The proposed bimodal suction stress method originates from the double structure typically exhibited by widely-graded soils, which are characterized by a bimodal pore-size distribution that is conceptually divided into micro and macrostructures.

The model is validated against literature data from soils with aggregated macrostructure or with a prevailing coarse fraction. Depending on the soil type and the range of suction investigated, the micro and macrostructures should prevail affecting the mechanical soil response subject to environmental loading, such as rainfall events. In order to investigate the bimodality effects in timing analysis the processes are dynamically described by a numerical solution of Richards' equations. A novel one-dimensional column Richards-based code (Ri.D1) have been developed using lognormal bimodal functions to describe the hydraulic properties. The work attempts to focus on the possible differences (and its magnitude) that occur between using conventional unimodal and bimodal interpretative models. The observed differences were investigated by comparing predictions in term of water contents and suction head profiles. In order to evaluate the effects of the hydraulic bimodality on the shallow landslides triggering processes, Ri.D1 includes a dedicated-module for simulating slope stability analysis. Comparisons between the results obtained from a “fully-unsaturated and bimodal approach” and a conventional slope stability analysis has been performed. From a practical point of view, taking into account the dual-structure network should be fundamental in the set-up of proper prediction models for shallow landslides induced by rainfall.

RINGRAZIAMENTI

Sono profondamente grato per l'opportunità ricevuta dalla Scuola di Dottorato di Ricerca in Ingegneria Civile per l'Ambiente e il Territorio dell'Università degli Studi di Salerno e per essa ai Direttori Professori Vincenzo Belgiorno e Leonardo Cascini.

Voglio esprimere la mia gratitudine alla Professoressa Maria Nicolina Papa e ai correlatori Professori Riccardo Rigon e Vicente Medina, per la preziosa guida, per il loro incoraggiamento e per l'amicizia concessami. Un sincero grazie va all'Ing. Francesca Casini dell'Università di Roma Tor Vergata, per l'importante supporto in questi ultimi due anni di ricerca. I miei ringraziamenti vanno anche ai Professori, ai Colleghi e agli Amici del Laboratorio di Idraulica Ambientale e Marittima (LIDAM) del Dipartimento di Ingegneria Civile dell'Università degli Studi di Salerno, per il tempo trascorso insieme e i preziosi consigli ricevuti. Grazie al Professore Allen Bateman del Sediment Transport Research Group (GITS) della UPC-Barcelona Tech, per avermi consentito di far parte del suo speciale gruppo di ricerca. Un grazie speciale va all'amico Francesco Bregoli. Non potrei mai smettere di ringraziare la mia famiglia. Sarò sempre grato ai miei genitori e ai miei fratelli per la loro immancabile presenza. Un ringraziamento particolare va alla mia compagna Simona: sono profondamente in debito con lei per il suo costante supporto e incoraggiamento che ha segnato la differenza soprattutto nei momenti più difficili.

ABOUT THE AUTHOR

Fabio Ciervo si laurea nel 2008 presso l'Università degli Studi di Salerno in Ingegneria per l'Ambiente e il Territorio. Nel 2009 collabora con il Consorzio inter-Universitario per la previsione e la prevenzione dei Grandi Rischi (CUGRI) nell'ambito del progetto europeo fp7 IMPRINTS, sviluppando conoscenza ed esperienza nel settore della modellazione matematico-numerica di innesco e propagazione di debris flow. Nel 2010 vince una borsa di studio dell'Università di Salerno per un periodo di perfezionamento all'esterno poi svolto presso il Sediment Transport Research Group (GITS), Department of Hydraulic, Maritime and Environmental Engineering, UPC-Barcelona Tech, Spagna, dove ritorna come Visiting Scientist nel 2013 e 2014. Nel 2011 vince una borsa di studio del CUGRI per attività di ricerca applicata nell'ambito della mitigazione del rischio da fenomeni di flash flood. Nel 2013 svolge un periodo di Scientist Training presso il Centro Universitario per la Difesa Idrogeologica nell'Ambiente Montano (CUDAM), Università di Trento. I suoi interessi scientifici riguardano: modellazione idrologica e idraulica, analisi idrologica in bacini non strumentati, idrologia dei suoli, suoli parzialmente saturi, stabilità dei versanti, soglie di pioggia critiche di innesco, applicazioni SAR nell'ambito di analisi idrologiche in aree semiaride. E' autore/coautore di pubblicazioni scientifiche su rivista internazionale e atti di convegno.

Fabio Ciervo received the Laurea degree in Civil and Environmental Engineering in 2008, from the University of Salerno, Salerno, Italy. In 2009, he received a grant from the Research Centre on Major Hazards (CUGRI) of Salerno University for research in the fields of debris flow initiation and propagation modeling (IMPRINTS fp7-European Project). In 2010, he obtained a research fellowship from the University of Salerno to be spent at the Sediment Transport Research Group (GITS), Department of Hydraulic, Maritime and Environmental Engineering, UPC-Barcelona Tech, Spain, where he came back as a Visiting Scientist in 2013-2014. In 2011, he obtained research fellowship at the CUGRI

for research in analysis and development of measures aimed to reducing risk from flash flood hazard. In 2013 he was a Visiting Scientist at the University Centre for Advanced Studies on Hydrological Risk in Mountain Areas (CUDAM), University of Trento, Italy. His research interest include modeling, flood/flow propagation in urban environment, hydrological and hydraulic analysis in ungauged basins, critical rainfall thresholds and early warning systems, unsaturated soil, slope stability, and synthetic aperture radar (SAR)-based hydrological and hydraulic analysis for semiarid regions. He has published several papers on international journals and conferences.

1 INTRODUCTION

1.1 ABOUT THE PROBLEM

During the last two decades, an increasing attention of scientific community has been focused on approaches and methodologies for modeling infiltration mechanism in unsaturated terrains. The unsaturated zone, or vadose zone, is located between the terrain surface and the groundwater level; the understanding of the vadose zone processes constitutes the key element to predict the slope response under meteorological forcing. A more reliable modeling description of time and energy of infiltration mechanisms in unsaturated zone can be crucial for predicting slope stability and implementing appropriate early warning systems.

Simulation of water flow in unsaturated terrain is a complicated issue; the reasons are different. The extremely non-linearity of the governing equations certainly constitutes one of the most difficult problem to be solved. At least two fluid phases (i.e. water and air) are present in the vadose zone; although in this condition the infiltration processes can be sufficiently described by a simplified unsaturated flow equation (Richards, 1931), the constitutive relationships used to solve the mathematical system remain still strongly non-linear.

A challenging problem that has recently received much attention in soil sciences is the heterogeneity of soil systems; because of its implications in affecting time-dependent variables the variability of the flow mechanisms due to complexity of soil porous system has become a concern for hydrologists and geophysicists.

Natural terrains generally exhibit heterogeneities at various observation scales. The scale of local heterogeneities is generally much smaller than of the processes that the modeler needs to simulate. Because of the extreme difficulty to explicitly define the local heterogeneities that affect the system, a detailed representation of the physical processes seems unachievable. All this results in terms of hampering accurate predictions of hydro-mechanical behavior of slopes.

The presence of the heterogeneities in the structure and the composition of partially-saturated slopes results in irregular wetting of the soil profiles. In common practice the soil system is treated as homogeneous and the simulations of the processes are performed by using average hydraulic parameters for the entire soil profile.

The last two decades have seen the development of a relatively large number of models that try to capture the effects of the soil structure heterogeneities on the infiltration mechanisms. A large class of heterogeneous porous systems that characterize the natural slopes can be well-described by double-porous, dual-permeability, dual-structure models. In this study, the above mentioned systems are conventionally defined as double-structured, that is composed by two structural domains, a macro-structure (macropores) and a micro-structure (micropores). Typically double-structured porous systems are those of aggregated or widely graded soil profiles.

Water may move through the macrostructure much faster than would be predicted with the Richards equation using area averaged moisture contents and pressure heads. The highly conductive structures of terrains with large fissures or macropores have often over capillary size; thus, the Richards equation may be inadequate to describe water flow and other mathematical formulations are needed. In this study the local scale (i.e. mesoscopic or Darcy scale) corresponds to the characteristic dimension of heterogeneities (macropores diameter). In other words, both porous domains (the macro and microstructural subsystem) are characterized by capillary pore-space, thus the water flow in both domain can be sufficiently well-described by the Richards equation. To mathematically represent the dual (-structure) implications in describing the hydraulic soil behavior several bimodal hydraulic functions have been presented and replaced the traditional sigmoidal/unimodal functions (i.e. van Genuchten).

It is therefore clear that the use of unimodal functions to describe the hydraulic properties of natural terrain is not always adequate. The widespread and not-contextualized use of unimodal approach may lead to considerable errors in predictive hydraulic simulations invalidating any possible subsequent and further analysis, as slope stability analysis and early warning system bulging up.

The knowledge of the infiltration processes and of the modeling techniques to perform them in unsaturated soil is still far to be “adequate” to enable reliable assessment of slope stability. It has been

widely established that the variation of pore pressure and hydraulic conductivity is very sensitive to the water content; this physical relationship can be significantly influenced by soil heterogeneities and consequently could critically affect the characteristics of slope stability processes as timing failure, failure depths and volume mobilization.

Slope stability analysis usually consists in analytical tools to assess the factor of safety of natural and man-made slopes. In common practice, the slope stability analysis is usually performed by using saturated shear strength parameters and completely neglecting the potential effects originated by “heterogeneities disturbances” on the hydraulic processes. In some cases (e.g. the slip surface dominantly passes through saturated terrain) this assumption can be a reasonable choice. However, it may be that the groundwater level is deep and the failure occurs in partially-saturated conditions. In these cases it may be necessary to use more sophisticated approaches to perform slope stability analyses; the conventional, limit equilibrium, slope stability analysis must be extended to incorporate more appropriate shear strength equations specifically developed for unsaturated soils. In the context of this more rigorous approach to describe the effects of the unsaturated processes on soil shear strength it seemed interesting to evaluate how soil heterogeneities can affect the slope stability.

1.2 RESEARCH LINE AND OBJECTIVES

This work attempts to provide response to key questions: how the double-structure can affect processes/mechanisms in cascade as the water flow infiltration and the unsaturated shear strength and how it can reflect in the reliability of slope stability analysis.

With the aim to give a response to the above mentioned questions, in this work some recent literature theories and models have been used and novel analytical and numerical model developed.

This work explores the influence of double-structure on the stress-strain behavior of unsaturated terrain and it proposes a new analytical method to assess the effects of the hydraulic properties on soil shear integrating a bimodal lognormal function proposed by Romano et al. (2011) to describe hydraulic behavior of unsaturated double-structured soils within the suction stress theory framework of Lu and Likos (2006). The model

is validated against literature data from soils with aggregated macrostructure or with a prevailing coarse fraction. From a practical point of view, taking into account the dual-structure network should be fundamental in the set-up of proper prediction models for shallow landslides induced by rainfall.

In order to investigate the bimodality effects in timing analysis, the processes are dynamically described by a numerical solution of Richards' equations. A novel one-dimensional column code (Ri.D1) have been developed in JAVA™ language, in Eclipse IDE environment; the bimodal hydraulic properties are described using Romano et al.'s model (2011) in which bimodal lognormal functions are matched with Mualem's conductivity model (Mualem, 1976). Ri.D1 implements a traditional van Genuchten-Mualem model too. In the (correct) assumption that a better retention-data fitting (by a generic function) should lead to more realistic reproduction of moisture and suction profiles, the effects of using unimodal and bimodal interpretative models of hydraulic properties were investigated by comparing predictions in term of water contents and suction head profiles. Obviously, the retention data-fitting by unimodal and bimodal functions have been previously performed on the same data-set by means of the same inverse method techniques.

In order to evaluate the effects of the hydraulic bimodality on the slope stability a proper module to perform slope stability analysis is implemented in Ri.D1 code. The work attempts to focus on the possible discrepancies (and its magnitude) that occur between using unimodal and bimodal interpretative models. The comparisons have been performed between the results as timing failure, failure depths and volume mobilization obtained from two approaches: 1) a fully-unsaturated approach in which the slope triggering is governed by Bishop's modified effective stress principle (Lu and Likos, 2006; Godt et al., 2008) and pore water pressure is mathematically defined by lognormal bimodal functions (Romano et al., 2011); 2) a conventional slope stability analysis where the slope triggering is governed by Terzaghi's effective stress principle and pore water pressure is mathematically defined by saturated infiltration theories.

1.3 THESIS LAYOUT

The structure of this work follows the outlined objectives.

In Chapter 2 an overview of the existing literature about the main theoretical topics treated is presented. Starting from the soil structure and related porosity definitions, the concept of dual-structure has been introduced. It focuses on the relationships between double-structure/double-porosity, pore size distributions and water retention functions giving a mathematical justification about how a multi-porous system can affect the hydraulic behavior of terrains. The mathematical formulation of infiltration at the local scale is recalled, including the Richards equation and the role of the parametric hydraulic functions. An overview about several unsaturated shear strength models and the phenomenological link between these and the hydraulic relationship is presented. In conclusion, more recent works about slope stability analysis and critical rainfall thresholds extrapolation methods are synthesized.

Chapter 3 describes the novel proposed bimodal suction stress method to assess the effects of bimodality on the shear-strain behavior; the method proposed originates from an extending of the suction stress theory of Lu and Likos (2006) and involves the lognormal hydraulic function proposed by Romano et al. (2011) to describe bimodal hydraulic behavior. After a description of the theoretical basis assumed by the shear strength expressions and hydraulic models used to formulate the proposal, the model is validated against literature data from soils with aggregated macrostructure or with a prevailing coarse fraction. A sensitivity analysis is performed in order to evaluate the effects of the variation of shape retention parameters on the suction stress. A physically based dependence of the soil shear on the bimodal hydraulic behavior is observable, the modified suction stress theory proves to be in agreement with the bimodality of suction and moisture change.

Chapter 4 describes a novel one-dimensional column code (Ri.D1) to numerically solve the Richards' equations is presented. The novelty consists in: 1) use of lognormal bimodal hydraulic functions (Romano et al., 2011) to describe the hydraulic behavior affected by double-structure; 2) include a slope stability model based on the suction stress theory (Lu and Likos, 2006; Godt et al., 2008) reformulated in a bimodal hydraulic response framework.

Chapter 3 contains the scientific manuscript submitted to Vadose Zone Journal (VZJ) (actually under review) entitled *Some remarks on bimodality effects of the hydraulic properties on shear strength of unsaturated soils* (Ciervo, Casini, Papa e Rigon, 2014).

In Chapter 5 comparison between the results (timing failure, failure depths and volume mobilization) obtained by using unimodal and bimodal hydraulic interpretative models is presented.

Finally, the obtained results are summarized in Conclusions and some recommendations about the possible perspective of the work are addressed.

2 LITERATURE REVIEW

This chapter presents an overview of the literature on the dual-structure soils and related hydraulic and mechanical processes. Furthermore, in the same chapter some theoretical key issues will be described.

The first part gives a brief and general description of the structure and pores space concepts in natural soils. Particular attention is paid to the heterogeneous terrains, the dual-structure concept and to the significances of these soil intrinsic characteristics to the hydro-mechanical behavior (Section 2.1).

Subsequently, common approaches of modelling transient infiltration into saturated-unsaturated soil are reviewed. Contextually, a particular care is given to the unimodal and bimodal constitutive hydraulic functions and to the modeling hydraulic processes in structured terrains (Section 2.2).

The second part of the chapter (Section 2.3) focuses on the effective stress concept (and its extensions) and shear strength models for soils under variably saturated conditions.

At the end, the chapter presents an overview of the available literature on the modeling of transient slope-stability (infinite slope stability). In order to stress the significances of the presented theories to the current engineering practice a particular attention is paid to the infinite slope stability analysis (Section 2.4).

2.1 SOIL PROPERTIES

2.1.1 Soil texture and structure

Natural soils consist of three separate phases: solid, liquid and gas. The solid phase of a soil includes sand, silt and clay fractions commonly expressed as a percentage of the whole. The sand and silt fractions

mainly consist of primary minerals that do not generally occur in the clay fraction.

Natural terrains are usually formed in layers. The ensemble of layers defines a soil profile. Each of these layers consist of structural units represented by different composition of sand, silt and clay (and organic matter).

In the context of analysis of soil water infiltration and flow-dependent mechanical response the role of the soil properties in vadose zone cannot overstated. Characteristics and physical properties of soils are the result of soil parent materials being acted upon by climatic factors (such as rainfall and temperature), and affected by topography (slope and direction, or aspect) and life forms (kind and amount, such as forest, grass, or soil animals) over a certain period of time. A change in any one of these influences usually results in a difference in the type of soil formed.

For purposes of this work the most significant physical properties of a soil are the texture and structure.

The texture refers to the relative proportions of primary particles of various sizes such as sand, silt and clay in the soil. Natural soils are almost never homogeneous, but are characterized by heterogeneities and structures at many scales (Carminati et al., 2008).

The structure refers to the aggregation of primary soil particles (sand, silt and clay) into compound particles or cluster of primary particles which are separated by the adjoining aggregates by surfaces of weakness (Southard and Buol, 1988). Soil structure can be described as the arrangements of variable size soil crumbs with their associated pore spaces. As a result, the various void spaces among the primary particles (micropores or intra-aggregate voids) and those created by the aggregation of these primary particles (macropores or inter-aggregate voids) lead to a complex set of void clusters that can effectively be characterized by a multimodal distribution of pore sizes (Horn and Smucker, 2005; Romano et al., 2011; Zhao et al., 2013).

The structure can be defined in terms of grade, class and type of aggregates. The grade of structure is the degree of aggregation, expressing the differential between cohesion within aggregates and adhesion between aggregates. As these properties vary with the moisture content of the soil, grade of structure should be determined when the soil is neither unusually moist nor unusually dry. Four grades of structure are defined: *Structureless*, *Weak*, *Moderate* and *Strong*. Structureless has no

observable aggregation or no definite orderly arrangement of natural lines of weakness. Some examples are massive structure (coherent) where the entire soil horizon appears cemented in one great mass and single-grain structure (non-coherent) where the individual soil particles show no tendency to cling together, such as pure sand. Weak structure is poorly formed from indistinct aggregates that can barely be observed in place. When removed from the profile, the soil material breaks down into a mixture of very few entire aggregates, many broken aggregates and much un-aggregated material. Moderate structure is well formed from distinct aggregates that are moderately durable and evident but not distinct in undisturbed soil. When removed from the profile, the soil material breaks down into a mixture of many distinct entire aggregates, some broken aggregates and little un-aggregated material. Strong structure is well formed from distinct aggregates that are durable and quite evident in undisturbed soil. When removed from the profile, the soil material consists very largely of entire aggregates and includes few broken ones and little or no non-aggregated material.

Class of structure describes the average size of individual aggregates. Usually, five distinct classes may be recognized in relation to the type of soil structure from which they come. They are very fine or very thin, fine or thin; medium; coarse or thick; very coarse or very thick.

Type of structure describes the form or shape of individual aggregates. Generally, soil technicians recognize seven types of soil structure, but here only four types are used. They are Granular, Blocky, Prismatic and Platy. Granular and crumb structures are individual particles of sand, silt and clay grouped together in small, nearly spherical grains. Widely-graded soils generally exhibit a granular-type structure (Figure 2.1)

Blocky and sub-angular blocky structures are soil particles that cling together in nearly square or angular blocks having more or less sharp edges. Prismatic and columnar structures are soil particles which have formed into vertical columns or pillars separated by miniature, but definite, vertical cracks. Platy structure is made up of soil particles aggregated in thin plates or sheets piled horizontally on one another.

The structure of a soil can have different grades of stability. Clay particles cohere to each other and adhere to larger particles under the conditions that prevail in most soils. Wetting and drying, freezing and thawing, root and mechanical agitation are involved in the rearranging of particles in soils-including destruction of some aggregates and the bringing together of particles into new aggregate groupings. Organic

materials, especially microbial cells and waste products, act to cement aggregates and thus to increase their strength. On the other hand, aggregates may be destroyed by poor tillage practices, compaction, and depletion of soil organic matter.

In this work soil texture (and related void space –micropores/intra-aggregate voids domain) will be conventionally called *micro-structure*, whereas the structure (and related void space – macropores/ inter-aggregate voids domain) will be defined as *macro-structure*.

All the applications presented in this work are implemented in soils characterized by granular-type structure.

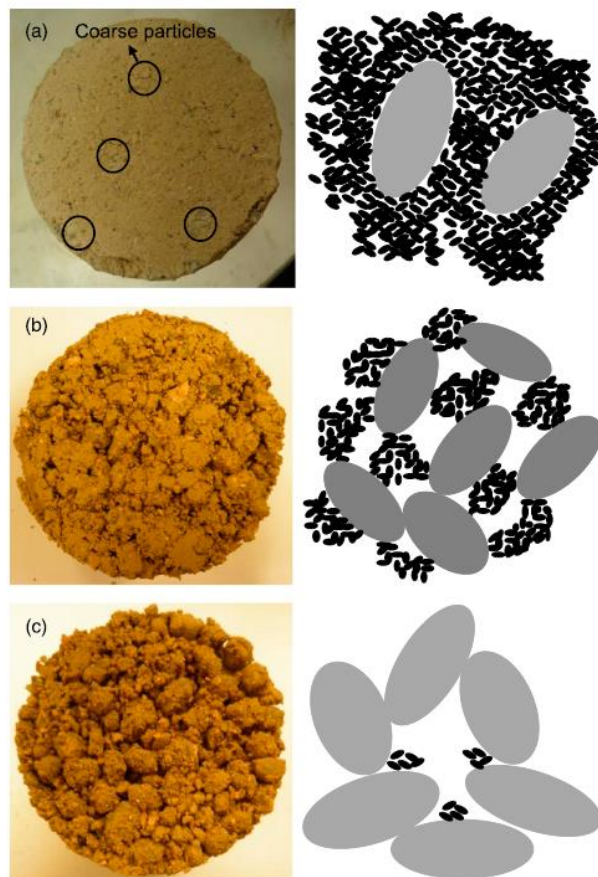


Figure 2.1 Three representative granular-type structured soils with different grade of macrostructure (increasing from a to c) (Zhao et al., 2013).

2.1.2 Pore size distribution and significance to soil hydraulic behavior

Porosity and pore size distribution (PSD) characterize terrain's pore space that portion of its volume that is not occupied by (or isolated) by solid material. The pores space affects the critical aspects of almost everything that occurs in the soil, including the water movement. The definition of pore space conventionally excludes fluid pockets that are totally enclosed within solid material vesicles or vugs (e.g. pumice) that have no exchange with the pore space that has continuity to the boundaries of the medium.

The soil medium is commonly conceptualized as having a single and contiguous pore space. The pore space defines fluid pathways and it could be tortuous, variably constricted or highly connected. This concept enables quantifications and assessments of the main features of pore space (and of related physics phenomena).

The terrain not contain discrete objects with obvious boundaries, so the precise definition of a pore unavoidably requires artificial assumptions and conceptualizations. The most common conceptualization takes the pore space as a collection of channels through which water can flow. The effective width of such a channel varies along its length (Nimmo, 2004).

The porosity is a single-value quantification of the amount of space available to water (or other fluids) within a specific volume of terrain, or alternately can be defined as the fraction of the total terrain volume that is taken up by the pore space. In natural terrain, the porosity typically ranges between 0.3 and 0.7. It depends on several factors (e.g. packing density, width of PSD, particle shape). Mathematically considering an idealized terrain of packed uniform spheres, porosity typically falls in the range 0.26~0.48, depending on the packing; spheres randomly mixed typically induce a porosity as about 0.30 or 0.35 (Nimmo, 2004). A monodisperse sand packs to about the same porosity as spheres. In a polydisperse sand (e.g. a granular-structured sand) the presence of small grains within the macropores can reduce the porosity to values generally less than 0.26. Re-arrangements to reduce porosity to 0.26 or less is highly improbable; however, the porosity generally falls within the 0.30-0.35 for polydisperse sands too. In many aggregate-structured soils (e.g. clay with high presence of organic substances) the porosity of the micro-structure might have a low value, but the additional pore space of the

macro-structure can induce on the whole to a porosity greater than that of the micro-structure. Terrains dominated by micro-structure the dimensions of pore space are comparable (generally slightly less) with those of the adjacent particles. Diversely, a wormhole, if it is essentially uniform in diameter along its length, might be considered a single pore. The porosity value could be representative (indicator) of complexity of structure (being greater for greater complexity); its spatial variability could be representative of granulometric heterogeneity (greater variability correlating with greater heterogeneity). Significant spatial variability on a small scale also implies greater structural complexity, independent of the magnitude of porosity.

Natural terrains generally exhibit heterogeneities at various observation scales. A large class of heterogeneous soils that characterize the natural slopes can be well-described by double-structured models. In heterogeneous natural soil modeled as double-structured the porosity is usually conceptually partitioned into two components, a microstructural and a macrostructural porosity. The microstructural component is that value assumed by the porosity for a random arrangement of the particles. The macrostructural porosity represents nonrandom structural influences, including macropores and it is arithmetically defined as the difference between the microstructural porosity and the total porosity (Romano et al., 2011). The microstructure of the soils relates in a general way to the pore size distribution, as large particles give rise to large pores between them, and therefore it is a major influence on the soil water retention curve. Additionally, the macrostructure substantially influences water retention.

Pore sizes are usually specified by an effective radius of the pore body. The effective radius relates to the radius of curvature of the air-water interface at which Haines jumps occur (i.e. the jump of the position of the meniscus where the air stops to fill the throats, in other words the discontinuous changes of the fluid content along the throats) (Crandall et al., 2009).

Alternative indicators of size include the cross-sectional area or the volume of a pore, and the hydraulic radius, defined as the ratio of the cross-sectional area to circumference, or of pore volume to specific surface. The Pore Size Distribution (PSD) can be defined as the relative abundance of each pore size in a representative volume of terrain.

Several attempts have been made to derive models for the pore radius distribution for the purpose of analyzing the moisture characteristic on

the basis of soil pore structure. Brutsaert (1966) applied several distribution laws, such as the incomplete gamma distribution, the lognormal distribution, and his own original distribution form, to the model for the pore radius distribution (Kosugi, 1994).

The PSD function $f(r)$ can be expressed by the following:

$$f(r) = \frac{d\theta}{dr} \quad (2.1)$$

where θ is the water content and r is the pore radius. Consequently, $f(r)dr$ represents the volume of full pores of radii $(r, r + dr)$ per unit volume of medium. Here r is assumed to be related to “the difference between the pore-air and the pore-water pressures” ψ , the matric suction (Fredlund and Rahardjo, 1993), for a given moisture content by the capillary pressure function:

$$r = \frac{-2\sigma\cos\alpha}{\psi} \quad (2.2)$$

where σ is the surface tension between the water and air, α is the contact angle. On the basis of this direct correspondence of r and ψ , the distribution $f(r)$ is transformed into the distribution $f(\psi)$ by the following equation:

$$f(\psi) = f(r) \frac{dr}{d\psi} \quad (2.3)$$

Substituting (1) into (3) yields:

$$f(\psi) = \frac{d\theta}{d\psi} \quad (2.4)$$

Hence $f(\psi)d\psi$ represents the volume of full pores in which water is retained by capillary pressure ψ to $\psi + d\psi$ per unit volume of medium. Therefore $f(\psi)$ can be regarded as the pore capillary pressure distribution function. From (2.4), it is evident that $f(\psi)$ is identical to the water capacity function $C(\psi)$. The relationship between θ and ψ (the water

retention curves) can be obtained by integrating (2.4). Thus the relationship between θ and ψ can be interpreted as statistical measure of its equivalent pore-size distribution (Durner, 1994; Kosugi, 1994). The water capacity function ($f(\psi)$ or $C(\psi)$) is defined as the slope of the water retention curves and is necessary for modeling water movement in unsaturated soil. The water capacity function is related to the pore radius distribution function by transforming variables under the assumption that there is a direct correspondence between the pore radius and the capillary pressure. At intermediate values of r , sometimes $f(r)$ has a pronounced peak. A peak in $f(r)$ corresponds to an inflection point in water retention curve. The common case of an retention curve that shows a wide range of slopes will have a defined peak in the PSD only if the middle portion of the retention curve has a slope that differs markedly from that of the two end segments. This is frequently true for monodisperse soils. For many terrain $f(r)$ does not have a pronounced peak and this especially likely for terrain that are polydisperse. Lognormal models can often still be applied but with the peak outside the measurable range. Some models (e.g. of hysteresis and hydraulic conductivity) may be unaffected by the lack of a measurable peak even though they were derived assuming the pore size distribution resembles some form of normal distribution.

In case of heterogeneous well-structured soils, similarly with porosity, $f(r)$ (thus $f(\psi)$) may be taken to comprise microstructural and macrostructural pores domains. The cumulative size distribution, by integration of $f(r)$, can be equivalently used. Often a normal or lognormal distribution can be useful to represent the data (Kosugi, 1994). In fact, Gaussian (or log-normal) density functions have been in many cases used for modeling pore-size and grain-size distributions in the open technical literature (Spencer 1963; Nimmo 2004). Structural features may give the soil a bimodal pore-size distribution, leading to several distinctive effects on water flow; bimodal or multimodal forms of PSD are possible, and generally they can be obtained by superposition of the normal or lognormal curves.

It is clear as soil structure critically affects the hydraulic behavior of terrains and related hydro-mechanical response. In case of not negligible structure not appropriate interpretative models for hydraulic properties may have negative effects on predicting physical behavior of heterogeneous natural soils. This is especially true for soils in which the presence of preferential flow paths whose size and flow characteristics

may require approaches other than darcian theory for laminar flow (Beven and Germann, 1982; Kutilek and Nielsen, 1994; Germann and Beven, 1985; Jarvis et al., 1991; Chen and Wagenet, 1992a,b; Gerke and van Genuchten, 1993; Coppola and Greco, 1997; Greco, 2002). In this case the conceptualization of the pore domain can be further complicated; in fact within the whole pore-system a non-capillary pore sub-system (no Darcian approachable) and a capillary pore sub-system can coexist; the latter comprises the capillary pore system further distinguishable as microstructure and macrostructure (Gerke and van Genuchten, 1993; Illman and Hughson, 2005; Kutilek and Jendele, 2008). In this work we only considered structured soils characterized by capillary pore systems. The fluxes interesting the macrostructure are faster than those in the pore system related to microstructure, but small enough to legitimate the assumption that Darcy's equation is either exact or at least a very good approximation for also describing accelerated flow (Kutilek and Nielsen, 1994). In this case the hydraulic properties of the whole soil medium can be described by darcian assumptions and linearly overlapping the hydraulic functions of each subsystem (bimodal hydraulic functions) (Othmer et al., 1991; Wilson et al., 1992; Ross and Smettem, 1993; Durner, 1994; Coppola, 2000). This implies that the whole pore-size distribution is assumed to be continuous and is obtained by weighted sum of the two partial pore-size distributions, such that no interacting term has to be explicitly considered (dual-porosity approach). Several studies of unsaturated flow in porous media exhibiting heterogeneities and conducted within a probabilistic framework have focused on the saturated hydraulic conductivity (Dagan and Bresler, 1983; Russo, 1984; Smith and Diekkruger, 1996; Indelman et al., 1998). A soil property that is important in the hydraulics of unsaturated flow and may strongly affect transport under unsaturated flow conditions is pore-size distribution (Russo, 1984; Destouni, 1993).

2.2 SOIL WATER FLOW

Infiltration is the process by which water passes across the atmosphere-soil interface and enters a given soil. The water movement through a saturated/unsaturated soil is more properly defined as *filtration*.

The time-rate at which water infiltrates the soil across is known as the infiltration rate, whereas the total volume of liquid crossing the interface is known as the cumulative infiltration. Quantitatively, infiltration rate is the volume of water (infiltrated) per unit area in a unit time.

With infiltration capacity is defined the maximum infiltration rate can be moved into the soil in a given condition. The infiltration capacity determines how much of the rainfall will run off and how much will infiltrates and propagate downward in the soil.

Considering an initially dry soil column under ponded conditions, the infiltration rate exhibits initially high values in time, then decreases rapidly and then more slowly decreases until the rate assumes a nearly constant value (stationary flow condition). The wetting front redistribution through a soil column consists in a progressively displacing air and filling pores spaces. In same conditions (ponding) infiltration processes can be described distinguishing three distinct zones. At upper layers the soil approaches to saturated condition. Below soil layers zone the water is being transmitted to the wetting front (transmission zone). Within the wetting zone, the infiltration front forms a sharp boundary between the wet and initially dry conditions (Tindall et al., 1999).

Infiltration and filtration processes can be affected by several factors: soil properties, water properties, meteorological forcing and soil surface factors. Soil characteristics affecting infiltration and filtration include the surface-entry characteristic and soil transmission characteristics. Soil properties as texture and structure affect the pore sizes and distribution in a soil, in turn influencing the hydraulic behavior. Both the total porosity and the pore size distributions determine the water capacity of the soil. In heterogeneous natural soils the initial infiltration will depend upon the volume, size, continuity, and relative stability of pores, which constitute the flow paths for the water. Sandy materials have relatively stable pores. In well-structured clay soils the pore space state is unstable with respect to hydraulic and mechanical loading. When loaded, aggregates are deformed and spatially rearranged, large inter-aggregate pores diminish in size and the bulk soil volume rapidly decreases (soil compaction) (Carminati et al., 2008). For an idealized condition of constant rainfall input and homogenous soil profile, two different mechanisms of the water front propagation can be considered. When the infiltration rate is less than the hydraulic conductivity (generally assumed as "saturated") the saturation occurs from bottom column layers (Dunne, 1970). Diversely, if the infiltration rate at the surface is greater

than the hydraulic conductivity, ponding or run off early occur and the saturation process “propagate” downward from the upper soil layers (Horton, 1933).

2.2.1 Darcy’s law

Darcy (1856) showed that the volume of water that passes through a bed of sand per unit time is mainly dependent on cross-sectional area of the bed, the bed thickness, the depth of ponded water above the bed and the hydraulic conductivity (K). This is known as Darcy’s law, expressed as:

$$Q = -K \cdot \frac{A \cdot \Delta H}{\Delta L} \quad (2.5)$$

where Q is the volume of water that passes the bed (or column), A is the cross section area of the column, ΔH is the difference in terms of head between the inlet boundary and outlet boundary and K is the constant called hydraulic conductivity and depends both on the porous medium and on the fluid passing through it. The negative sign was introduced to obtain a positive value for the discharge; indeed, the groundwater flows in the direction of the head loss, which is negative.

Dividing (2.5) by the cross-sectional area, A, a specific discharge (flux density) is obtained. The flux density is the rate of water movement through a medium; in other word the volume of water that passes a plane perpendicular to the direction of flow, per unit time. The Darcy flux is often called Darcy velocity. Still, the term "velocity" is misleading, because not the entire cross-section is available for flow, but only a part of it, since the solid material represents the most important part. Therefore, the Darcy velocity is an apparent velocity as if the whole cross-section would be available for the water transfer. In fact the real porous medium reflecting the microscopic concept of the flow is replaced by a representative continuum, derived from a macroscopic concept. The microscopic concept would involve the use of the microscopic velocities, associated with the actual paths of the water particles. Because in practice it is impossible to measure the real microscopic velocities, an average value of the real velocities is accepted. Hydraulic conductivity as well as Darcy's law provides thus a global description of the microscopic behavior. The specific discharge (Darcy's

flux) is an average value of the microscopic fluxes from a Representative Elementary Volume (REV), considered homogeneous from a macroscopic point of view.

Darcy's law was established in certain circumstances: laminar flow in saturated granular media, under steady-state flow conditions, considering the fluid homogenous, isotherm and incompressible, and neglecting the kinetic energy. Still, due to its averaging character based on the representative continuum and the small influence of other factors, the macroscopic law of Darcy can be used for many situations that do not correspond to these basic assumptions (Freeze and Cherry, 1979): saturated flow and unsaturated flow; steady-state flow and transient flow; flow in granular media and in fractured rocks; flow in aquifers and flow in aquitards; flow in homogeneous systems and flow in heterogeneous systems; flow in isotropic media and flow in anisotropic media.

The most restrictive hypothesis of Darcy's law is the one that considers the flow laminar, and the fluid movement as dominated by viscous forces. This occurs when the fluids are moving slowly, and the water molecules move along parallel streamlines. When the velocity of flow increases, the water particles move chaotically and the streamlines are no longer parallel. The flow is turbulent, and the inertial forces become significant relative to viscous forces (Fetter, 2001).

The hydraulic conductivity values fall in a wide range; generally, K can range from 10^{-9} cm/s for clay to 1 cm/s for clean sand. Lower values of K for a clay medium (with smaller pore size) are likely due to the drag exerted on the viscous fluid by the walls of the pores. A terrain with a wide range of pores size conducts fluid much more rapidly than a terrain with a narrow range of pore sizes; this is especially true if pores, preferential flowpaths, or macropores form continuous paths through the body of the terrain.

Particles of smaller sized individual grains (such as clays compared to sands) have a larger surface area, increasing the drag on water molecules that flow through the medium affecting the hydraulic conductivity.

2.2.2 The Richards' model

The theory of Richards is formulated within the framework of the modern continuum theory of mixtures, provided that one recognizes from the outset the existence of the separate solid, liquid, and gaseous phases (Raats, 1984). It can also be justified on the basis of the principles

of surface tension and viscous flow at the pore scale (Miller and Miller, 1956; Whitaker, 1986). Richards theory combines the balance of mass, expressed in the equation of continuity, and of momentum, expressed in Darcy's law.

In a two-phase flow model the air pressure in the vadose zone is generally assumed as constant and equal to the atmospheric pressure (Richards, 1931; Hillel, 1980; Kutilek & Nielsen, 1994). This hypothesis seems to be justified in many practical situations, although the question about its validity is quite controversial (Gray & Hassanizadeh, 1991a,b; Vachaud et al., 1973; Touma & Vauclin, 1986; Tegnander, 2001). The additional hypothesis of incompressibility of the water allows to obtain the basis on which a simplified description used for describing the water flow unsaturated zones is developed.

In the vadose zone, the fluid movement is generally well described by the Richards equation (Richards, 1931). The water-mass balance equation for saturated and variably saturated conditions is:

$$-\rho \left(\frac{\partial q_x}{\partial x} + \frac{\partial q_y}{\partial y} + \frac{\partial q_z}{\partial z} \right) = \frac{\partial(\rho\theta)}{\partial t} \quad (2.6)$$

Here ρ represent the water density (assumed constant), $q_{x,y,z}$ are the water fluxes in the several directions, t is the time and θ is the volumetric water content. The Darcy's law is generalized to the unsaturated condition by assuming hydraulic conductivity as a function of the suction (Buckingham, 1907):.

$$q_x = -K_x(\psi) \frac{\partial H}{\partial x}; \quad q_y = -K_y(\psi) \frac{\partial H}{\partial y}; \quad q_z = -K_z(\psi) \frac{\partial H}{\partial z} \quad (2.7)$$

Where ψ is the matric suction and $K(\psi)$ is the unsaturated hydraulic conductivity function. The total head H , in case of assuming negligible the osmotic head, is given by the sum of the suction and the elevation head. Thus, inserting the equation (2.7) into equation (2.6), the following expression is obtained:

$$\frac{\partial \theta}{\partial t} = \frac{\partial}{\partial x} \left[K_x(\psi) \frac{\partial \psi}{\partial x} \right] + \frac{\partial}{\partial y} \left[K_y(\psi) \frac{\partial \psi}{\partial y} \right] + \frac{\partial}{\partial z} \left[K_z(\psi) \left(\frac{\partial \psi}{\partial z} + 1 \right) \right] \quad (2.8)$$

The first term of the above equation can be rewritten as:

$$\frac{\partial \theta}{\partial t} = \frac{\partial \theta}{\partial \psi} \cdot \frac{\partial \psi}{\partial t} = C(\psi) \frac{\partial \psi}{\partial t} \quad (2.9)$$

where $C(\psi)$ is the soil water capacity. The equation (2.9) can be rewritten as:

$$C(\psi) \frac{\partial \psi}{\partial t} = \frac{\partial}{\partial x} \left[K_x(\psi) \frac{\partial \psi}{\partial x} \right] + \frac{\partial}{\partial y} \left[K_y(\psi) \frac{\partial \psi}{\partial y} \right] + \frac{\partial}{\partial z} \left[K_z(\psi) \left(\frac{\partial \psi}{\partial z} + 1 \right) \right] \quad (2.10)$$

The equation (2.10) is the Richards' equation that in a more general form may be written as:

$$C(\psi) \frac{\partial \psi}{\partial t} = \nabla \cdot [K(\psi) \cdot \nabla(\psi + z)] \quad (2.11)$$

To solve the equation (2.11) constitutive hydraulic functions to describe the relationship $\theta(\psi)$ and hydraulic conductivity function $K(\psi)$ are required.

2.2.3 Constitutive hydraulic functions

A transient isothermal unsaturated soil water flow is well described by the Richards' equation. The solution of Richards' equation *a priori* requires the knowledge of the constitutive hydraulic relationships. The relationship between suction and water content is mathematically described by the soil water retention functions, of which the slope is the so-called soil water capacity. Both the soil water retention and unsaturated hydraulic conductivity relations (in combination referred to as soil hydraulic functions) are highly nonlinear, with both suction and hydraulic conductivity varying many orders of magnitude over the water content range of significant water flow.

For use in simulation applications, hydraulic properties are often represented through analytical expressions in which there are parameters to be defined with reference to the soils in question (van Genuchten and Nielsen, 1985; Bruce and Luxmoore, 1986; Mualem, 1986; Santini et al.,

1995) (see for example Kosugi et al., 2002 for a more detailed presentation and comparison of different propositions). The equation proposed by van Genuchten (1980) for the water retention curve is widely adopted and generally combined with Mualem's expression (1976) for the estimation of hydraulic conductivity. Many studies have discussed the validity of the van Genuchten–Mualem model on the basis of direct comparisons between estimated and measured values of hydraulic conductivity (Michiels et al., 1989), as well as on the basis of theoretical analyses (Mualem, 1986; Vogel and Cislserova, 1988; Sidiropoulos and Yannopoulos, 1988).

The van Genuchten–Mualem (van Genuchten, 1980) and Brooks–Corey (Brooks and Corey, 1964) models generally allow a good fit of measured data and are widely used. The parameters of these models can be obtained by fitting the functions to experimental water retention and conductivity data. Alternatively, they can be evaluated by more easily measured soil properties (Bloemen, 1980; Saxston et al., 1986; Vereecken et al., 1989) or calibrated by parameter estimation techniques when the inverse problem is solved.

The above mentioned functional descriptions generally represent pores systems with unimodal pore-size distribution (Durner, 1994). The forms of the curves represented by these functions are fully sigmoidal.

Table 2.1 lists a summary of unimodal water retention functions commonly used.

Table 2.1 Summary of some unimodal water retention functions

References	Equation	Parameter
Brooks and Corey, 1964	$\theta = (\psi_a/\psi)^\lambda$	θ volumetric water content, λ PSD index, ψ_a air entry value
Van Genuchten, 1980	$S_e = [1 + (\alpha\psi)^n]^{-m}$	S_e effective water content, α , n , m constant
Fredlund and Xing, 1994	$S_e = [\ln(e + (\psi/a)^n)]^{-m}$	α , n , m constant
Kosugi, 1996	$S_e = 0.5 \cdot \operatorname{erfc} \left[\ln \left(\frac{\psi_a - \psi}{\psi_a - \psi_c} \right) - \sigma^2 / \sqrt{2\pi}\sigma \right]$	ψ_c mode related to PSD, σ constant, erfc complementary error function

Vanapalli et al. (1996) in order to develop a physical model for explaining the unsaturated shear strength behavior identified the three different

saturation stages when the desaturation process of soil takes place: the boundary stage, the transition stage (i.e., primary and secondary transition stage) and residual stage (Figure 2.1). The soil is essentially saturated in the boundary stage. The area of water in the soil does not change with the increasing matric suction. In the transition stage, the matric suction is greater than the air entry value. The water content reduces with the increasing matric suction. In the residual stage, the variation of water content changes is fairly small. The water content that soils have at this stage is generally referred to as the residual water content.

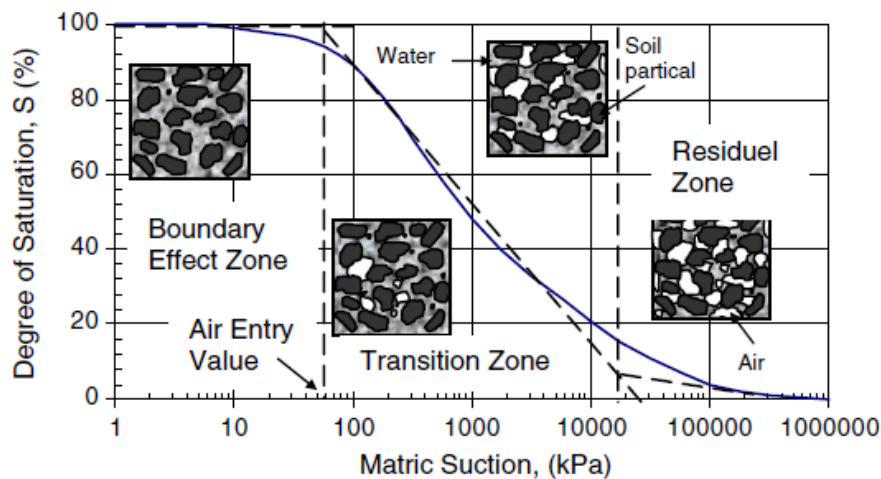


Figure 2.2 A typical soil water characteristic curve showing desaturation Stage (Kayadelen et al., 2007).

Contrary to these simple models, natural soils often exhibit more complicated pore-size distributions which may greatly influence the hydraulic properties. Natural soils are almost never homogeneous, but are characterized by heterogeneities and structures at many scales. Soil structure critically affects the hydrological behavior of soils. So, the use of unimodal functions to describe the hydraulic properties of such terrains is not always adequate and may lead to considerable errors in predictive hydraulic simulations (Othmer et al., 1991; Durner, 1992, 1994; Wilson et al., 1992; Ross and Smettem, 1993; Durner, 1994, Coppola, 2000).

The last two decades have seen the development of a relatively large number of models that try to capture the effects of the soil structure heterogeneities on the infiltration mechanisms. A large class of heterogeneous soil systems can be well-described by dual-structure approach analysis.

At the local scale (Darcy scale), the water movement is adequately governed by the Richards' equation in both sub-structural domains assuming the same order of magnitude of the hydraulic parameters for both pore domains. This assumption led to an equilibrium model. The retention model is characterized by a single macroscopic pressure field and two macroscopic water content (bimodal functions). An overview of bi-porous model can be found in Simunek et al. (2003). In the vadose zone modeling composite hydraulic functions are often used (Othmer et al., 1991; Durner, 1994; Peters & Klavetter, 1988; Smettem et al., 1991; Simunek et al., 1998). They allow to account for rapid changes of the soil properties in the near-saturation region, which is caused by the presence of macropores.

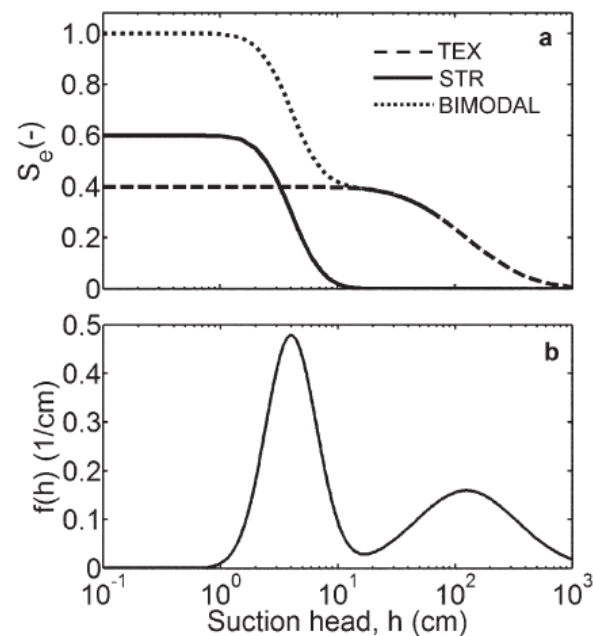


Figure 2.3 Bimodal (a) effective saturation and (b) PSD $f(h)$ for an hypothetical soil. (Romano et al., 2011).

The medium is conceptualized as two or more overlapping regions. Each region is characterized by its own pore size distribution and hydraulic functions (Fredlund et al., 2000; Romano et al., 2011). The characteristic of entire bi-modal or multi-modal system is obtained by the linear superposition of the local functions (Figure 2.3). Zhao et al. (2013) identified four different drainage stage processes in a dual-structured soil (Figure 2.4). The first drainage phase (Stage a) consists in the water retention domain that falls in the suction range between 0 and the air entry value; the pore space is completely filled by the water. When the suction is larger than the air entry value, air breaks into the macrostructural void domain where the first drainage period starts (Stage b); the water stored in the macrostructure begins to drain and becomes unsaturated. As soil suction increases, the drainage of the meniscus water in the macrostructure follows (Stage c); a large increase in matric suction results in little changes in water content. The pore water becomes discontinuous except for the water bounded between the primary particles (microstructure) in the form of water bridges. In Stage d the water stored in the microstructure begins to drain (Stage d). The macrostructure subsequently becomes unsaturated.

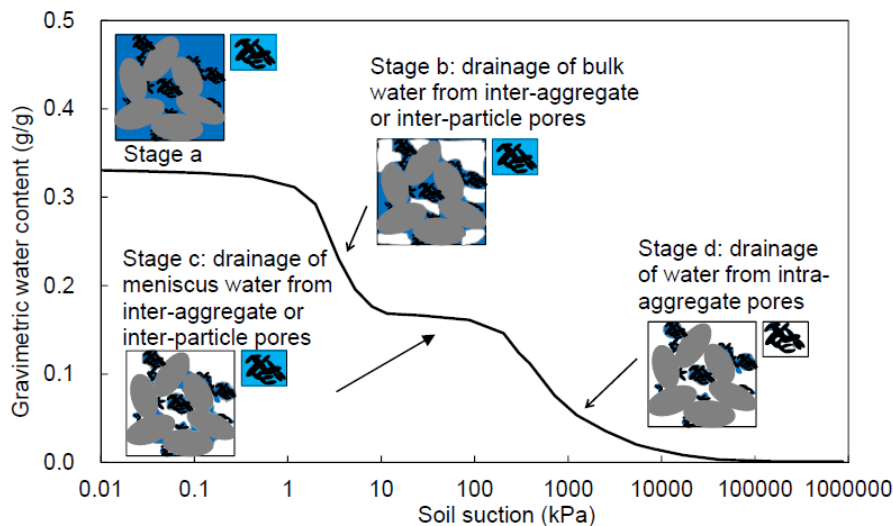


Figure 2.4 A typical bimodal soil water characteristic curve showing desaturation Stage (Zhao et al., 2013).

To model water flow in such media bimodal hydraulic functions are widely used in many applications. However, a large part of these models rely on effective hydraulic properties that are mostly based on empirical relationships or fitted data; several research proposals fall in this set of models (e.g., Othmer et al., 1991; Durner, 1994; Ross and Smettem, 1993). More recently, Priesack and Durner (2006) derived a closed-form parametric expression for the van Genuchten-Mualem model in the case of soils showing a multimodal PSD, described by bimodal or trimodal forms of van Genuchten's water retention function. Tuller and Or (2002) and Kutilek and Jendele (2008) used more physically based, but different, approaches for modeling hydraulic functions of unsaturated structured porous media. Specifically, Tuller and Or (2002) considered equilibrium liquid configurations in dual-continuum pore space as the basis for the calculation of liquid saturation and the subsequent introduction of hydrodynamic considerations, while Kutilek and Jendele (2008) used the lognormal hydraulic model of Kosugi (1994) and partitioned the structural and textural soil pore domains by defining a soil-specific suction head value that corresponds with the air-entry value of the soil textural domain (Romano et al., 2011). Fredlund et al. (2000) proposed a bimodal water retention curve by using a four-parameter unimodal model described by Fredlund and Xing (1994). Romano et al. (2011) proposed a bimodal lognormal model by using Kosugi-type Gaussian probability distribution functions linking the structure domains through weighting factors that represent the probability of the pore space being part of either the micro- or the macro-structural domain.

2.3 SHEAR STRENGTH BEHAVIOR

2.3.1 Stress state variables

Stress state variables constitute the model to characterize the mechanical behavior of terrains. The stress states in terrain consist of combinations of stress variables that can be referred to as stress state variables. For saturated or dry conditions Terzaghi defined *effective stress* as stress representing “that part of the total stress which produces measurable effects such as compaction or an increase of the shearing resistance” (Terzaghi, 1943), which takes the form:

$$\sigma' = \sigma - u_w \quad (2.13)$$

where σ^s is the effective stress tensor (single tensor variable), σ is the total stress tensor and u_w is the pore pressure. The stress state variable as above represented is actually (in practical engineering) considered to fully describe the measurable effects induced by variable stress changes on the mechanical response of terrains under different water content conditions. In the specific case of unsaturated terrains, several authors investigated on the specific contribution of matrix forces that should not be negligible into the stress state definition (Bishop, 1959; Lambe and Whitman, 1969; Mitchell, 1976). Bishop (1959) suggested (in a similar form to Terzaghi) the following expression of effective stress in partially-saturated terrain:

$$\sigma' = \sigma - u_a + \chi \cdot (u_a - u_w) \quad (2.14)$$

where $(\sigma - u_a)$ is the net normal stress, $(u_a - u_w)$ is the matric suction and χ is the coefficient of effective stress to be experimentally defined and it is generally associated to the degree of saturation but it can incorporate information regarding the microstructure of the deformable medium and can be mainly envisioned as a scaling factor that captures the weight of the contribution of each fluid pressure to the effective stress (Mainka et al., 2014).

The magnitude of the capillary forces are complex functions of the soil properties and the properties of the multiphase fluid interface. Manifestation of capillary forces to the macroscopic engineering behavior of unsaturated soil is readily apparent by associated increases in shear and tensile strength or by volume changes commonly observed under changing moisture conditions (Lu and Godt, 2013). Lu and Likos (2004, 2006) and Lu (2008) demonstrate the conceptual validity of Bishop's effective stress but underline several deficiencies in Bishop's relation, such as the need for zero effective stress in nearly dry condition, where suction is high (particularly for silt and clay, for which the magnitude of inter-particle stress could be very large for low saturation conditions).

Several authors put substantial efforts toward the proper identification of a single effective stress for partially-saturated terrain, commonly referred to as Bishop-type effective stress (Jennings, 1960; Aitchison, 1961; Sheng et al., 2008b; Laloui and Nuth, 2009).

However, the concept of using a single stress state variable was widely shown to be not representative for mechanical behavior of unsaturated terrains. Jennings and Burland (1962) concluded that the Bishop's equation not adequately predict the "collapse compression" (Al-Sharrad, 2013) for decreasing suctions under a constant total stress. This deficiency was also acknowledged by other researchers (e.g. Bishop & Blight, 1963; Burland, 1965 and Matyas & Radhakishna, 1968). Therefore, the proposals to represent the mechanical behavior of partially-saturated through expressions in terms of a single stress state variable was widely not accepted. It was recognized that the choice of the stress space to thermodynamically describe volume changes in unsaturated media was more complex.

The variables of unsaturated soils are generally the net stress and suction. The two variables are treated independently in terms of their roles in the mechanical behavior of unsaturated soil so that the use of a single valued effective stress equation for unsaturated soil can be eliminated (Fredlund and Rahardjo, 1993).

In the two independent stress state variable approach (Coleman, 1962; Fredlund and Morgenstern, 1977), the total stress (net stress) and suction are hypothesized to be sufficient stress variables for predicting the mechanical behavior of terrain in unsaturated conditions. Bishop and Blight (1963) proposed a validation of the two variables approach by experimental tests (oedometer tests and triaxial tests). The two independent stress approach take relevance with the extension to the elastoplasticity by some proposed models (Alonso et al., 1990; Wheeler and Sivakumar, 1995; Gallipoli et al., 2003).

Two significant obstacles characterize the two independent stress state variable theory: a) the need of additional and variable parameters difficult to determine experimentally; b) the no-flexibility of the model along the smooth transition between saturated and dry conditions. Other discussible aspect of the original two independent stress-state variable theory consists in considering a unique relationship between degree of saturation and suction (hysteresis) inducing to significant errors. Some interesting works aimed at allowing a continuous transition between unsaturated and saturated states and also reducing the number of constitutive model parameters (Houlsby, 1997; Loret and Khalili, 2002; Khalili et al., 2004; Nuth and Laloui, 2008).

The model of Wheeler et al. (2003) is a particular example of the use of two stress state variables where the first is a Bishop's type stress state

variable; the models assumes that the yielding behavior is also affected by the effective water content, with changes related to the variation of a second stress state variable defined as “modified suction”.

Alonso et al. (2010) suggested a “microstructurally based effective stress” based on the concept that the portion of soil water captured by clay minerals does not contribute to water movement processes.

Lu and Likos (2006) and Lu et al.(2010) proposed the effective stress of unsaturated soil with a form similar to that of Terzaghi’s classic effective stress equation:

$$\sigma' = \sigma - u_w - \sigma^s \quad (2.15)$$

where σ^s is the suction stress. The suction stress theory of Lu and Likos (2004, 2006) is based on the conceptualization of the energy exchange interaction at the surface of soil skeleton as the amount of different inter-particle interactions due to matric suctions (van der Waals, capillarity, tensile forces). Lu et al.(2010) proposed a close-form equation for the suction stress of unsaturated soil, in which the suction stress is mathematically described by the product between the suction and the effective water content, in turn described by van Genuchten hydraulic model. Toker et al. (2014) theoretically showed that the effective stress principle may be represented by the suction-stress of Lu and Likos (2006).

An interesting research proposal by Mainka et al. (2014) extends the effective stress to unsaturated porous media with dual porosity by taking into consideration electro-chemo-mechanical effects. Their approach uses the self-consistent homogenization technique and shows that the resulting expression reduces to the Bishop’s expression for unsaturated single porosity media and swelling saturated porous media.

2.3.1 Soil shear strength

Stress and strength concepts are used to define the failure state. The definition of the soil strength varies widely dependent on the perspective on the aims of the applications. The soil strength can be defined in different ways. Soil strength is the ability of the terrain to resist deformation by compressive, tensile or shear strength stresses; diversely, it can be considered as the ability of the terrain to resist abrasion or to

resist being transported by a fluid. In this work, the first strength definition is contemplated.

Both the shear and tensile strengths are mainly controlled by the soil composition, stress and pore-water pressure history, and prevailing loading conditions. The presence of water in soil constitutes a significant difference in its mechanical behavior compared with other materials.

The soil characteristic shear strength parameters (i.e. cohesion and friction angle) would be different depending on the consideration of pore-water pressure and grade of saturation. Because the condition of natural soils likely are oscillating between several conditions (i.e. drained and undrained) effective stress, together with effective shear strength parameters, should be used in slope stability analysis.

Slope stability analysis is usually performed by using saturated shear strength parameters. In some cases (e.g. the slip surface dominantly passes through saturated terrain) this assumption can be a reasonable choice. However, it may be that the groundwater level is deep and the failure occurs in partially-saturated conditions. In these cases it may be necessary to use more sophisticated approaches to perform slope stability analyses; the conventional, limit equilibrium, slope stability analysis must be extended to incorporate more appropriate shear strength equations specifically developed for unsaturated soils.

Shear strength data experimentally measured suggests that there is a non-linear increase in strength as the terrain desaturates as a result of an increase in matric suction (Oloo and Fredlund 1996; Oberg and Sallfors 1997; Miao et al. 2002; Xu 2004; Gan and Fredlund 1982; Escario and Juca 1989; Fredlund et al. 1996; Oloo and Fredlund 1996; Rassam and Williams 1997; Bilotta et al., 2005; Sorbino et al., 2012). Due to the phenomenological relationship between the shear strength of an unsaturated soil and the amount of water in the voids of the soil, and therefore with matric suction, it is presupposed that the shear strength of an unsaturated soil should also bear a relationship to the soil water characteristic curve. Oloo and Fredlund (1996) defined this non-linearity as being the result of the decreasing contribution of the matric suction to the shear strength as the water content approaches the residual water content of the terrain.

The two independent stress-state variables approach is commonly adopted by most of the researchers for studying the unsaturated terrains (Vanapalli et al. 1992; Gan and Fredlund 1996; Miao et al. 2002; Toll and Ong 2003).

Basing on the single effective stress theory proposed by Bishop (1959), Bishop and Donald (1961) substituted the Bishop's stress into the Mohr-Coulomb equation to define one of more widespread equation for describing the shear strength of unsaturated terrains:

$$\tau = c' + [(\sigma - u_a) + \chi \cdot (u_a - u_w) \cdot \tan\varphi'] \quad (2.16)$$

Bishop's equation consists of two components; the first part is a function of normal stress, since the shear strength parameters, cohesion (c') and friction angle (φ') are constant for a saturated terrain. The first component of the equation is related to saturated shear strength when the pore-air pressure (u_a) is equal to the pore-water pressure (u_w). The second component is the contribution in shear strength of matric suction.

Fredlund et al. (1978) proposed the modified Bishop's relationship introducing the angle φ_b (experimentally evaluated) that expresses the increasing of strength due to a change in suction:

$$\tau = c' + (\sigma - u_a) \cdot \tan\varphi' + (u_a - u_w) \cdot \tan\varphi^b \quad (2.17)$$

More recently some studies have proposed empirical approaches to predict the shear strength of unsaturated terrains by using the water retention curve parameters and saturated shear strength parameters. Vanapalli et al. (1996) developed a physical model for describing the unsaturated shear strength behavior by making use of the water retention curve in addition to shear strength parameters for saturated conditions:

$$\tau = c' + (\sigma - u_a) \cdot \tan\varphi' + (\Theta^k) \cdot (u_a - u_w) \cdot \tan\varphi' \quad (2.18)$$

where Θ is the normalized volumetric water content and k is a fitting parameter; the authors reintroduce the friction angle at saturation (φ') and erasing the practical complexity of the φ^b evaluation through experimental tests.

The authors identified three different saturation stages as the desaturation processes advance: the boundary, the transition and residual stage (Figure 2.1). In the boundary stage the variation of shear strength is assumed to be linear. In the transition stage the shear strength typically exhibits a non-linear behavior. In the residual stage, the shear strength with respect to the suction decreases or remains approximately constant for sandy and silty soils.

Oberg and Sallfors (1997) proposed another equation for suction strength exclusively for sands and silts; the form of the equation is quite similar to that of Bishop (1959):

$$\tau = c' + (\sigma - u_a) \cdot \tan\phi' + S \cdot (u_a - u_w) \cdot \tan\phi' \quad (2.19)$$

The authors assumed that the χ is equal to the effective water content. The variation of the χ factor with matric suction was investigated by Khalili and Khabbaz (1998) using experimental data published in the literature; the authors proposed to calculate χ through empirical expression that relates the current matric suction to the air entry value of the terrain.

Another equation relating the suction strength to the soil–water characteristic curve was put forward by Rassam and Cook (2002). Similarly to Vanapalli et al. (1996) Rassam and Cook (2002) proposed a new shear strength relationship requiring the further knowledge of the unsaturated shear strength at residual suction .

$$\tau = c' + (\sigma - u_a) \cdot \tan\phi' + (u_a - u_w) \cdot \tan\phi' - \alpha[(u_a - u_w) - (u_a - u_w)_r]^b \quad (2.20)$$

where:

$$\begin{cases} \alpha = \frac{(u_a - u_w)_r \cdot \tan\phi' - \tau_{sr}}{[(u_a - u_w)_r - (u_a - u_w)_b]^\beta} \\ \beta = \frac{[(u_a - u_w)_r - (u_a - u_w)_b] \cdot \tan\phi'}{[(u_a - u_w)_r \cdot \tan\phi' - \tau_{sr}]} \end{cases}$$

where α and β are estimated fitting parameters, $(u_a - u_w)_r$ is residual suction and the τ_{sr} contribution of matric suction to the shear strength at residual suction, which should be experimentally evaluated. Due to the complication related to the dependence on the residual state determination this model turned out not extensively suitable.

The relationship proposed by Zhao et al., (2013) is based on the definition of four different drainage stages (n) of the water retention curves and three micro-structural relative effective water contents, therefore shear strength results a composite expression of different

contributions. The model is specifically developed for granular soils that exhibit bimodal retention behavior.

$$\tau = c' + (\sigma - u_a) \cdot \tan\varphi' + \tau_s \quad (2.21)$$

where:

$$\tau_s = \begin{cases} s \cdot \tan\varphi' \\ s \cdot (1 - S_r^{1e}) \cdot \tan\varphi' \\ \sigma_c \cdot S_r^{2e} \cdot \tan\varphi' \\ (1 - f_c) \cdot s \cdot (1 - S_r^{3e}) \cdot \tan\varphi' \end{cases}$$

Other authors have questioned the physical justification for relating shear strength to the water retention behavior arguing that the physical reasons for an increase of shear strength with increasing suction are not entirely the same as those for a decrease of degree of saturation with increasing suction.

Other unsaturated shear strength expression is based on the suction stress theory proposed by Lu and Likos (2006):

$$\tau = c' + [(\sigma - u_a) - \sigma^s] \cdot \tan\varphi' \quad (2.22)$$

where:

$$\sigma^s = -\frac{S_e}{\alpha} \left(S_e^{\frac{n}{1-n}} - 1 \right)^{\frac{1}{n}} \quad 0 \leq S_e \leq 1$$

where α and n are the empirical curve-fitting parameters of the van Genuchten parametric model. The suction stress refers to the net interparticle forces generated within the unsaturated matrix due to the combined effects of negative pore water pressure and surface tension (Song, 2014). The hydraulic shape parameters demonstrate the characteristic values of the unsaturated soil and have different ranges according to the terrain type. The relationship between suction stress and effective water content is defined by the authors as the Suction Stress Characteristic Curves (SSCC, Lu and Likos, 2006). This approach avoids the many challenging difficulties in experimental determination or theoretical development of the Bishop's effective stress parameter χ (Lu

et al., 2014). Lu and Likos (2006) showed that, using the ample existing experimental data in the literature, the suction stress-based effective stress principle is valid for describing the shear strength of variably saturated soils. Baille et al. (2014) experimentally demonstrated that the closed form equation proposed for the suction stress of unsaturated soil can be used to describe void ratio-effective stress relationships for different clays under unsaturated oedometer conditions. Recently, several researchers have investigated the validity of the suction stress obtained using this approach (Lu et al., 2009; Kim et al., 2010; Lehmann and Or, 2012; Song, 2014; Ciervo et al., 2015 *submitted*).

2.4 INFINITE SLOPE STABILITY ANALYSIS

Quantify the impact of infiltration conditions and subsurface flow processes (soil heterogeneity, dual-structure, preferential flow, interaction with matrix flow) upon slope stability is of significant importance to improve landslide hazard forecast (Debieche et al., 2012).

The triggering of landslides is strongly related to hydrological processes, which conditioning the mechanical behavior of the terrain ultimately cause slope failure; the rainfall is between the main triggering factor of landslides, and its pattern controls their behavior in time.

Slope failure is a physically consequence of both a decrease in the shear strength due to a matric suction reduction (increase of pore-water pressure) and an increasing of the destabilizing forces on the slope (soil weight). Thus, the knowledge of spatial and temporal distribution of strength parameters, and of infiltration dynamics is of significant importance for the prediction of landslides.

In the last decade several hydro-mechanical models have been proposed in literature in order to explain physical processes and to comprehend the cause–effect relationship between heavy rainfall occurrence and initial instability in terrains.

The classical methods of slope stability analysis are based on the concept of “limit equilibrium”, which defines the limiting state when the shear stress in a slope is in just-stable mechanical equilibrium with the shear strength of the slope material (Fellenius, 1936; Morgenstern and Proce, 1965). To quantitatively assess the stability of a slope, a parameter (FoS)

known as “Factor of Safety” is introduced. The FoS is the ratio between the resistive forces and gravity force pull. Thus, the transition between stability to failure may be envisaged mathematically as a decrease in the FoS to values below unity along a failure surface. In many circumstances, the failure surfaces are shallow and quite parallel to the slope surface. Under these conditions, stress concentration is usually ignored due to its negligible effect and one-dimensional limit equilibrium model is generally used (i.e. infinite-slope stability model).

Several theoretical models of rainfall-triggered landslides are based on the infinite-slope stability analysis in which the slope triggering is governed by the increase in groundwater pressure due to rainfall, or rather by Terzaghi’s effective stress principle in which pore water pressure is mathematically defined by saturated infiltration theories. These models are often implemented in codes that through a spatial discretization of landscape in cells allow to spatially extend the analysis computing FoS in each cell. Many of the approaches proposed in literature are based on the hypothesis of steady groundwater flow conditions (Montgomery and Dietrich, 1994).

However shallow failures may occur within the vadose zone under unsaturated terrain conditions (e.g., Wolle and Hachich, 1989; de Campos et al., 1991; Godt et al., 2007) indicating that stability analyses assuming saturated conditions are often physically inconsistent and in some case completely invalid. Iverson (2000) showed that for the limiting case of nearly saturated terrains, the dominant direction of strong pore pressure transmission resulting from rainfall can be assessed using two time scales. In an isotropic, homogeneous slope, the time scale for strong pore pressure diffusion *normal* to the slope is H^2/D_0 where H is the slope normal depth and D_0 is a reference soil water diffusivity. The time scale for strong pore pressure diffusion *parallel* to the slope to some point located below a catchment with contributing area A is A/D_0 . In the circumstances where the ratio of the time scales is 1, the long- and short-term pressure head responses to rainfall can be adequately described by one-dimensional linear and quasi-linear approximations to Richards equation (Iverson, 2000).

Casadei et al. (2003) coupled an infinite slope stability model with a dynamic hydrologic model inspired by the Topmodel (Beven and Kirkby, 1979). Simoni et al. (2008) proposed a model (GEOtop-FS) that computes soil moisture and matric suction within soil layers by numerically integrating the Richards equation in a 3-D scheme.

Additionally Bathurst et al. (2006) developed another hydrological model (Shetran model), including an infinite slope stability module. Lanni et al. (2012) proposed a new hydrological model in which a dynamic topographic index is used to describe the transient lateral flow. In this model the lateral flow initiates only if hydrological connectivity is determined by rainfalls exceeding a threshold value.

The failure is strongly influenced by spatial and temporal variations in seepage induced pore water pressure (Fannin et al. 2000). An adequate characterization of the terrain strength is essential over an appropriate stress range for a reliable stability analysis and a clear understanding of the likely failure mechanisms (Fannin et al. 2005). Negative pore-water pressures above the water table have been quantified in many slope-stability analyses (e.g., Cho and Lee, 2002; Collins and Znidarcic, 2004). However, the distribution of stress within the vadose domain is generally considered using the distribution of total stress since Terzaghi's effective stress that is not able of accounting for the stress at skeleton scale under unsaturated conditions (Lu and Godt, 2008; Casini et al., 2011; Godt et al., 2012). In fact, fluctuation in skeletal stress as a consequence of changes in content or suction have been generally largely ignored in the practical applications. Fredlund et al. (1978) proposed a soil shear strength modification to account for soil suction fluctuations; this modification of shear strength due to soil suction has been recently used for slope stability analysis (e.g., Ng and Pang, 2000; Rahardjo et al., 2007; Godt et al., 2009). The time needed to reach potential instability in the unsaturated zone for a given rainfall was investigated by Godt et al. (2012). In order to assessing the slope failure under transient variably saturated conditions Godt et al. (2012) analyzed suction and water content profiles and FoS variability within the framework of the effective stress form proposed by Lu and Likos (2004, 2006); they aimed to define a mean for rigorous quantification of changes in stress state due to infiltration and thus the analysis of slope stability over the range of volumetric water contents and pressure heads relevant to shallow landslide initiation.

The heterogeneity of terrain properties (intrinsic and variable properties) within slope domain is other significant issue that may complicate the mostly used mechanism concepts to analyze landslide inception (Bogaard and Greco, 2014). Capparelli and Versace (2014) highlight the effects induced on the infiltration dynamics by coarse pumiceous layers situated below layers of fine volcanic ashes in Sarno (Italy). Unsaturated

properties and hydrological regime of pyroclastic soils were also considered a key factor for the understanding of hydro-mechanical behaviour of the pyroclastic mantle (Cascini et al. 2003; Picarelli et al. 2004; Sorbino et al., 2012). Lepore et al. (2013) proposed a distributed eco-hydrological model to evaluate the spatial and temporal distribution of the local FoS; the focus of the research is on the introduction of anisotropy of hydraulic conductivity to better reproduce the fast lateral redistribution of water observed in macroporous forest soil. The results show that, especially in layers with small hydraulic conductivity, a higher horizontal conductivity leads to a more realistic prediction of the unstable areas.

3 BIMODALITY EFFECTS OF THE HYDRAULIC PROPERTIES ON SHEAR STRENGTH OF UNSATURATED SOILS

An analytical method to assess the effects of the hydraulic properties on soil shear is developed integrating a bimodal lognormal function to describe water retention behavior within the suction stress theory framework. Hydraulic properties affect the shear strength of unsaturated soils in terms of suction, predicted as a function of water volume in the pores. The proposed bimodal suction stress method originates from the double structure typically exhibited by widely-graded soils, which are characterized by a bimodal pore-size distribution that is conceptually divided into micro and macrostructures. The model is validated against literature data from soils with aggregated macrostructure or with a prevailing coarse fraction. A physically based dependence of the soil shear on the bimodal hydraulic behavior is observable, the modified suction stress theory proves to be in agreement with the bimodality of suction and moisture change. Depending on the soil type and the range of suction investigated, the micro and macrostructures should prevail affecting the mechanical soil response subject to environmental loading, such as rainfall events. From a practical point of view, taking into account the dual-structure network should be fundamental in the set-up of proper prediction models for shallow landslides induced by rainfall. Hydro-mechanical approaches to modeling complex-graded or compacted materials may be pivotal to understanding the behavior of unsaturated soils in engineering practice. Several equations have been proposed linking strength models to water retention curves (WRC) (Vanapalli et al., 1996; Fredlund et al., 1995; Öberg and Sällfors 1997; Kim, 2001; Miao et al, 2001; Rassam and Cook, 2002; Vaunat et al, 2002; Springman et al 2003; Lee et al., 2005; Likos et al., 2010, Sheng et al., 2011 Lu et al.; 2010; Zhao et al., 2013). Owing to its intrinsic dual-porous structure, widely-graded porosity systems usually manifest bimodal hydraulic properties affecting the shear response of the soil. Current research studies come from experimental investigations on multi-modal pore-size distributions (PSD) and correlated hydro-

mechanical behavior (Zhang and Li, 2010; Zhao et al., 2013); some recent works have focused on processes related to fine-grained soils and its own microstructural component (Romero and Vaunat 2000; Romero et al., 2011; Della Vecchia et al 2014), others have been devoted to understanding the behavior of unsaturated silty materials (Casini et al, 2012).

Volcanic soils usually exhibit a composite hydraulic behavior where the macro- and microstructure domains interact (Miyamoto et al., 2003; Basile et al., 2007; Sorbino et al., 2006). Hamamoto et al., (2009) adopts bimodal functions to describe the hydraulic behavior of variably compacted unsaturated volcanic ash soils. Recently, by analyzing the effects of infiltration in a flume test, a fully hydro-mechanical model has been used to describe the behavior of pyroclastic soils in conditions ranging from unsaturated to saturated by Villaraga et al (2014). By experimental investigation, Zhao et al. (2013) identified a critical coarse content of soil, above which the hydro-mechanical behavior of widely graded soils moves from a fines-controlled to a coarse-controlled structure. Soils with an appreciable content of clay that are compacted dry of optimum moisture content generally exhibit a structure made up of aggregates of varying sizes and tend to have a bimodal hydraulic behavior (Casini et al., 2012).

The WRC represents the relationship between water content and suction in unsaturated soils (van Genuchten, 1980; Brooks and Corey, 1966; Fredlund and Xing, 1994). The most common approaches to describe WRCs consist of the sigmoidal form of smooth empirical functions (Kutilek and Jendele, 2008). More physically-based expressions of WRCs are generally related to probability laws of PSD (Brutsaert, 1966); natural soils are often characterized by complex pore-systems for which the existence of an intrinsic, multimodal PSD is demonstrated by means of experimental proofs (Burger and Shackelford, 2001; Bird et al., 2005). Several bimodal water retention curve (BWRC) models use linear superposition of various types of unimodal functions (Ross & Smettern, 1993; Durner et al 1994; Burger and Shackelford, 2001). Fredlund et al. (2000) (equation 8, in reference) proposed a bimodal WRC by using a four-parameter unimodal model described by Fredlund and Xing (1994). Romano et al. (2011) proposed a bimodal lognormal model by using Kosugi-type Gaussian probability distribution functions linking the structure domains through weighting factors that represent the

probability of the pore space being part of either the micro- or the macro-structural domain (equation 3a, in reference).

From a mechanical point of view, Bishop (1959) linked the suction contribution to effective stress by trying to condense the magnitude of process variability into the χ parameter; the χ parameter includes the effects the degree of saturation (S_e), the “disturbances” due to structure complexity, wetting-drying history, loading path and boundary effects in the case of its experimental determination. Fredlund et al. (1978) taken into account the partial saturation introducing the friction angle φ^b (evaluated experimentally) that expresses increasing strength relative to a change in suction; Vanapalli et al. (1996) proposed an unsaturated shear strength relationship by reintroducing the friction angle at saturation (φ') and eliminating the practical complexity of evaluating φ^b through experimental tests (equation 16, in reference). Similarly, Rassam and Cook (2002) proposed an equation requiring further knowledge of the unsaturated shear strength at residual suction, however, due to the complication of dependence on residual state determination, the model is not extensively suitable. The suction contribution to strength proposed by Zhao et al., (2013) is composed of four different drainage stages of the WRC and three relative and effective micro-structural water contents; the equation is specifically developed for granular soils that exhibit bimodal retention behavior (equation 9, in reference). Lu and Likos (2006) use Bishop’s effective stresses introducing the *suction stress* term (σ^s) (equation 9, in reference); it is defined as the amount of physiochemical force generated within a matrix of unsaturated soil particles due to the combined effects of suction and surface tension (Song, 2014).

In practical applications a “bimodal approach” to the study of hydro-mechanical behavior of natural soils (by means of proper models) could lead to variable differences in results if compared with those obtained by more classic unimodal models. The use of BWRC and non-conventional saturated properties may be crucial to improving slope-stability analysis and design of hazard countermeasures. Moreover, extending the dual-structure concept to the hydraulic conductivity framework (i.e. Mualem, 1976) could significantly affect the forecasting of process timing; this should be of fundamental importance in a context of operational early warning systems, physically-based derivation of critical rainfall thresholds

(Papa et al., 2014) or, more in general, for the prevention of natural hazards induced by atmospheric loading (De Vita et al., 2014).

In this work, the term *microstructure* is used to refer the micro-pore domain, whereas *macrostructure* refers to the macro-pore domain. The microstructure is given by the amount of pore space between the primary soil particles (sand, silt or clay). It is generally limited to the finer soil fraction. The macrostructure, diversely, consists of the interspaces between stable aggregates of primary particles or coarser particles (Dexter and Richard, 2009).

The main aim of this work is to develop an analytical method to analyze the effects of bimodal hydraulic properties on shear strength assessments. To achieve this goal, we have integrated a bimodal lognormal retention model (Romano et al. 2011) into the suction stress framework of Lu and Likos (2004, 2006). Thence, a new, closed-form equation for estimating shear strength in unsaturated soils with bimodal hydraulic behavior is validated. To better understand the capabilities of the proposed model, however, a mathematical exploration and a sensitivity analysis of the equation has been carried out. A discussion on the theoretical and practical suitability of the model concludes the work.

3.1 EXTENDING THE SUCTION STRESS THEORY

The suction stress theory of Lu and Likos (2004, 2006) is based on the conceptualization of the energy exchange interaction at the surface of soil skeleton as the amount of different inter-particle interactions due to matric suctions (van der Waals, capillarity, tensile forces). The suction stress σ^s is expressed as follows:

$$\sigma^s(\psi) = S_e \cdot \psi \quad \psi \geq 0 \quad (3.1)$$

and the equation for effective stress is reformulated as:

$$\sigma' = \sigma - u_a + \sigma^s \quad \psi \geq 0 \quad (3.2)$$

where S_e is the effective water content, s is the suction (positive by convention), σ' and σ are effective and total stresses respectively, and u_a is the atmospheric air pressure.

A closed-form expression for suction stress (σ^s) has been experimentally validated representing S_e with the sigmoidal retention function of van Genuchten (1980) (Lu et al. 2010). In the following section the suction stress theory has been contextualized into a bimodal hydraulic response framework and a bimodal unsaturated σ^s has been validated.

3.2 BIMODAL UNSATURATED SUCTION STRESS EQUATION

As a model for BWRC the parametric function of Romano et al. (2011) is used:

$$S_e(\psi) = \frac{S - S_r}{1 - S_r} = \frac{w_{micro}}{2} \operatorname{erfc} \left[\frac{\ln(\psi/\psi_{micro})}{\sigma_{micro} \cdot \sqrt{2}} \right] + \frac{w_{macro}}{2} \operatorname{erfc} \left[\frac{\ln(\psi/\psi_{macro})}{\sigma_{macro} \cdot \sqrt{2}} \right] \quad (3.3)$$

S_e is the effective water content; w is a weighting factor ($0 \sim 1$), respectively for micro- and macrostructure; erfc is the complementary error function; s the matric suction, σ_{micro} , σ_{macro} and ψ_{micro} , ψ_{macro} are the soil water retention function shape parameters for the micro-structure and macro-structure components respectively. The equation (3.3) is composed of the superposition of two lognormal Gaussian distributions, each defined by three shape-parameters (Kosugi, 1994; Kosugi et al., 2002). The suction heads ψ_{micro} , ψ_{macro} ($\psi_{micro} > \psi_{macro} > 0$) are related to the median of the effective cylindrical pore-throat radius, r_m (Young-Laplace equation). Whereas σ_{micro} and σ_{macro} ($\sigma_{micro}, \sigma_{macro} > 0$) represent the widths of the r_m distribution (standard deviations of $\log-r_m$), consequently they define the width range of the suction head to which the structural components belongs. The σ_{micro} and σ_{macro} are “indicators” of the pore sizes and the tortuosity of the pore network. The ψ_{micro} and ψ_{macro} values control the position of the inflection points on the two limbs of the BWRC, whereas the σ_{micro} and σ_{macro} control the steepness of the curve limbs. The weight w represents the probability of the pore space being part of the soil micro-structural pore-throat domain. When soil behavior is essentially monomodal ($\psi_{micro}/\psi_{macro} \rightarrow 1$ or $\psi_{micro}/\psi_{macro} \gg 1$) the parameters lose their physical relevance; this aspect is intrinsically linked to the conceptualization of composite soil retention and to the impossibility of identifying a perfect range that is either

macro-structural or micro-structural for soil hydraulic behavior (Romano et al., 2011).

An expression of σ^s for soils with bimodal hydraulic properties is obtained by substituting equation (3.3) into (3.1):

$$\sigma^s(\gamma) = (w \cdot \gamma)_{micro} + (w \cdot \gamma)_{macro} \quad (3.4)$$

where:

$$\gamma_{micro}(\psi) = \frac{\psi}{2} \cdot \operatorname{erfc} \left[\frac{\ln(\psi/\psi_{micro})}{\sigma_{micro} \cdot \sqrt{2}} \right]$$

$$\gamma_{macro}(\psi) = \frac{\psi}{2} \cdot \operatorname{erfc} \left[\frac{\ln(\psi/\psi_{macro})}{\sigma_{macro} \cdot \sqrt{2}} \right]$$

$(w \cdot \gamma)_{micro}$ is the suction stress contribution related to the water volume connected by small pore sizes; the water in the domain of small pore sizes preferentially resides during the drainage and contributes marginally to the infiltration processes. It can therefore be inferred that smaller variability in the suction stress rate against water loading is attributable to the microstructure; diversely, the water volume fraction related to the $(w \cdot \gamma)_{macro}$ is characterized by high mobility being connected by large pore-size. Water preferentially resides in the large pore domain during imbibition processes (Xu et al., 2013); this leads to retain that in the macrostructure the strength contribution due to suction stress reacts more quickly to loads than in the microstructure.

3.3 VALIDATION

Similarly to the methodology proposed in Lu et al. (2010), an experimental validation of the equation (3.3) is carried out comparing the results (σ_H^s) with data extracted from mechanical testing (σ_M^s). The σ_H^s have been obtained by fitting retention data to bimodal lognormal functions; the hydraulic curve-fitting parameters (w , ψ_{micro} , ψ_{macro} and

3. Bimodality effects of the hydraulic properties on shear strength of unsaturated soils

σ_{micro} , σ_{macro}) univocally identify the results in terms of suction stress curves (σ^s_{H}). Therefore, in order to achieve the validation, soils for which retention and shear strength data are available in literature have been chosen carefully.

Table 3.1 Data used

Soil -type	Hydraulic (H)		Mechanical (M)		References
	Data points	Test	Data points	Test	
A sand	14	Automated apparatus	9	--	Song, 2014
B limestone agglomerates	15	--	8	DSS	Schubert, 1984
C ash	27	Transient inflow/outflow tests	61	DSS	Bilotta et al., 2005 Sorbino et al., 2012
D ashly silty sand	36	Minitensiometer And STCX	34	SCTX	Damiano et al., 2010 Greco et al., 2010
E low plasticity silty sand	7	Oedometer	7	DSS	Casini et al., 2011
F silty sand	18	Pressure-plate Extractor and temp cell	18	SCTX	Lee et al., 2005

To achieve an appreciable fitting of the hydraulic data a coupled approach, consisting of a traditional trial-and-error method and an inverse method, is implemented. To estimate the shape parameters by inverse analysis the optimization algorithm UCODE_2005 (Hill et al., 2007) has been used; the code performs inverse modeling, posed as a parameter-estimation problem, using non-linear regression that is solved by minimizing a weighted least-squares objective function using a modified Gauss-Newton method.

A first attempt to estimate the weighting factor (w) is made by visual inspection of the “matching point”; the matching point consists in the

pair of values, effective water content (S_e) and related suction head (ψ), that conceptually separates the wetting processes from microstructure to macrostructure domain (or vice versa drainage processes). It must be pointed out that the validity of the calibrated BWRCs may be restricted to only usable data (Chirico et al., 2007). The optimal parameters obtained with the abovementioned method are listed in table 2. In accordance with the previously fitted BWRCs, the curves in terms of σ_H^S have been obtained with equation (3.4).

A first attempt to estimate the weighting factor (w) is made by visual inspection of the “matching point”; the matching point consists in the pair of values, effective water content (S_e) and related suction head (ψ), that conceptually separates the wetting processes from microstructure to macrostructure domain (or vice versa drainage processes). It must be pointed out that the validity of the calibrated BWRCs may be restricted to only usable data (Chirico et al., 2007). The optimal parameters obtained with the abovementioned method are listed in table 2. In accordance with the previously fitted BWRCs, the curves in terms of σ_H^S have been obtained with equation (3.4).

Table 3.2 Optimal bWRC-fitting parameters

Soil-type	w	ψ_{micro} [kPa]	ψ_{micro} [kPa]	σ_{micro}	σ_{micro}	R^2
A	0.890	2.6	1.1	0.18	0.15	0.9978
B	0.257	8.5	2.5	0.80	0.30	0.9928
C	0.250	90	9.0	0.50	0.35	0.8896
D	0.430	1500	30	0.50	1.50	0.9499
E	0.510	298	4.0	0.80	1.50	0.9998
F	0.400	425	6.0	1.65	0.80	0.9993

Typically, shear strength tests are usually either direct shear stress (DSS) or triaxial tests (STCX) on unsaturated specimens where the suction can be controlled or measured by the apparatuses. For soil A (Song et al., 2014) and soil B (Schubert, 1984) the suction stress data are available, while for soils C-D-E-F the σ_M^s has been obtained from the shear strength measures.

The following equations are obtained for DSS (equation 3.5) and SCTX (equation 3.6) (after Lu et al 2010):

$$\tau_f = c' + [(\sigma_n - u_a) - \sigma_M^s] \cdot \tan\varphi' , \quad \sigma_M^s = \left| -\frac{\tau_f - c'}{\tan\varphi'} - (\sigma_n - u_a) \right| \quad (3.5)$$

$$q = M(p - u_a - \sigma_M^s) + C' , \quad \sigma_M^s = \left| \frac{q - C'}{M} - (p - u_a) \right| \quad (3.6)$$

where τ_f , c' and φ' are the failure shear strength, cohesion and friction angle respectively;

$$\sin\varphi' = \frac{3M}{6+M} \quad (3.7)$$

$$c' = \frac{3 - \sin\varphi'}{6\cos\varphi'} C' \quad (3.8)$$

$q = \sigma_1 - \sigma_3$ is the deviatoric stress and $p = (\sigma_1 + 2\sigma_3)/3$ is the mean total stress in triaxial conditions (axis-symmetry). The maximum total principal stress σ_1 and the minimum total principal stress σ_3 are related to τ_f and σ_n through the following equations:

$$\sigma_1 = \sigma_n + \tau_f \left(\frac{1 + \sin\varphi'}{\cos\varphi'} \right); \quad \sigma_3 = \sigma_n - \tau_f \left(\frac{1 - \sin\varphi'}{\cos\varphi'} \right) \quad (12.9)$$

For each pairing of soils investigated (A-B, C-D, E-F), the following panels of figures 1- 3, show: a) BWRCs fitted by the bimodal lognormal functions; b) comparison between model results (equation 3.4) and measurements for suction stress (σ_M^s) versus suction head; c) suction stress prediction versus S_e ; d) suction stress obtained by hydraulic approach (σ_H^s , equation 4) versus suction stress by mechanical approach (σ_M^s equations 5 - 6).

The following figures show: a) BWRCs fitted by the bimodal lognormal functions; b) comparison between model results (equation 3.4) and measurements for suction stress (σ_M^s) versus suction head ψ ; c) suction stress prediction versus effective water content Se ; d) suction stress obtained by hydraulic approach (σ_H^s , equation 3.4) versus suction stress by mechanical approach (σ_M^s equations 3.5 and 3.6).

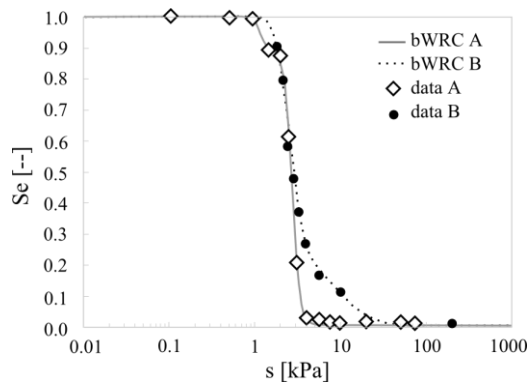


Figure 3.1 BWRC - soils A and B.

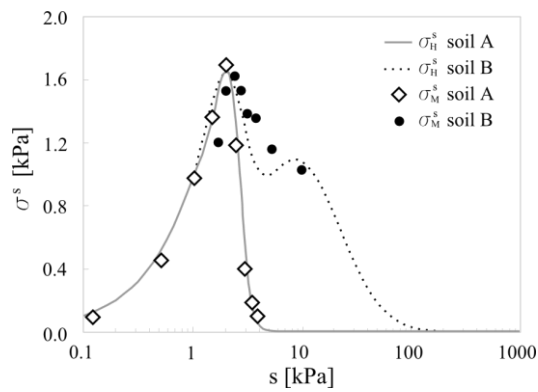


Figure 3.2 Comparison σ_H^s/ψ with σ_M^s - soils A and B.

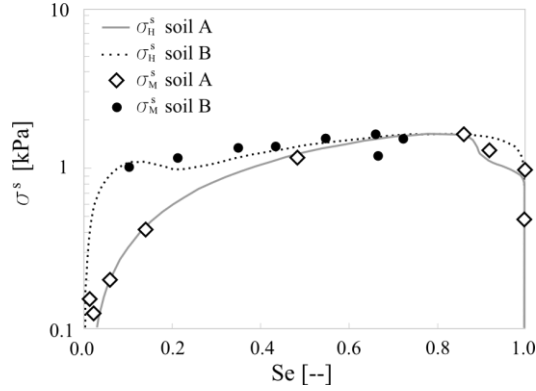


Figure 3.3 Comparison σ^s/Se with σ^s_M - soils A and B.

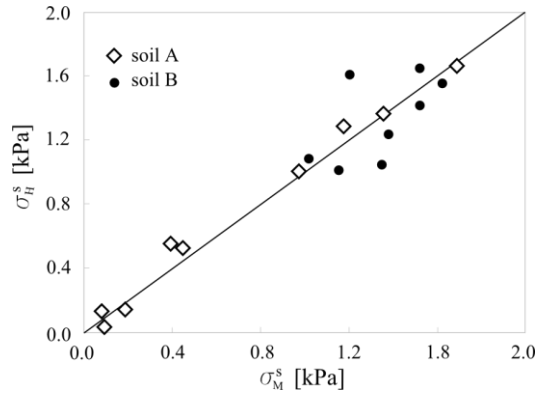


Figure 3.4 σ^s versus σ^s_M - soils A and B.

The equation proposed for the estimation of suction stress (equation 4) fits reasonably well to the experimental data. BWRCs for soils A (Song et al., 2014) and B (Schubert, 1984) (Figure 3.1) show no pronounced bimodal features, proving to be affected by a weak structuration. The effective water content change between 1 and 0 in a very low suction range (0.1 ~ 10 kPa; Figure 3.2 and Figure 3.3) is consistent with the soil physics (sand). In sand the water is retained essentially in the macrostructural domain characterized by low values of suction, the hydro-mechanical behavior of soils A and B appears to be controlled essentially by the macrostructure. The weighting factor w_{micro} in soil A (0.89) apparently reveals an unexpectedly significant role of the microstructure, while a gap from the unimodal state affects the BWRC close to saturation ($Se = 0.90 \sim 1.0$), conditioning the fitting. The “distortion”

assumed by the retention data at saturation may be due to the granular-type structure of loose sand that entails a dual porous-behavior within a domain typically definable as macro-structured. This apparent inconsistency can be explained as strictly due to the conceptualization of dual-structure problem. The degree of agreement between predicted and measured suction stress (Figure 3.2, Figure 3.3 and Figure 3.4) reflects the goodness of the fitted bimodal model.

Figure 3.5 show the results of two pyroclastic soils, soil C (Bilotta et al., 2005; Sorbino et al., 2012) and soil D (Damiano et al., 2010; Greco et al., 2010), originating from explosive activities of the Somma-Vesuvius volcano (Italy). The BWRCs (Figure 3.5) confirm the hydraulic properties of pyroclastic soils as coarse-grained type, with low air-entry value and complete drying at approximately 100 kPa of suction (Sorbino et al., 2012). Relating to soil C the amplitude of the envelope of the water retention data point can be considered a consequence of both soil variability and hydraulic hysteresis (Sorbino & Nicotera 2012); the fitted curve spans a wider suction head range (0 ~ 1000 kPa) because composed of soil fractions ranging from coarse- (sand) to fine-grained domains (silt) (Sorbino & Foresta, 2002). The presence of a fine component translates into a fitted w_{micro} of about 0.43, which statistically confirms a significant contribution of the microstructure within the suction head range of 120 ~ 1500 kPa. This also reflects upon the high values of σ_H^s (≈ 250 kPa, Figure 3.6), consistently with the functional view of suction stress theory that the magnitude of the effective water content represents the share of suction that effectively contributes to the shear strength of soils. The extrapolation of the σ_M^s has been carried out based on DSS data (using equation 4) obtained for different net vertical stresses (σ_n): 10, 20, 40, 50, 80 and 100 kPa; the variance between model and measurements is, on average, the same and appears not to be strongly influenced by the net vertical stress. Generally, the agreement with the measurements is better within the macrostructural dominium.

Soil D manifests strong bimodal features (Figure 3.5) and a significant macrostructural contribution ($w_{macro} \approx 0.75$); both micro- and macrostructure curve components are very steep, confirming typical coarse-type hydraulic behavior of the soil (large increase in S_e for small changes in suction). Shear strengths are measured with SCTX tests (Olivares & Picarelli, 2003) and reduced through equation (3.5) to σ_M^s .

The σ_H^s clearly reflects the bimodality of the hydraulic properties (dotted line in Figure 3.6 and Figure 3.7). The matching between experimental-based data and the model is consistent with the fitted BWRC; slight underestimates of σ_H^s versus higher σ_M^s (Figure 3.8) are attributable to the different mean net stress (from 20 to 200 kPa) in the SCTX tests: in fact, the effects of compaction on hydraulic behavior could be appreciable, particularly in strong coarse-grained soils, and there could be no unique BWRC.

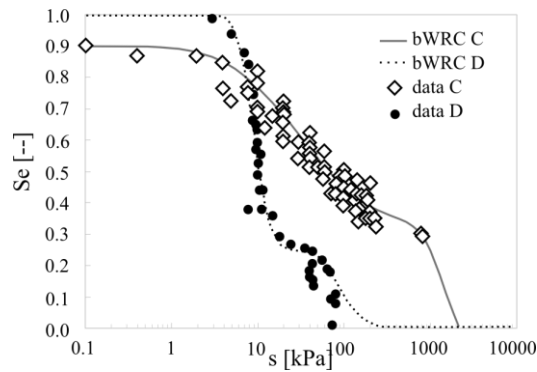


Figure 3.5 BWRC - soils C and D.

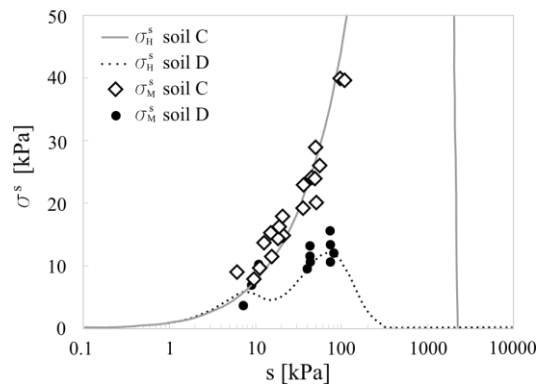


Figure 3.6 Comparison σ_H^s/ψ with σ_M^s - soils C and D.

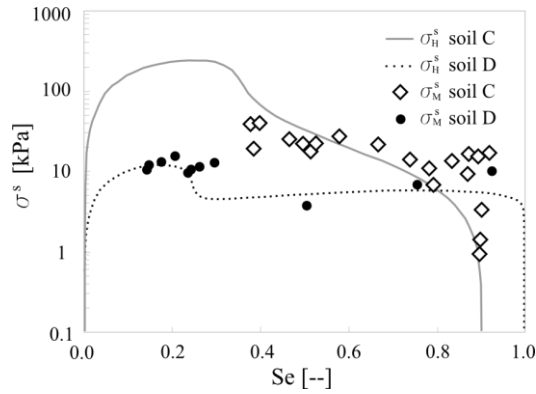


Figure 3.7 Comparison σ^s_H/Se with σ^s_M - soils C and D.

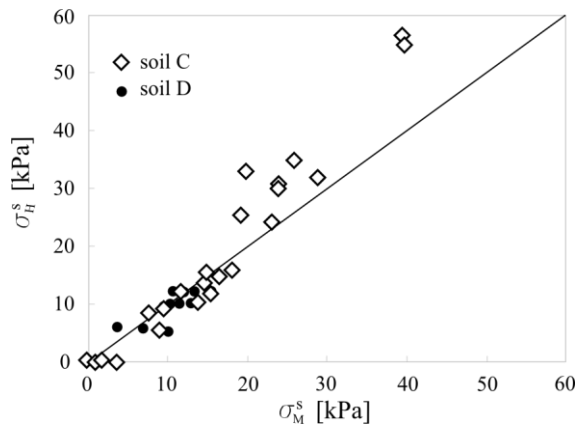


Figure 3.8 σ^s versus σ^s_M - soils C and D.

The fitting of data for the Ruedlingen silty sand (soil E, Casini et al 2011) is reported in Figure 3.9. The shear strength has been obtained with a direct shear box under constant volume of water. The soil has been compacted at dry part of the optimum water content under different compaction water content then compressed to the target vertical stress. As a first approximation, neglecting the hysteresis of the water retention curve, the main drying was chosen to obtain the suction known as the compaction water content. A bimodal retention function was chosen because the soil was compacted on the “dry part” of the Proctor curve, which usually leads to a bimodal distribution of voids. This assumption is also supported by Mercury Intrusion Porosimetry (MIP) tests performed by Colombo (2009). The optimal fitting of the BWRC leads

to a w_{macro} of about 0.51 (Figure 3.9). The available σ^s_M data exclusively concern the macrostructural domain and are reasonably well fitted by the model.

Similarly to the pyroclastic soil C, soil F has characteristics of a silty sand (Lee et al., 2005); the hydraulic behavior (Figure 3.9) is evidently affected by a fine-grained contribution spanning a wide suction head range (0 ~ 1000 kPa). The position of the matching point is given by 0.41 in Se and is ≈ 20 kPa in the suction head; the role of the dominium structures appears to be reasonably equivalent. Comparison between results and measurement show a gradual overestimation of the model toward the microstructure and an apparent sensitivity to variation in net normal stress (0, 100, 200, and 300 kPa).

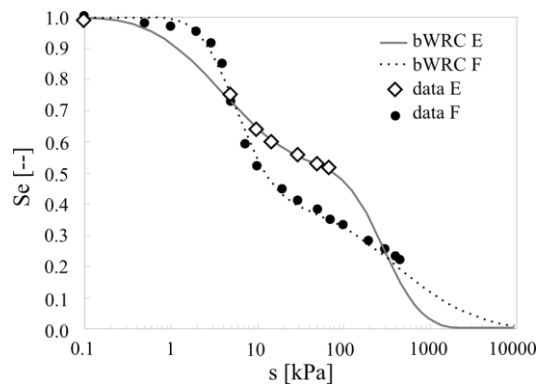


Figure 3.9 BWRC - soils E and F.

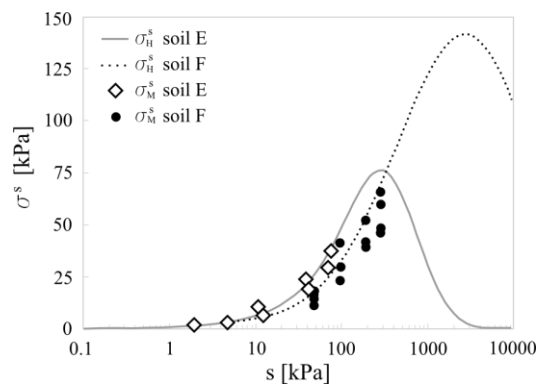


Figure 3.10 Comparison σ^s_H/ψ with σ^s_M - soils E and F.

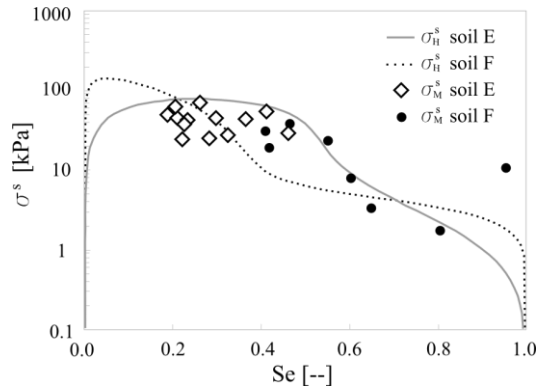


Figure 3.11 Comparison σ^s_H/Se with σ^s_M - soils E and F..

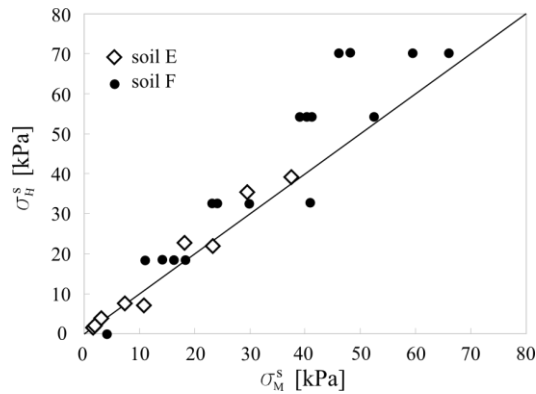


Figure 3.12 σ^s_H versus σ^s_M - soils E and F.

3.4 NUMERICAL MAXIMA EXPLORATION AND SENSITIVITY ANALYSIS

In order to clarify the influence of the shape parameters on the function (3.4) a coupled study of function maxima and sensitivity analysis is presented. The maxima of equation (3.4) cannot be expressed in closed-form and, therefore, the problem has been solved numerically. To separately investigate the influences that originate from variations of the related shape parameters on the maxima of suction stress, normalized forms of equation (3.4) with respect to macro- and microstructural components have been obtained, reducing the suction head ($\psi^* = \psi / \psi_{\text{macro}}$

3. Bimodality effects of the hydraulic properties on shear strength of unsaturated soils

relatively to macro-, and $\psi^* = \psi / \psi_{\text{micro}}$ for micro-structure) and introducing the ratios $I = \psi_{\text{micro}} / \psi_{\text{macro}}$ and $J = \sigma_{\text{micro}} / \sigma_{\text{macro}}$.

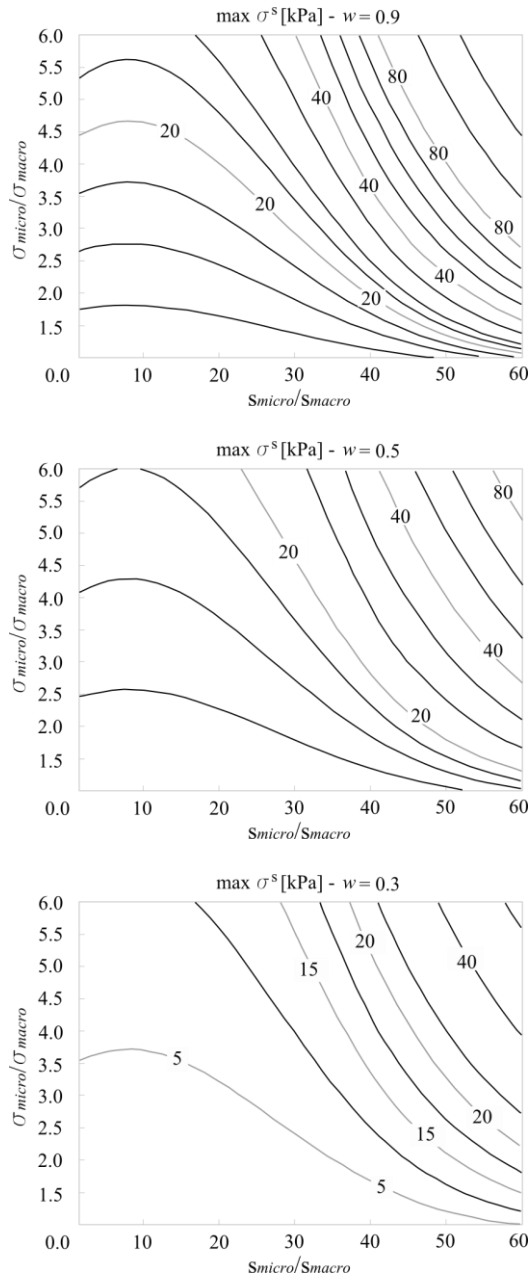


Figure 3.13 . Numerical exploration of maximum suction stress

Generally, the results indicate that variations in macrostructural parameters do not significantly contribute in defining the maxima values; diversely, the microstructure weighs on the maxima. The Figure 3.13 shows iso-lines of suction stress maxima on the plane as defined by the abovementioned ratios for different values of the weighting factor (w); the results are related to the normalized expression of the equation related to macrostructural component.

It is not possible to trace a general trend for the maxima iso-lines because the expression depends on the normalizing values. An increasing of the maxima has been found for $I \gg 3.5$ and $J \gg 30$, independently by the value assumed by w ; decreasing the weighting factor w (i.e. increasing the macro-structural contribution) does not affect the shape of the curves but does produce a general lowering of the maxima; this confirms that, by moving towards the prevailing macrostructural conditions, the effect of variations in parameters on the maxima values is reduced. It also indicates that the microstructure plays a dominant role on shear strength generation.

A parametric sensitivity of equation (3.4) is quantified in the form of a relative sensitivity coefficient (RSC). The RSC is useful when calculating the absolute change in the model result due to a known change in a single shape parameter; RSC consists of the ratio between the model result and the relative parameter variation.

The parametric sensitivity analysis is performed computing a relative sensitivity coefficient (RSC) that consists of the ratio between the model result, in this case the σ^s , and the relative parameter variation (δvar). The general form of the RSC is the following:

$$\Theta(\sigma^s(var)) = \frac{[\delta\sigma^s(var)]/(\sigma^s(var))}{\delta var/var} \quad (3.10)$$

The following equations are the analytical expressions of equation 3.4 with respect to the σ^s and, respectively, the parameters ψ_{micro} , ψ_{macro} , σ_{micro} and σ_{macro} :

$$\Theta(\sigma^s(\psi_{micro})) = \frac{w_{micro} \sqrt{2} e^{\theta_{micro}}}{S_e \sqrt{\pi} \sigma_{micro}} \quad (3.11)$$

$$\Theta(\sigma^s(\psi_{macro})) = \frac{w_{macro} \sqrt{2} e^{\theta_{macro}}}{S_e \sqrt{\pi} \sigma_{macro}} \quad (3.12)$$

$$\Theta[\sigma^s(\sigma_{micro})] = \frac{w_{micro} \sqrt{2} e^{\theta_{micro}} \ln\left(\frac{\psi}{\psi_{micro}}\right)}{S_e \sqrt{\pi} \sigma_{micro}} \quad (3.13)$$

$$\Theta[\sigma^s(\sigma_{macro})] = \frac{w_{macro} \sqrt{2} e^{\theta_{macro}} \ln\left(\frac{\psi}{\psi_{macro}}\right)}{S_e \sqrt{\pi} \sigma_{macro}} \quad (3.14)$$

with:

$$\theta_{micro} = -\frac{1}{2} \left[\frac{\ln\left(\frac{\psi}{\psi_{micro}}\right)}{\sigma_{micro}} \right]^2 ; \theta_{macro} = -\frac{1}{2} \left[\frac{\ln\left(\frac{\psi}{\psi_{macro}}\right)}{\sigma_{macro}} \right]^2$$

Figure 3.13 and Figure 3.14 show a comparison between RSC values with respect to macrostructural shape parameters obtained for three different degrees of bimodality (Table 3.3):

Table 3.3 Idealized bWRC parameters

	w	I	J
Strong	0.3	2.6	60
Moderate	0.5	8.5	15
weak	0.9	90	6

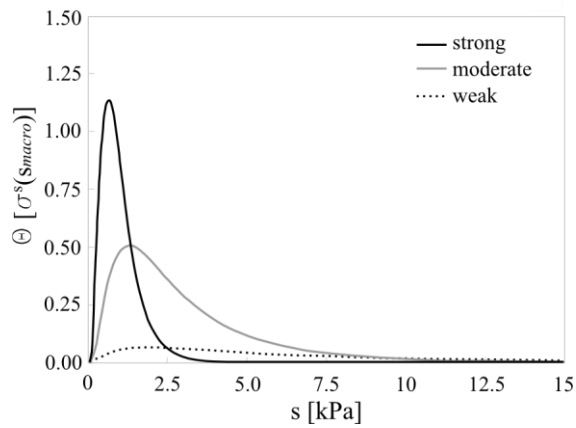


Figure 3.14 RCS versus suction head respect to ψ_{macro} .

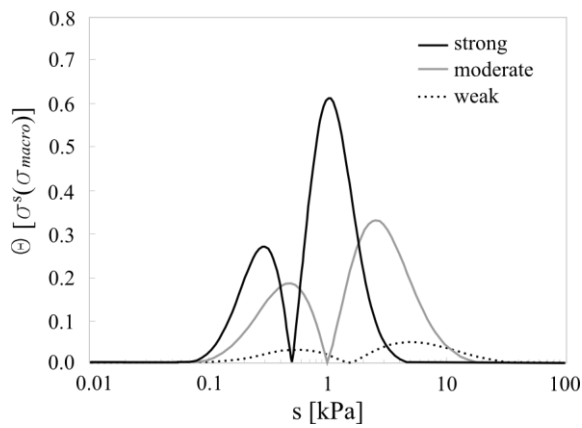


Figure 3.15 RCS versus suction head respect to σ_{macro} .

The RSC highlights the physical meaning of the shape parameters: consistent with the theory, in BWRC characterized by strong bimodality, the role of the macrostructure becomes evident at low suction values (0.1 to 3.0 kPa) close to the saturation. The RSC related to σ_{macro} tends to 0 as the suction head approaches the ψ_{macro} value due to the presence of the logarithm of $\psi / \psi_{\text{macro}}$. Conversely, for poor-structured soils (weak bimodality), the macrostructural parameters lose incidence and the “peak” of the RSC shifts toward higher suction heads; the RSC is practically null when the retention curve approaches a unimodal shape.

3.5 FINAL REMARKS

Natural soils can be seen as an assemblage of particles and aggregation (or simply widely-graded soils) having sizes that mainly depends on the grain size distribution, the mineralogy, the void ratio and the water content. This structural complexity affects the hydro-mechanical behavior of natural soils, which can be properly described with the bimodal equation. An analytical method has been developed to analyze the effects of bimodal hydraulic properties on the shear stress exhibited by different type of soils in literature. The bimodal lognormal model developed by Romano et al. (2011) has been integrated into the suction stress framework of Lu and Likos (2004, 2006) and a new closed-form expression for suction stress has been proposed and validated. The chosen bimodal lognormal model is firmly grounded on physical principles, it use the particle size distribution to describe the soil hydraulic behavior, thus overcoming the limits of the classic empirical functions.

The suction stress of micro- and macrostructures obtained from water retention data has been compared to that obtained by mechanical experimental results on different soils such as sand with gravel or silt and volcanic ash soils.

The bimodal lognormal function adopted fits quite well to the data over the range of suction investigated. The model developed gives an accurate description of water retention behavior at quasi-saturation dominium, dominated by the macrostructure, and over a range of suction up to 1000 kPa, dominated by microstructure. A discrepancy between the model adopted and the experimental data has been observed for

3. Bimodality effects of the hydraulic properties on shear strength of unsaturated soils

materials with higher fine content. This should be due to the dependency of the BWRC on the void ratio, which has been neglected as a first approximation, and to the value of suction acting on the shear band, which should be different from that imposed at the boundary of the sample.

Further investigation must be done to take into account the evolution of the water retention curve with mechanical loading and to take into account the coupled hydro-mechanical features typical of unsaturated soils, such as collapse from saturation or the swelling nature of soils.

4 MODELING TRANSIENT WATER AND SLOPE STABILITY IN DUAL-STRUCTURE SOILS

Most analytic models commonly used for landslide hazard assessment assume that the position of the failure surface is beneath the water table. The assertion that the shallow landslides commonly are triggered under saturated rather than unsaturated conditions is quite controversial (essentially due to the scarcity of survey measurements on the hydrologic conditions in natural setting); several authors indicated that shallow failures may occur within the vadose zone under unsaturated terrain conditions (e.g., Wolle and Hachich, 1989; de Campos et al., 1991; Lu and Godt, 2008; Godt et al., 2009) and that the stability analyses considering saturated conditions are often physically inconsistent.

The method prediction of stress conditions leading to landslides is largely based on Terzaghi's effective stress principle for saturated soils. However, this approach may not be adequate for assessing the stress state of slope and for describing the failure processes under variable saturated conditions "*since it neglects the cohesive forces present in wet, but not saturated, soils and granular materials*" (Godt et al., 2009).

To the need to use more appropriate mathematical expressions for describing hydro-mechanical soil processes, a second problem relates to the need of considering the effects induced by soil heterogeneities on the physical mechanisms. In fact, an actual significant problem for modelers is to having to take into account the implications of the heterogeneities in affecting time-dependent hydro-mechanical variables. Natural terrains generally exhibit heterogeneities. The presence of the heterogeneities in partially-saturated slopes results in irregular propagation of the moisture and suction front. A large class of heterogeneous natural soils can be well-described by double dual-structure models. To mathematically represent the dual (-structure) implications in describing the hydraulic soil behavior several bimodal hydraulic functions have been presented in literature (Othmer et al., 1991; Durner, 1992, 1994; Wilson et al., 1992; Ross and Smettem, 1993; Romano et al., 2011) and replaced the

conventional sigmoidal/unimodal functions (e.g. van Genuchten). About these some details have been introduced in Paragraph 2.2.3.

In this work the infiltration is strictly modeled by Darcy's law. In other words the scale of the macropores that characterize the macro-structure domain of the soil is assumed comparable with the local scale (Darcy scale), thus the Richards' model can be assumed adequate to mathematically reproduce the processes. To achieve the above mentioned objectives a novel numerical code written in JAVA™ language and developed in Eclipse IDE environment is presented (Ri.D1). In R1.D1 code, a one-dimensional vertical transient water flow has been simulated by numerically solving the Richards' equation. Several hydraulic constitutive models can be selected. In this work the simulations have been performed by means of the widespread used van Genuchten–Mualem's model (unimodal), whereas to describe bimodal hydraulic behavior the Romano et al.'s functions are implemented.

4.1 INFILTRATION MODEL

The transient saturated/unsaturated flow of water in porous media is described by Richards equation:

$$C(\psi) \frac{\partial \psi}{\partial t} = \frac{\partial}{\partial z} \cdot \left[K(\psi) \cdot \frac{\partial \psi}{\partial z} - K(\psi) \right] \quad (4.1)$$

where $C(\psi)$ is the soil water capacity (describes the available storage in partially-saturated soil), t denotes the time, z is the vertical coordinate being positive upward, K is the hydraulic conductivity, and ψ is the pressure head. To solve the equation (4.1), the water content $\theta(\psi)$ and the hydraulic conductivity $K(\psi)$ (or equivalently $K(\theta)$) need to be a priori specified by prescribing their constitutive relationships. The Richards' equation describes the movement of water in unsaturated, isothermal, rigid soils, with the air pressure everywhere and always at atmospheric pressure.

4.1.1 Unimodal and bimodal hydraulic functions

For the unimodal model Ri.D1 implements the well-known function of van Genuchten (1980) to describe the water retention characteristic:

$$S_e(\psi) = \frac{\theta - \theta_r}{\theta_s - \theta_r} = \left[\frac{1}{1 + (\alpha \cdot \psi)^n} \right]^m \quad (4.2)$$

Where S_e is the effective saturation, θ_s and θ_r denote the saturated and the residual volumetric water content, respectively, and α , n and m are shape parameters for the water retention characteristic. The parameter m is given by $m=1-1/n$. This constraint allows a closed-form prediction of the unsaturated hydraulic conductivity function using the model of Mualem (1976):

$$K(S_e) = K_s \cdot S_e^\tau \cdot \left[(1 - S_e^{1/m})^m \right]^2 \quad (4.3)$$

where K is the hydraulic conductivity, K_s is the hydraulic conductivity in saturated conditions and τ [dimensionless] is a factor to account for eccentricity of the flow path (tortuosity factor).

For the bimodal model Ri.D1 implements Romano et al.'s functions (2011). Romano et al. (2011) proposed a bimodal lognormal model by using Kosugi-type Gaussian probability distribution functions (Kosugi, 1994) linking the structure domains through weighting factors that represent the probability of the pore space being part of either the micro- or the macro-structural domain. Romano et al. (2011) developed the following bimodal lognormal water retention function (bWRF):

$$S_e(\psi) = \frac{S - S_r}{1 - S_r} = \frac{w_{micro}}{2} \operatorname{erfc} \left[\frac{\ln(\psi/\psi_{micro})}{\sigma_{micro} \cdot \sqrt{2}} \right] + \frac{w_{macro}}{2} \operatorname{erfc} \left[\frac{\ln(\psi/\psi_{macro})}{\sigma_{macro} \cdot \sqrt{2}} \right] \quad (4.4)$$

S_e is the effective water content; w is a weighting factor ($0 \sim 1$), respectively for micro- and macrostructure; erfc is the complementary error function; s the matric suction, σ_{micro} , σ_{macro} and ψ_{micro} , ψ_{macro} are the soil water retention function shape parameters for the micro-structure and macro-structure components respectively. The equation (4.4) is

composed of the superposition of two lognormal Gaussian distributions, each defined by three shape-parameters (Kosugi, 1994; Kosugi et al., 2002). The suction heads ψ_{micro} , ψ_{macro} ($\psi_{micro} > \psi_{macro} > 0$) are related to the median of the effective cylindrical pore-throat radius, r_m (Young-Laplace equation). Whereas σ_{micro} and σ_{macro} ($\sigma_{micro}, \sigma_{macro} > 0$) represent the widths of the r_m distribution (standard deviations of $\log-r_m$), consequently they define the width range of the suction head to which the structural components belongs. The σ_{micro} and σ_{macro} are “indicators” of the pore sizes and the tortuosity of the pore network. The ψ_{micro} and ψ_{macro} values control the position of the inflection points on the two limbs of the BWRC, whereas the σ_{micro} and σ_{macro} control the steepness of the curve limbs. The weight w represents the probability of the pore space being part of the soil micro-structural pore-throat domain.

Inserting the equation (4.4) into Mualem’s model framework with $K_0=K_s$ under, the following analytical expression for the bimodal hydraulic conductivity function can be obtained (bHCF):

$$K(S_e) = K_s \cdot \frac{S_e^2}{4 \cdot (a + b)^2} \cdot [a \cdot \operatorname{erfc}(\alpha) + b \cdot \operatorname{erfc}(\beta)]^2 \quad (4.5)$$

where:

$$\begin{cases} \alpha = \frac{\sigma_{micro}}{\sqrt{2}} + \frac{\ln(\psi/\psi_{micro})}{\sigma_{micro} \cdot \sqrt{2}} \\ \beta = \frac{\sigma_{macro}}{\sqrt{2}} + \frac{\ln(\psi/\psi_{macro})}{\sigma_{macro} \cdot \sqrt{2}} \end{cases}$$

and

$$\begin{cases} a = \frac{w_{micro}}{\psi_{micro}} \exp\left(\frac{\sigma_{micro}^2}{2}\right) \\ b = \frac{w_{macro}}{\psi_{macro}} \exp\left(\frac{\sigma_{macro}^2}{2}\right) \end{cases}$$

4.2 INFINITE SLOPE STABILITY MODEL

When the failure surfaces are shallow and parallel to the slope surface, stress concentration is usually ignored and one-dimensional limit-equilibrium model called the *infinite-slope stability model* is generally used (Lu and Godt, 2013). To quantitatively assess the stability of a slope, a parameter known as “Factor of Safety” (FoS) is introduced. The FoS is the ratio between the resistive forces and gravity force pull. The transition between stability to failure is usually considered mathematically as a decrease in the FoS to values below unity along a failure surface.

4.2.1 “Saturated” and “unsaturated” approaches to assess FoS

A unified approach to analyzing the saturated stability under both hydrostatic and seepage conditions employs Terzaghi’s effective stress in place of total stress for both normal stress and shear strength.

For effective stress conditions a different set of material properties for cohesion (drained c') and friction angle (drained φ') are appropriate to well-describe the strength behavior under saturated conditions. The FoS for a one-dimensional infinite slope under saturated conditions as a function of vertical depth Z can be expressed by the following equation:

$$FoS(Z, t) = \frac{\tan\varphi'}{\tan\alpha} + \frac{2 \cdot c'}{\gamma_s \cdot Z \cdot \sin 2\alpha} - \frac{\psi(Z, t)}{\gamma_s \cdot Z} \cdot (\tan\alpha + \cot\alpha) \cdot \tan\varphi' \quad (4.6)$$

where φ' is the internal frictional angle, c' is the cohesion, α is the slope angle and γ_s is the saturated soil unit weight. The negative sign of the third term indicates that an increase in pore-water pressure has a destabilizing effect on the slopes.

However shallow failures may occur within the vadose zone under unsaturated terrain conditions (e.g., Wolle and Hachich, 1989; de Campos et al., 1991; Godt et al., 2007) indicating that stability analyses assuming saturated conditions are often physically inconsistent and in some case completely invalid.

A generalized FoS equation for infinite-slope model under variably saturated soil conditions based on a Bishop’s modified/extension

effective stress principle (i.e. the suction stress theory of Lu and Likos (2006)) is proposed by Lu and Godt (2008):

$$FoS(Z, t) = \frac{\tan\varphi'(Z)}{\tan\alpha} + \frac{2 \cdot c'}{\gamma(Z, t) \cdot Z \cdot \sin 2\alpha} - \frac{\sigma^s(Z, t)}{\gamma(Z, t) \cdot Z} \cdot (\tan\alpha + \cot\alpha) \cdot \tan\varphi' \quad (4.7)$$

where σ^s is the suction stress; γ and φ' are the water-content dependent soil unit weight and soil-depth dependent friction, respectively, and they can be described by the following expressions:

$$\begin{cases} \gamma = \gamma_w \cdot \frac{G_s + e \cdot S_e}{1 + e} \\ \varphi' = \varphi'_0 + \frac{\Delta\varphi'}{1 + \frac{Z_w}{Z}} \end{cases}$$

where G_s is the specific gravity, γ_w is the weight of the water and e is the void ratio. φ'_0 and $\Delta\varphi'$ are the friction angle at ground surface and the range of variation in friction angle respectively; Z_w is the generic depth and Z is the slope thickness. In the context of analysis of potential effects induced by bimodal hydraulic behavior on slope stability analysis, in this work the suction stress term will be expressed with positive sign as follow (Chapter 3):

$$\sigma^s(\gamma) = (w \cdot \gamma)_{micro} + (w \cdot \gamma)_{macro} \quad (4.8)$$

where:

$$\gamma_{micro}(\psi) = \frac{\psi}{2} \cdot erfc \left[\frac{\ln(\psi/\psi_{micro})}{\sigma_{micro} \cdot \sqrt{2}} \right]$$

$$\gamma_{macro}(\psi) = \frac{\psi}{2} \cdot \operatorname{erfc} \left[\frac{\ln(\psi / \psi_{macro})}{\sigma_{macro} \cdot \sqrt{2}} \right]$$

where w , σ_{micro} , σ_{macro} , ψ_{micro} and ψ_{macro} are the shape parameters of the bimodal hydraulic functions of Romano et al. (2011).

4.3 NUMERICAL IMPLEMENTATION

Equation (4.1) is known as the *mixed form* of Richards' equation. Its peculiarity is that can be expressed either in terms of θ or in terms of ψ . The significant advantage of the θ -based expression is that it can be solved perfectly by mass conservative methods. This form, however, can degenerate under fully saturated conditions. The ψ -based form allows for both unsaturated and saturated conditions, but in highly nonlinear cases, however, it can suffer from large mass balance errors (Casulli et al., 2010).

Similarly to that adopted in HYDRUS-1D model (Simunek et al., 1998), a mass-lumped linear finite elements scheme was used for discretization of equation (5.1). Since the mass-lumped scheme results in an equivalent standard implicit, backward, finite difference scheme (Vogel et al., 1996):

$$\begin{aligned} \frac{\theta_i^{j+1,k+1} - \theta_i^j}{\Delta t} = & \\ = \frac{1}{\Delta x} \cdot & \left(K_{i+\frac{1}{2}}^{j+1,k} \cdot \frac{\psi_{i+1}^{j+1,k+1} - \psi_i^{j+1,k+1}}{\Delta x_i} - K_{i-\frac{1}{2}}^{j+1,k} \cdot \frac{\psi_i^{j+1,k+1} - \psi_{i-1}^{j+1,k+1}}{\Delta x_{i-1}} \right) + \\ & + \frac{K_{i+1/2}^{j+1,k} - K_{i-1/2}^{j+1,k}}{\Delta x} \end{aligned} \quad (4.9)$$

where

$$\Delta t = t^j - t^{j+1}$$

$$\Delta x = \frac{x_{i+1} - x_{i-1}}{2}, \quad \Delta x_i = x_{i+1} - x_i, \quad \Delta x_{i-1} = x_i - x_{i-1}$$

$$K_{i+1/2}^{j+1,k} = \frac{K_{i+1}^{j+1,k} - K_i^{j+1,k}}{\Delta x}, \quad K_{i-1/2}^{j+1,k} = \frac{K_i^{j+1,k} - K_{i-1}^{j+1,k}}{\Delta x}$$

$i-1$, i , and $i+1$ indicate the position in the finite difference mesh; superscripts k and $k+1$ indicate the previous and current iteration levels, respectively; superscripts j and $j+1$ represent the previous and current time levels, respectively.

$K_{i+1/2}^{j+1,k}$ represents the “interblock” hydraulic conductivities. Equation (5.9) is based on a fully implicit discretization of the time derivative; in order to solve the large system of algebraic equations an iterative solution scheme, Picard-type scheme, is implemented and the linearization approach proposed by Celia et al. (1990) is used. Similarly to the θ - and ψ -based algorithms, the “modified Picard” of Celia et al. (1990) is based on a fully implicit (backward Euler) time approximation of equation (4.9). However, instead of directly solving the discretized equation, the water content at the new time step and iteration level ($\theta_i^{j+1,k+1}$) of equation (4.9) is replaced with a truncated Taylor series expansion with respect to ψ about the expansion point ($\theta_i^{j+1,k}$), thus:

$$\theta_i^{j+1,k+1} = \theta_i^{j+1,k} + \left(\frac{d\theta}{d\psi}\right)^{j+1,k} (\psi_i^{j+1,k+1} - \psi_i^{j+1,k}) + O[(\delta^k)^2] \quad (4.10)$$

where

$$\delta^k = \theta_i^{j+1,k+1} - \theta_i^{j+1,k}$$

is the difference between the solved pressure heads at the j and $j + 1$ iteration levels. Neglecting the higher-order terms in (4.10) and substituting this equation into (4.9), omitting the detailed development, gives the following expression:

$$\begin{aligned}
 \left(\frac{1}{\Delta t} C_i^{j+1,k}\right) \delta_i^{j+1,k} + \frac{\theta_i^{j+1,k+1} - \theta_i^j}{\Delta t} &= \frac{K_{i-1/2}^{j+1,k}}{\Delta Z^2} (\psi_{i-1}^{j+1,k+1} - \psi_i^{j+1,k+1}) + \\
 &+ \frac{K_{i-1/2}^{j+1,k}}{\Delta Z^2} (\psi_{i-1}^{j+1,k+1} - \psi_i^{j+1,k+1}) \\
 &+ \frac{K_{i+1/2}^{j+1,k} - K_{i-1/2}^{j+1,k}}{\Delta Z}
 \end{aligned} \tag{4.11}$$

where $C_i^{j+1,k}$ represents the nodal value of the soil water capacity. Substituting in the above equation the increment of pressure head at two subsequent iteration level:

$$\delta_i^{j+1,k+1} = (\psi_i^{j+1,k+1} - \psi_i^{j+1,k}) \quad (j=i-1, i+1) \tag{4.12}$$

or

$$\delta_i^{j+1,k+1} = (\theta_i^{j+1,k+1} - \theta_i^{j+1,k}) \quad (j=i-1, i+1) \tag{4.13}$$

obtain:

$$\begin{aligned}
 C_i^{j+1,k} \frac{\delta_i^{j+1,k}}{\Delta t} + \frac{K_{i-1/2}^{j+1,k}}{\Delta Z^2} (\delta_{i-1}^{j+1,k} - \delta_i^{j+1,k+1}) + \frac{K_{i+1/2}^{j+1,k}}{\Delta Z^2} (\delta_{i-1}^{j+1,k} - \delta_i^{j+1,k+1}) &= \\
 = \frac{K_{i-1/2}^{j+1,k}}{\Delta Z^2} (\psi_{i-1}^{j+1,k} - \psi_i^{j+1,k}) + \frac{K_{i+1/2}^{j+1,k}}{\Delta Z^2} (\psi_{i-1}^{j+1,k} - \psi_i^{j+1,k}) +
 \end{aligned}$$

$$-\frac{K_{i+1/2}^{j+1,k} - K_{i-1/2}^{j+1,k}}{\Delta z} - \frac{\theta_i^{j+1,k} - \theta_i^j}{\Delta t} (\psi_{i-1}^{j+1,k} - \psi_i^{j+1,k}) = Q_i^{j+1,k} \quad (4.14)$$

The above equation can be rewritten in the following forms:

$$\left\{ \begin{array}{l} \alpha_i^{j+1,k} = \frac{K_{i-1/2}^{j+1,k}}{\Delta z^2}; \\ \beta_i^{j+1} = \frac{C_i^{j+1,k}}{\Delta t} + \frac{K_{i-1/2}^{j+1,k}}{\Delta z^2} + \frac{K_{i+1/2}^{j+1,k}}{\Delta z^2}; \\ \gamma_i^{j+1} = -\frac{K_{i+1/2}^{j+1,k}}{\Delta z^2}; \\ Q_i^{j+1,k} = \frac{K_{i-1/2}^{j+1,k}}{\Delta z^2} (\psi_{i-1}^{j+1,k} - \psi_i^{j+1,k}) + \frac{K_{i+1/2}^{j+1,k}}{\Delta z^2} (\psi_{i-1}^{j+1,k} - \psi_i^{j+1,k}) + \\ -\frac{K_{i+1/2}^{j+1,k} - K_{i-1/2}^{j+1,k}}{\Delta z} - \frac{\theta_i^{j+1,k} - \theta_i^j}{\Delta t} \end{array} \right.$$

Where the first three coefficients are the components of a symmetrical tridiagonal matrix $P_w^{j+1,k}$:

$$[P_w]^{j+1,k} \{\psi\}^{j+1,k+1} = \{Q\}^{j+1,k} \quad (4.15)$$

The matrix coefficients are dependent upon the prescribed boundary conditions. Dirichlet (first-type) boundary condition is applied at the top or bottom of the soil column, whereas Neumann (third-type) boundary condition at the bottom is specified.

For each iteration a system of linearized algebraic equations is first derived from (4.15), which, after incorporation of the boundary conditions, is solved using Gaussian elimination. This elimination

algorithm takes advantage of the tridiagonal and symmetric features of the coefficient matrix in (4.15). After the first time-step, the coefficients in (4.15) are recalculated by using this first solution, and the new equations are again solved. The iterative process continues until the convergence is obtained (i.e. until the change in value between two iterations becomes less than the value tolerance).

In order to obtain computationally faster performances, a preprocessing consisting in generating a data-set of hydraulic characteristic values from the specified set of hydraulic parameters (i.e. shape retention parameters, saturated hydraulic conductivity, residual and saturated volumetric water content) is programmed. By means a linear interpolation between the values of the above mentioned data-set the hydraulic properties are computed during the iterative solution process.

In case of bimodal simulations, for the bimodal retention relationship (equation 4.4) is not possible to find a closed-form inverse function; in this case the inverse function is evaluated by numerical integrating equation the equation using bisection method.

4.4 VALIDATION

Validation is achieved by comparing the results with other numerical solutions to Richards equation for idealized tests. Specifically, the tests are performed by comparing Ri.D1 with HYDRUS-1D model (Simůnek et al., 1998); the two numerical solvers are the same. The comparisons are performed basing on the sigmoidal hydraulic relationship of van Genuchten-Mualem model. Comparisons in term of suction and moisture obtained for an idealized test are depicted for a general time instant in the follow Figure 4.1. The comparing-based validation shows that the model is able to correctly solve the equation.

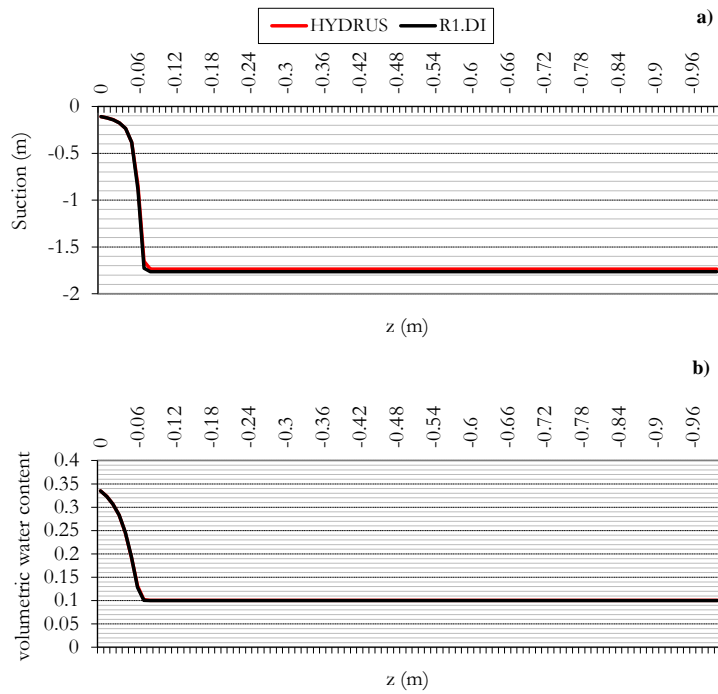


Figure 4.1 Comparisons in terms of suction (a) and volumetric water content (b)

5 COMPARING UNI- AND BIMODAL WATER INFILTRATION AND SLOPE STABILITY MODELING RESULTS

In this section the differences in the soil hydraulic response that result from using different hydraulic interpretative models (unimodal and bimodal hydraulic functions) are discussed. Moreover, discussions are carried out on the effects induced by “bimodal assumptions” on slope stability analysis. The purpose of this work is to focus on the differences in simulated flow infiltration and slope stability originate from a preliminary choice of definite hydraulic models and contextually between different, “saturated” and “unsaturated” approaches to evaluate the factor of safety (FoS).

To achieve the above mentioned objectives a novel numerical code (Ri.D1) have been developed. Description and details about R1.D1 model have been introduced in the previous chapter (Chapter 4). In R1.D1 a one-dimensional vertical transient water flow is simulated by numerically solving the Richards’ equation.

In this work the simulations are performed by means of the widespread used van Genuchten–Mualem’s model (unimodal), whereas to describe bimodal hydraulic behavior the Romano et al.’s functions are implemented (Chapter 4). A one-dimensional infinite slope model under saturated conditions has been compared with a generalized FoS equation under variably saturated soil conditions based on a Bishop’s modified/extension effective stress principle (i.e. Lu and Likos, 2006; Lu and Godt, 2008).

5.1 SIMULATION SCENARIOS

5.1.1 Soil properties

Data and soil characterization available in literature are carefully chosen. The simulations are carried for two different soil types that show evident bimodal features (chosen in literature): a) clay loam (Durner, 1994); ashy silty sand (Damiano et al., 2010; Greco et al., 2010).

The experimental retention data were fitted by the unimodal van Genuchten–Mualem model (equations 4.2 and 4.3) and by the bimodal Romano et al. model (equations 4.4 and 4.5) respectively. The best data fitting was obtained by means a nonlinear least-square optimization method application (Hill et al., 2007, UCODE); the algorithm, similarly to other optimization algorithms, use a modified Gauss-Newton method to adjust the value of user selected input parameters in an iterative procedure to minimize the value of the weighted least-squares objective function. A set of fitted shape parameters was obtained for each soils and for each model; the optimal fitting parameters are listed in the following tables (Table 5.1, Table 5.2):

Table 5.1 Optimal fitting parameters for soil 1 (Durner, 1994)

	Unimodal (R²=0.990)	Bimodal (R²=0.998)
θ_r [cm ³ cm ⁻³]	0.0	0.132
θ_s [cm ³ cm ⁻³]	0.439	0.473
α [mm ⁻¹]	0.00027	--
n	1.13	--
W_{micro}	--	0.88
ψ_{micro} [kPa]	--	880
ψ_{macro} [kPa]	--	0.28
σ_{micro}	--	2.4
σ_{macro}	--	0.4

Table 5.2 Optimal fitting parameters for soil 2

	Unimodal (R²=0.881)	Bimodal (R²=0.949)
θ_r [cm ³ cm ⁻³]	0.25	0.25
θ_s [cm ³ cm ⁻³]	0.69	0.69
α [mm ⁻¹]	0.0014	--
n	2.01	--

	Unimodal ($R^2=0.881$)	Bimodal ($R^2=0.949$)
W_{micro}	--	0.25
ψ_{micro} [kPa]	--	90
ψ_{macro} [kPa]	--	9.5
σ_{micro}	--	0.5
σ_{macro}	--	0.3

The water retention and hydraulic conductivity curves obtained for fitted values of the hydraulic parameters are shown for each investigated soil in the following Figure 5.1 and Figure 5.2.

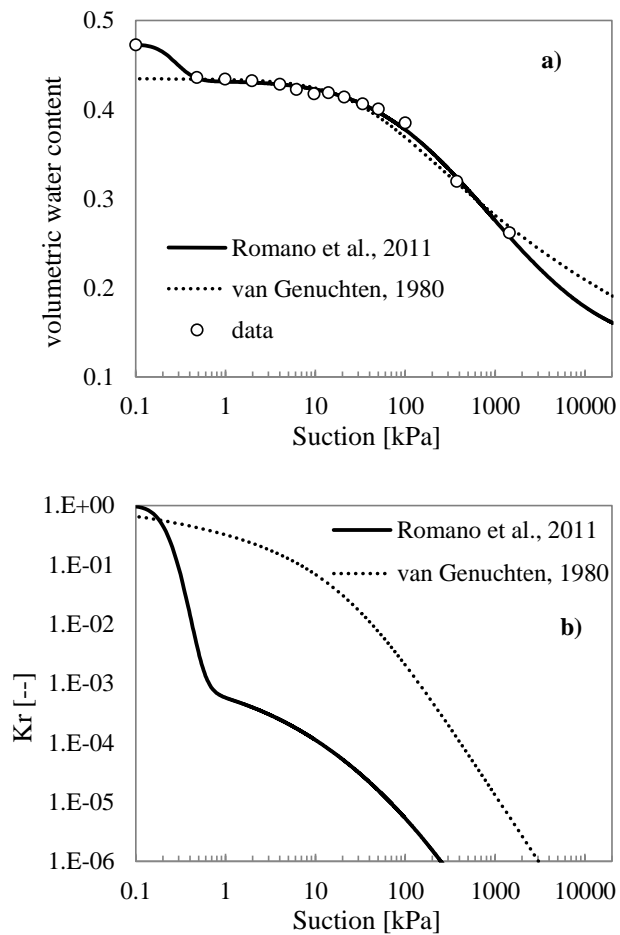


Figure 5.1 Unimodal and bimodal hydraulic functions of soil 1: a) water retention curve; b) relative hydraulic conductivity curves

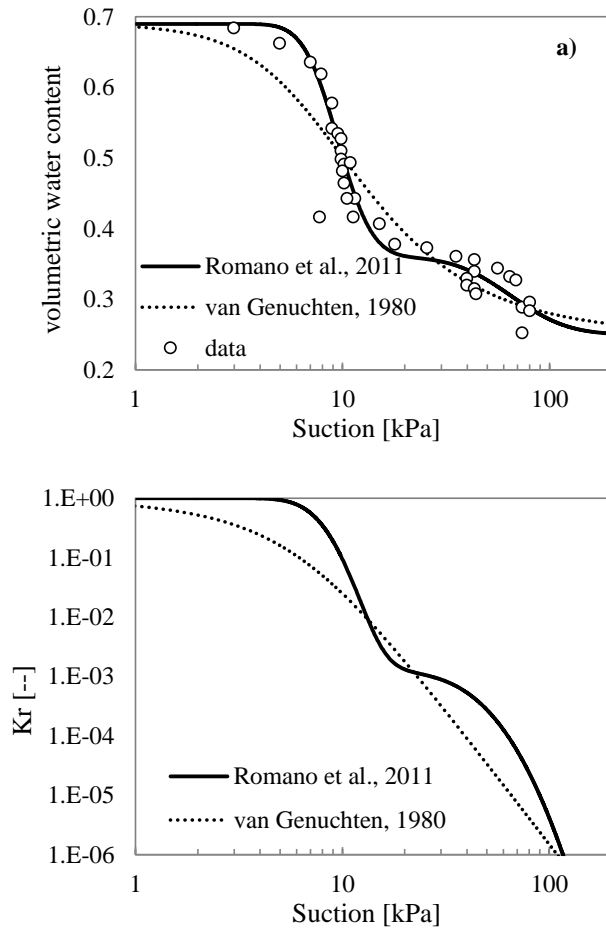


Figure 5.2 Unimodal and bimodal hydraulic functions of soil 2: a) water retention curve; b) relative hydraulic conductivity curves

The bimodal function provides a good fit of data; compared to the unimodal fit the bimodal functions describe the data of each soil more accurately. The retention data of soil 1 denotes a clear increasing in water content near saturation; this behavior is typical of structured soil with a secondary pore system in the large-pore range; when the curve flattens considerably indicate that the hydraulically active pore system consists of pores of more similar size (Durner, 1994).

The saturated hydraulic conductivity (K_s) is for each soil arbitrarily fixed at 100 mm day^{-1} .

From a preliminary comparison between unimodal and bimodal hydraulic functions the attempting to represent bimodal hydraulic behavior by means of simplified sigmoidal functions should lead to significant errors, especially if the fitting evaluations are applied to the conductivity measures.

The suctions stress characteristic curves (in terms of $\sigma^S-\psi$ and σ^S-S_e) are depicted in Figure 5.3 and Figure 5.4. For the clay loam soil (soil 1), the pattern of variation of suction stress shows some distinct characteristics related to that of sandy soil (soil 2). Suction stress is zero when matric suction is zero but increases monotonically as matric suction increases. The minimum suction stress for soil 1 is on the order of several hundreds of kilopascals in magnitude. Diversely, suction stress pattern of soil 2 clearly shows as the suction strength contribution (in sandy soils) for progressing toward dry conditions decreases.

The determination of the slope stability analysis parameters (i.e. slope surface and friction angle) is arbitrarily established. The cohesion is chosen null. The friction angle is assumed equal to the surface slope. Basing on this data setting the comparisons in terms of slope stability can be made exclusively on suction and suction stress strength contributions.

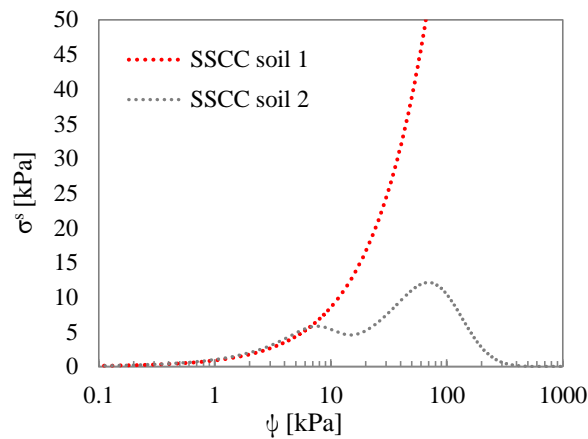


Figure 5.3 Suction stress characteristic curves $\sigma^S-\psi$

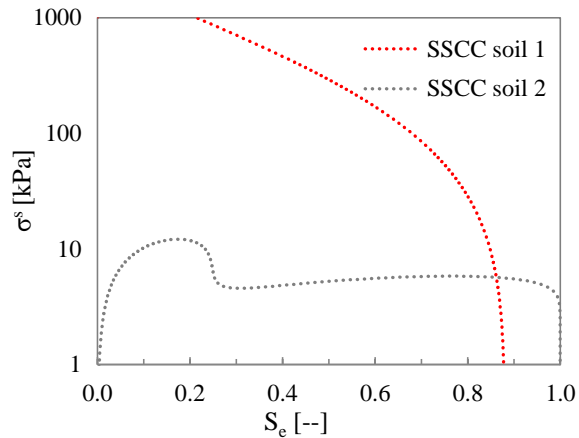


Figure 5.4 Suction stress characteristic curves σ^s - S_e

5.1.2 Rainfall scenarios

In order to investigate the effects induced by using different hydraulic interpretative models (unimodal and bimodal), numerical simulations of soil infiltration and slope stability are performed along 2 meters of homogenous soil column.

Soil 1 is undergone by three rainfall impulses similarly to the simulation performed by Zurmühl and Durner (1996). Diversely, for soil 2 the upper boundary condition is given by a steady rainfall. In all simulations the bottom boundary condition is a “no flow” condition (i.e. impermeable bed) and the initial condition is given by an hydrostatic profile in suction. Scenarios and conditions imposed for each investigated soil are listed in the following Table 5.3.

Table 5.3 Configuration performed simulations

Cod.		Upper boundary condition	Rainfall intensity	Bottom boundary condition
Id1	Soil 1	unsteady	5 cm/day	0 kPa
Id2	Soil 1	unsteady	5 cm/day	10 kPa
Id3	Soil 2	steady	2.5 cm/hour	0 kPa
Id4	Soil 2	steady	5.0 cm/hour	10 kPa
Id5	Soil 2	unsteady	20 cm/day	0 kPa

Unsteady rainfall input is given by three different duration-time impulse separated by two no-rainfall (evaporation intensity) intervals (Table 5.4):

Table 5.4 Unsteady rainfall

intervals		
no rainfall	$0 \leq t < 1$ days	1 st impulse
rainfall	$1.0 \leq t < 1.1$ days	
no rainfall	$1.1 \leq t < 1.2$ days	
evaporation	$1.2 \leq t < 2.0$ days	
rainfall	$2.0 \leq t < 2.2$ days	2 th impulse
no rainfall	$2.2 \leq t < 2.3$ days	
rainfall	$2.3 \leq t < 3.0$ days	
no rainfall	$3.0 \leq t < 4.0$ days	3 th impulse
evaporation	$4.0 \leq t < 4.1$ days	
rainfall	$4.0 \leq t < 10.0$ days	

The rainfall intensity for each impulse is constant.

5.2 RESULTS AND DISCUSSIONS

In this section, after a preliminary analyses about the differences revealed in the water moisture propagation and suction variation by comparing the results obtained from using unimodal and bimodal interpretative hydraulic models, the consequences obtained in terms of slope stability are discussed.

The comparisons here presented are:

- a. unimodal (UNI_s) and bimodal (BIM_s) suctions;
- b. unimodal (UNI_{wc}) and bimodal (BIM_{wc}) water contents;
- c. unimodal suction (UNI_s) and bimodal suction stress (BIM_{ss});
- d. unimodal “saturated” slope stability (SAT_{FOS}) and bimodal “unsaturated” slope stability ($UnSAT_{FOS}$).

UNI_s and BIM_{ss} represent the “strength contributions” to slope stability analyzed by SAT_{FOS} and $UnSAT_{FOS}$ respectively. The $UnSAT_{FOS}$ approach includes a generalized FoS equation for infinite-slope model under variably saturated soil conditions (Par. 5.2.1, Equation 4.6) and the bimodal Romano et al.’s functions to describe the hydraulic response (Par. 5.1.1, Equations 4.4 and 4.5). The SAT_{FOS} approach includes the

“conventional” expression of the factor of safety under saturated conditions (Par. 5.2.1, Equation 4.7) and the widespread used hydraulic model of van Genuchten-Mualem (Par. 5.1.1, Equations 4.2 and 4.3).

The simulations are set up in order to remark (and stress) some differences between the two adopted approaches. All the choices meet the need to explore a wide range of possibilities. For easier reading, the general definitions “unimodal model” and “bimodal model” will be replaced with acronyms UM and BM respectively.

5.2.1 Transient ψ and S_e profiles (Soil 1)

Id1 - Unsteady rainfall – bottom condition 0 kPa (Figure 5.5 and Figure 5.6)

Because of high unsaturated hydraulic conductivity of UM (related to the BM, see Figure 5.1b) the response of the soil to each rainfall-impulse appears clearly more pronounced than those of BM. Although the saturated hydraulic conductivity is the same, the profiles obtained by the BM exhibit a delay in propagating downward the infiltration front. The infiltration front of the BM is significantly sharp if compared with the front of the unimodal results and the first layers of the soil column are quickly saturated. There is no sharp infiltration front in the UM, even during and immediately after the rain events. During the entire imbibition processes a stationary flux is established by the BM through the upper layers of soil column; this occurs when the infiltration rate at the surface is greater than the unsaturated hydraulic conductivity, ponding or run off early occur and the saturation process “propagate” downward. During the time between two different rainfall-impulse (before the second impulse) the moisture content redistribution reflects in a gradual increasing of the suction head at top layers according with the hydraulic characteristic functions; in these time interval the behavior described by the UM exhibits the same strong sensitivity observed during the imbibition phases. Diversely, the infiltration front resulted by BM seems only slightly affected at the surface layer.

Id2 - Unsteady rainfall – bottom condition 10 kPa (Figure 5.7 and Figure 5.8)

Compared to the previous case in this simulation the bottom condition (in suction) has been changed to 10 kPa. As mentioned in above section,

the wetting processes described by the BM concern only the upper soil layers (wetting downward). Consequently, the profiles obtained by the simulations not appear affected by the new bottom condition and the suction and moisture content fronts continue to propagate similarly to previous case showing a shape significantly sharp.

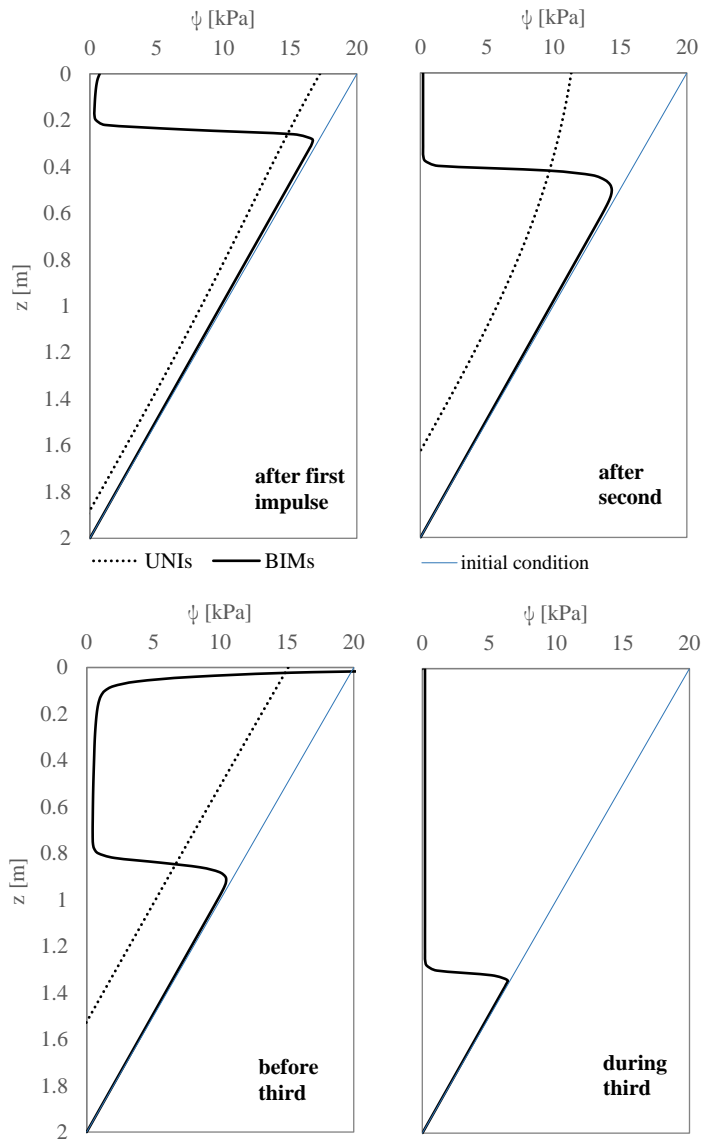


Figure 5.5 Simulated suction profiles for soil 1, Simulation Id1

5. Comparing uni- and bimodal water infiltration and slope stability modeling results

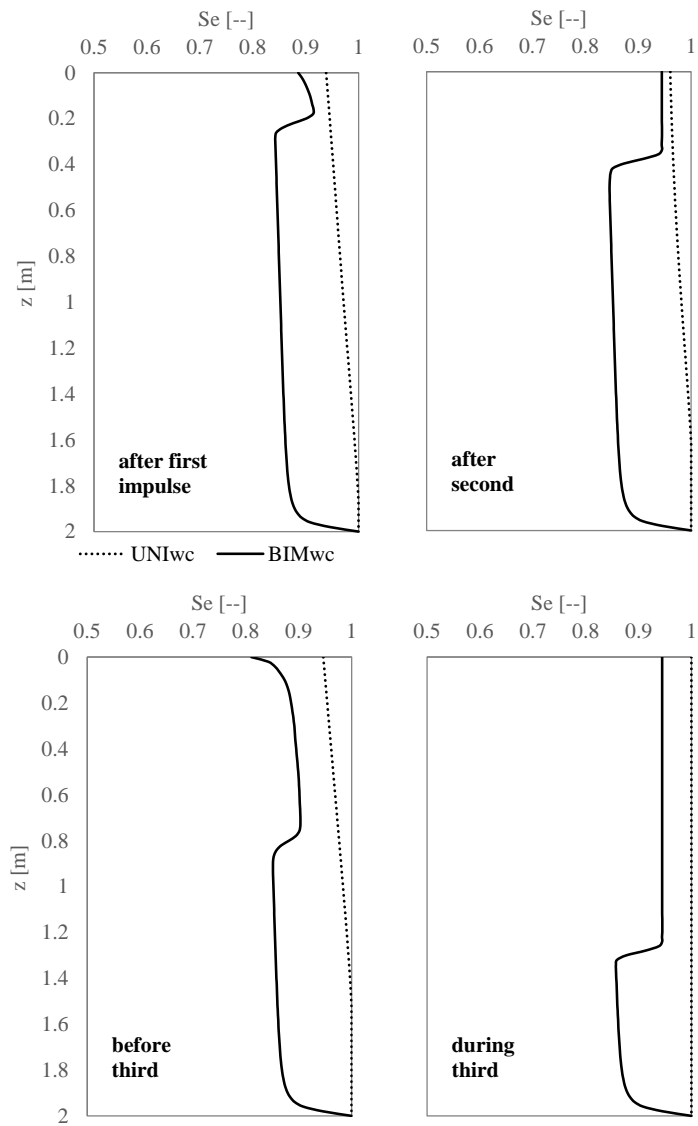


Figure 5.6 Simulated water content profiles for soil 1, Simulation Id1

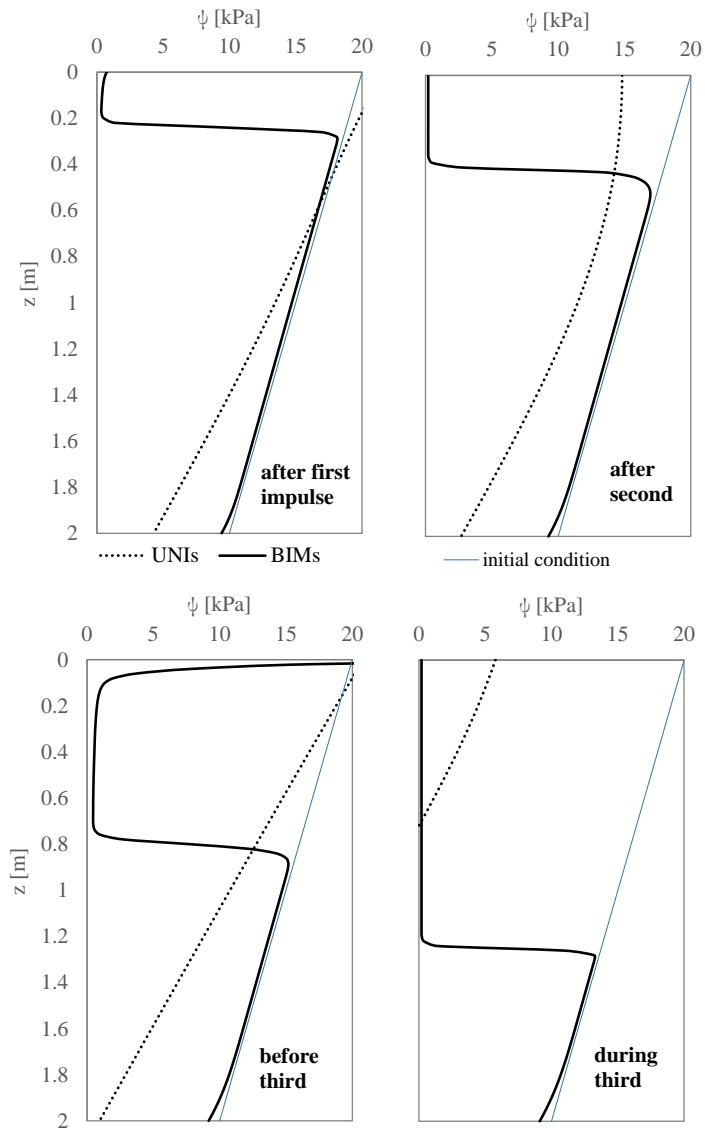


Figure 5.7 Simulated suction profiles for soil 1, Simulation Id2

5. Comparing uni- and bimodal water infiltration and slope stability modeling results

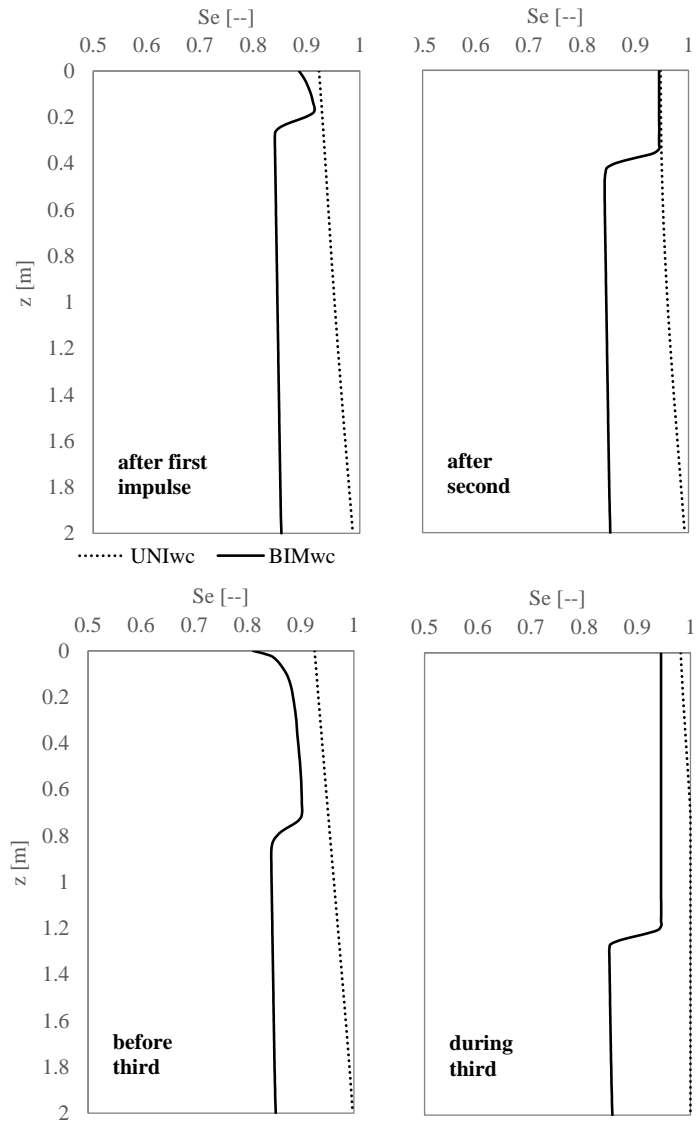


Figure 5.8 Simulated water content profiles for soil 1, Simulation Id2

5.2.2 Transient σ^s and FoS profiles (Soil 1)

Id1 - Unsteady rainfall – bottom condition 0 kPa (Figure 5.9, Figure 5.10 and Figure 5.11)

The mechanical behavior of the soil column can be quantitatively investigated by examining the suction stress patterns. In the Figure 5.9 the bimodal suction stress are compared with the unimodal suction at two different depths (0.5 m and 1.5 m). The aim of the comparison is to stress the differences between the two strength contribution between the compared model SAT_{FOS} and $UnSAT_{FOS}$. The temporal pattern of suction stress corresponds with the variations in moisture content (Figure 5.6) and suction head (Figure 5.5). The UNI_s exhibits “fluctuations” as a consequence of the rainfall-impulses. At 0.5 m depth the sensitivity of the UM to the un-steady-rainfalls is significantly more emphasized respect to the BIM_{ss} . The same behavior, but more feeble, is found at 1.5 m depth.

UNI_s and BIM_{ss} maintain approximately the same values order at the both depths until the second rainfall impulse is begun; after which the BIM_{ss} rapidly “falls” whereas the UNI_s approximately maintains for one day the same value (≈ 10 kPa). At 1.5 m depth the phenomena is completely reversed. In fact, the UNI_s rapidly decreases to zero just after the second rainfall impulse, whereas the BIM_{ss} has a delay of about 1 day.

It is interesting to observe the significant differences in terms of time-failure between the two approaches used (Figure 5.10). The shape of the suction stress (BIM_{ss}) and suction (UNI_s) profiles are quite similar to FoS profiles as the suctions (and the suction stress) being the main variable contribution to the soil strength. Shallower failures (0.5 m depth) quickly occur as a consequence of rapid water front propagation of the BM at upper column layers; the failure occurs well in advance of the SAT_{FOS} (≈ 1 day). Unlike at 1.5 m depth where due to the more generalized along-column processes described by the UM, the failure (of the UM) occurs before (≈ 1 day before the failure in BM).

At the upper soil layers the abruptness with which the $UnSAT_{FOS}$ (Figure 5.10) clearly reflects the shape of the wetting front propagation. In these simulations the FoS profiles appear profoundly conditioned by the

suction value (0 kPa) fixed to the bottom boundary of the soil column that involves a monotonically decreasing of FoS toward the bottom. Anyway, it can be said that as a consequence of the more in depth propagation of the hydraulic processes, the UM compared to BM generally (for the specific case) predicts the failures at deeper depths.

Id2 - *Unsteady rainfall – bottom condition 10 kPa* (Figure 5.12, Figure 5.13 and Figure 5.14)

At the 0.5 m depth, the UnSAT_{FOS} profiles (Figure 5.13 and Figure 5.14), analogously with the suction and moisture content profiles, does not seem to be significantly affected by the new bottom boundary condition; diversely, the SAT_{FOS} profile at the same depth initially exhibits a feeble FOS increment (≈ 4 against ≈ 3 of previous case). The higher value in suction at the bottom layer (1.5 m) causes a feeble distributed increment in FoS along the column. The more significant difference respect to the previous case consists of a delay reduction at 1.5 m depth between the time-failure achievements predicted by UM and BM. This is clearly a consequence of the major contribution in strength due to the higher initial suctions. Due to the same reasons, the time interval between the failures predicted by the SAT_{FOS} and UnSAT_{FOS} models is wider (≈ 1.2 day) than the case argued in the previous section. FoS-depth profiles (Figure 5.14) more clearly display as the SAT_{FOS} model quickly reaches low critical values at deeper depth respect to the UnSAT_{FOS} simulations.

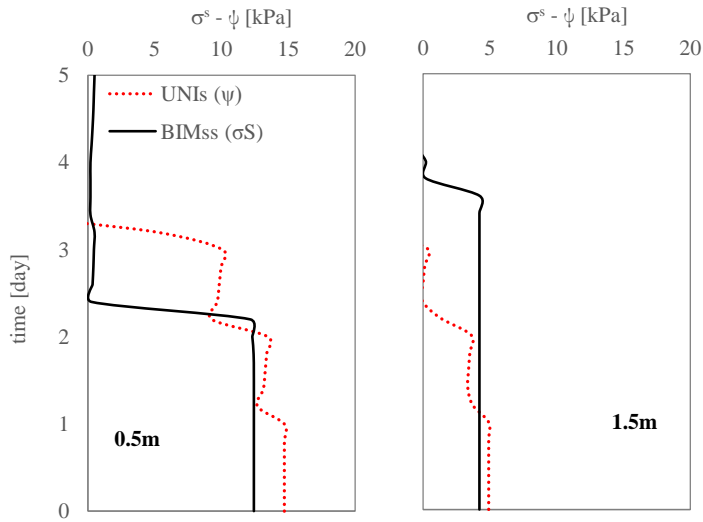


Figure 5.9 Simulated suction and suction stress at two different depths for soil 1, Simulation Id1

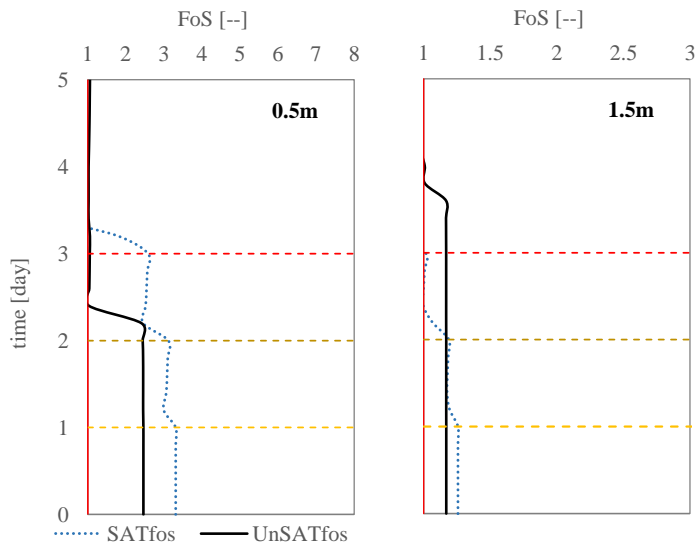


Figure 5.10 Simulated FoS at two different depths for soil 1, Simulation Id1

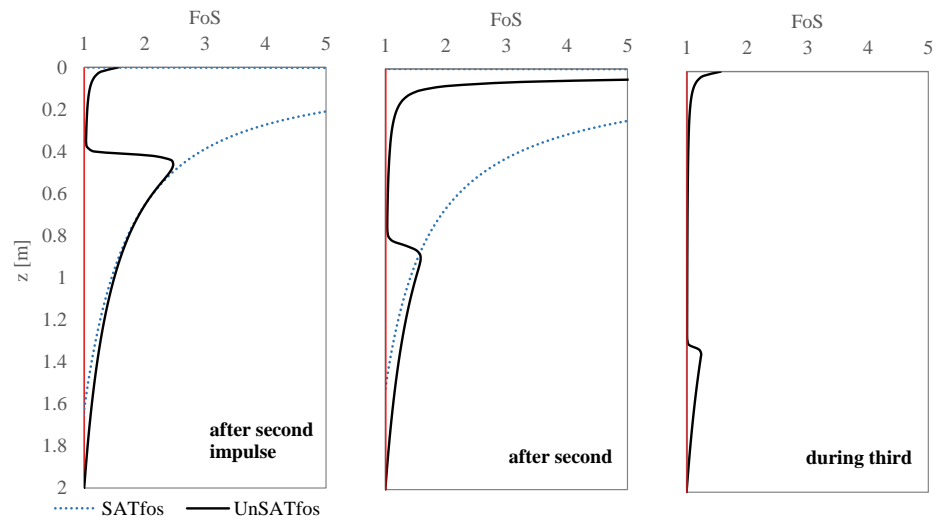


Figure 5.11 Simulated FoS profiles for soil 1, Simulation Id1

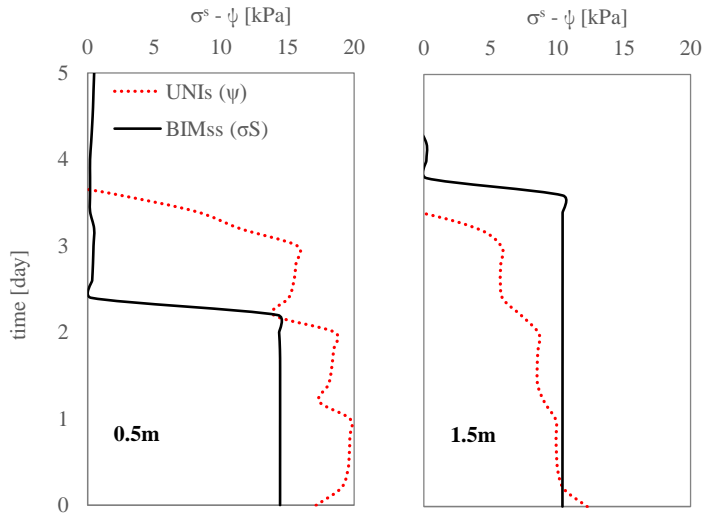


Figure 5.12 Simulated suction and suction stress at two different depth for soil 1, Simulation Id2

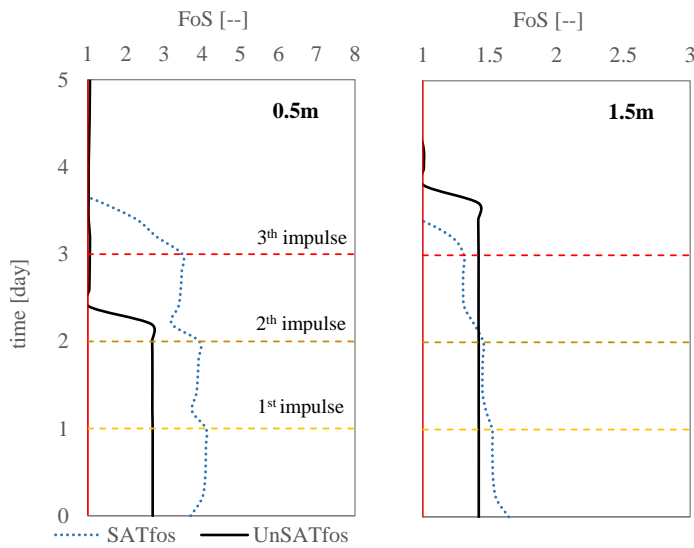


Figure 5.13 Simulated FoS at two different depths for soil 1, Simulation Id2

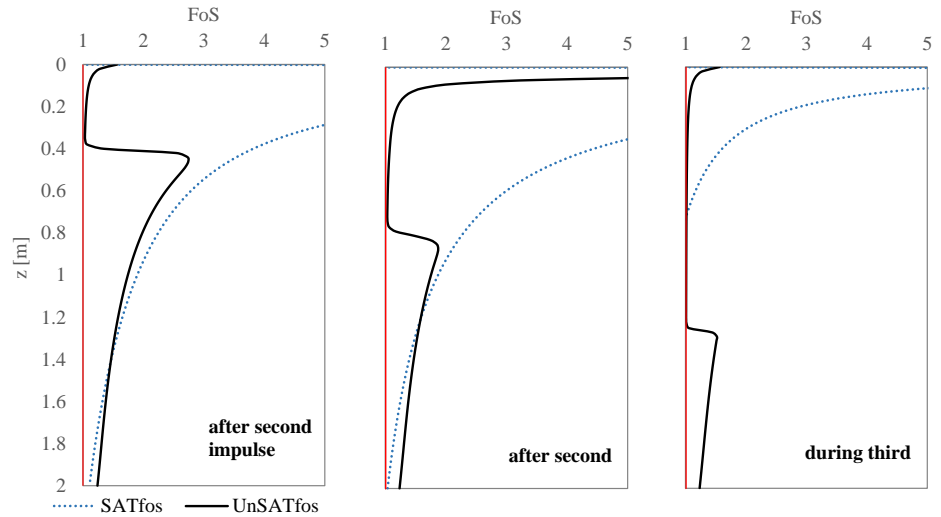


Figure 5.14 Simulated FoS profiles for soil 1, Simulation Id2

5.2.3 Transient ψ and S_e profiles (Soil 2)

Id3 - Steady rainfall – bottom condition 0 kPa (Figure 5.15 and Figure 5.16)

The both models rapidly reaches a stationary infiltrating flux condition at about 3.5 kPa (UM) and 8 kPa (BM). The quasi-saturated initial condition at the deeper layers combined with the faster increasing of the hydraulic conductivity in approaching to the saturation state cause a more pronounced progress of the wetting front from the bottom in BM case.

The moisture content profiles clearly display the simulated saturation mechanisms; an hortonian saturation process (saturation from the top) initially occurs; after that the stationary flux is established in both models a dunnian process prevails (saturation from the bottom).

The order of discrepancies between the two models is consistent with the shapes of the hydraulic functions respectively.

Id4 - Steady rainfall – bottom condition 10 kPa (Figure 5.17 and Figure 5.18)

A bottom boundary condition fixed to 10 kPa changes in part the profiles described in the above section. In the both simulated profiles (suction and moisture) a dominant hortonian-type mechanism of saturation (downward wetting front) is found. The both models rapidly (quasi)saturate the upper soil layers. The relatively high suction observed at quasi-saturation of the BM's profiles is a consequence of the shape of the water retention curve (Figure 5.2a); in fact, along a wide range of suction (0.1~5 kPa) the BM water content maintains approximately the same high value (0.65 ~ 0.7 in volumetric values).

The moisture content profiles clearly display the simulated saturation mechanisms; an hortonian saturation process (saturation from the top) initially occurs; after that the stationary flux is established in both models a dunnian process prevails (saturation from the bottom). The order of discrepancies between the two models is consistent with the shapes of the hydraulic functions respectively.

Compared with the results obtained by using a conventional unimodal approach (SAT_{FOS}), the $UnSAT_{FOS}$ simulations uniformly exhibit a delay of the wetting front. By a not accurate comparison of the water retention curves this may seem to be apparently a nonsense. In fact, the rapid increasing of the water content (and unsaturated hydraulic conductivity) for small changes in suction would lead to consider the hydraulic processes described by the BM always in advance of those resulted by UM. Instead, the hydraulic behavior reproduced is significantly controlled by the water initially present into the dry layers of the soil. The UM water retention curve (Figure 5.2) exhibits higher values in moisture contents in the range 10~20 kPa than the bimodal curve; the differences between the two curves for the same suction range are medially 0.1 of volumetric water content. This initially condition allows to the UM to progress in advance respect to BM.

Id5 - Unsteady rainfall – bottom condition 0 kPa (Figure 5.19 and Figure 5.20)

The hydraulic conductivity described for soil 2 by the two models, although characterized by different shapes, are quite similar. The UNI_s and BIM_s profiles shown in the Figure 5.19 vary approximately between 10 kPa and 20 kPa. Entering into the hydraulic conductivity curves (Figure 5.2b) with the above suction range we note that an “inversion” of the hydraulic behavior occurs between the two models. Due to the faster increasing of the unsaturated bimodal hydraulic conductivity, the

model rapidly reaches (after the second impulse) a stationary infiltrating flux condition at about 9 kPa. During the redistribution time between the second and third rainfall impulses the above mentioned condition vanishes, thus it occurs again during the third rainfall impulses. During the last rainfall a stationary flux is established (at ≈ 5 kPa) by the UM too.

The UNI_s and BIM_s are quite similar. Diversely, the UNI_{wc} and BIM_{wc} profiles display more significant differences. The profiles exhibit the same characteristics of the water retention curves falling in the range 0 kPa and 20 kPa (Figure 5.2a) it is interesting to observe how the BM profile appears almost saturated at bottom.

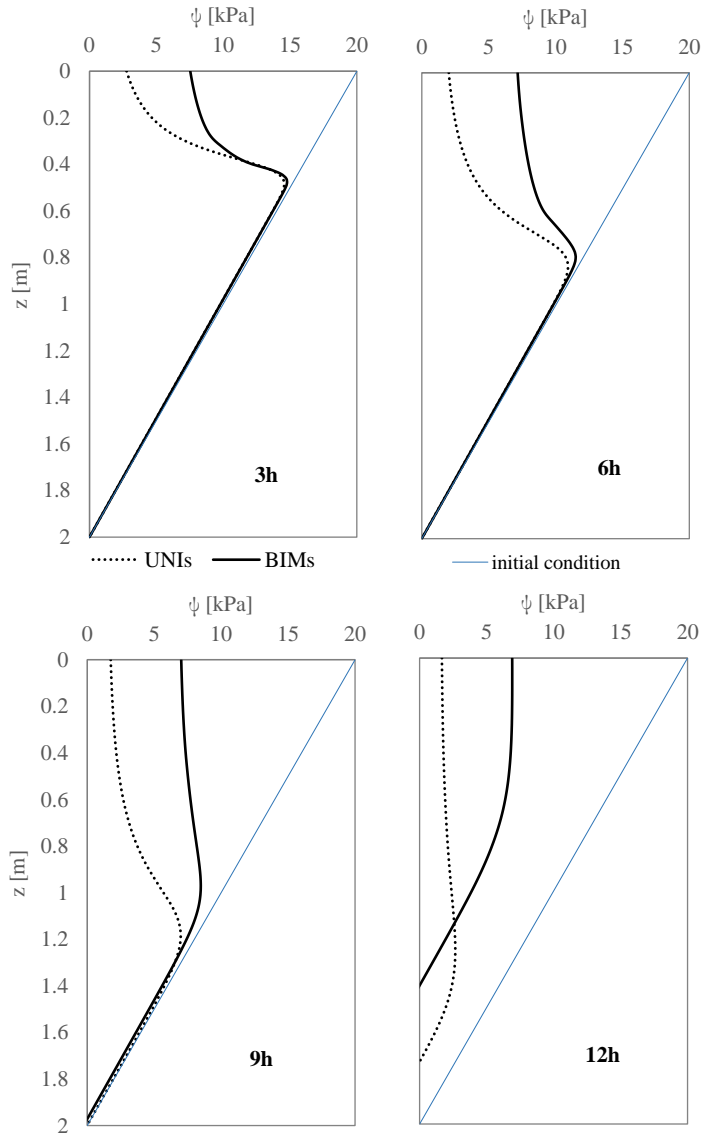


Figure 5.15 Simulated suction profiles for soil 2, Simulation Id3

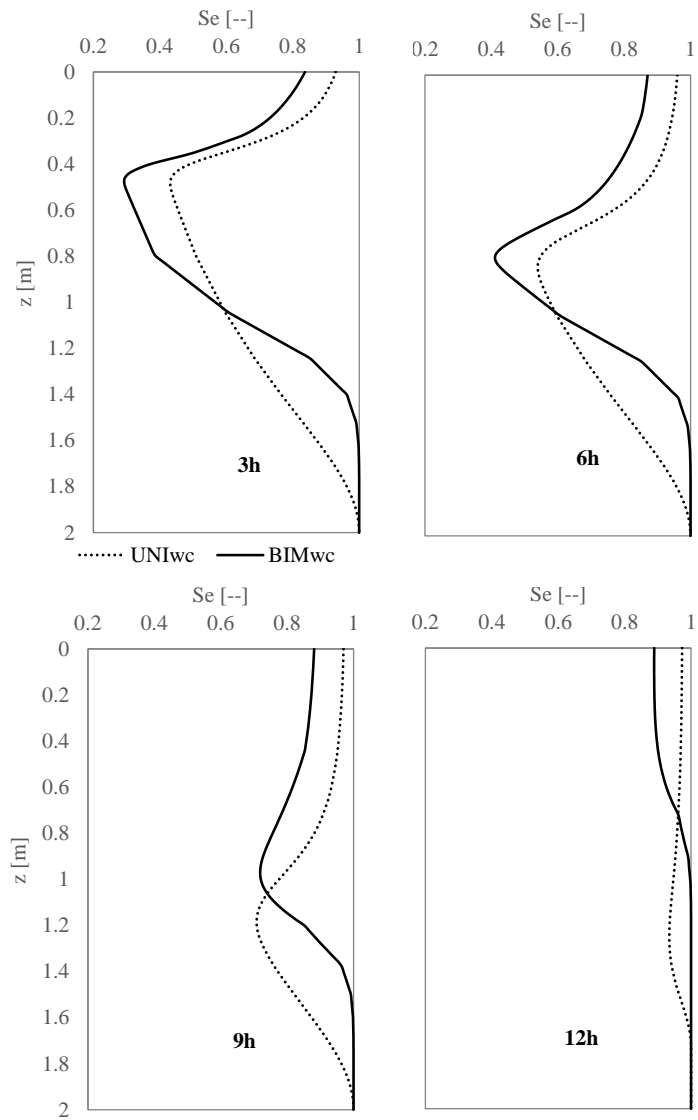


Figure 5.16 Simulated water content profiles for soil 2, Simulation Id3

5. Comparing uni- and bimodal water infiltration and slope stability modeling results

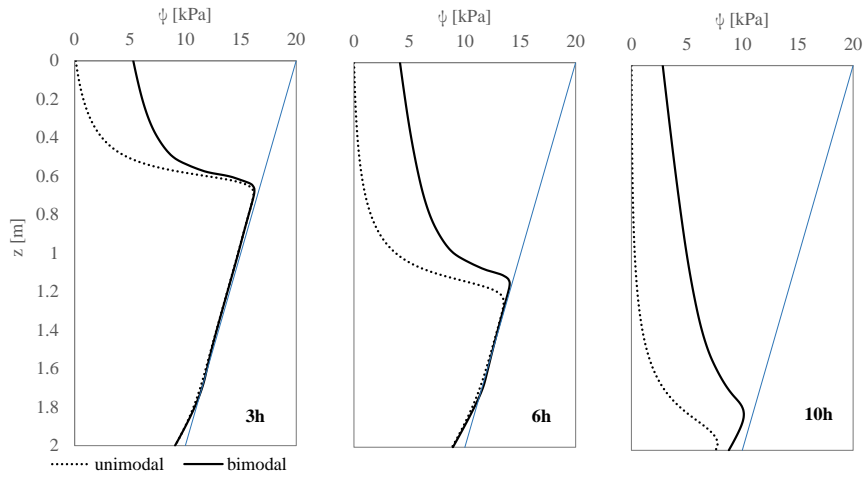


Figure 5.17 Simulated suction profiles for soil 2 – Simulation Id4

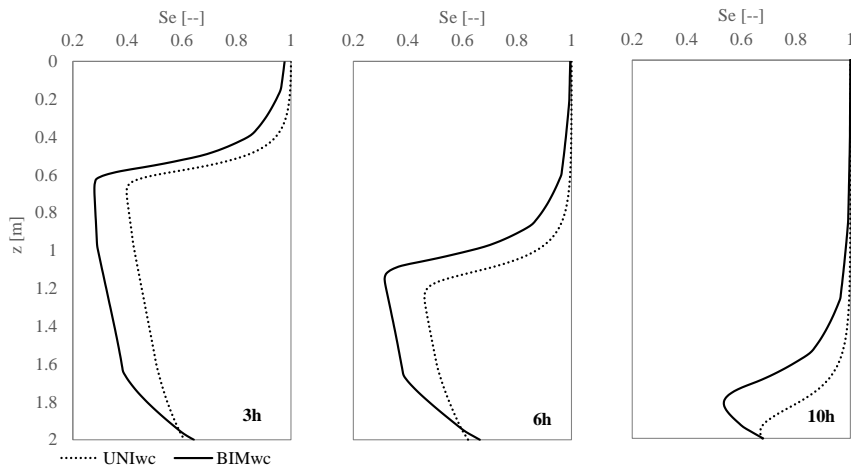


Figure 5.18 Simulated water content profiles for soil 2, Simulation Id4

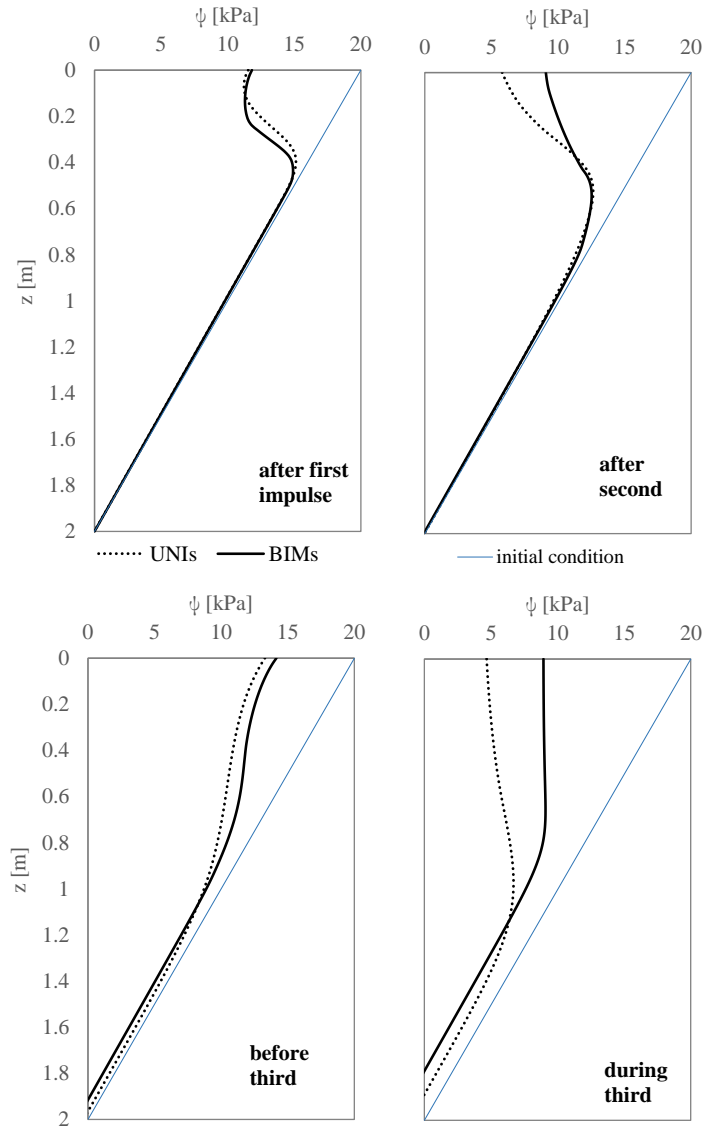


Figure 5.19 Simulated suction profiles for soil 2, Simulation Id5

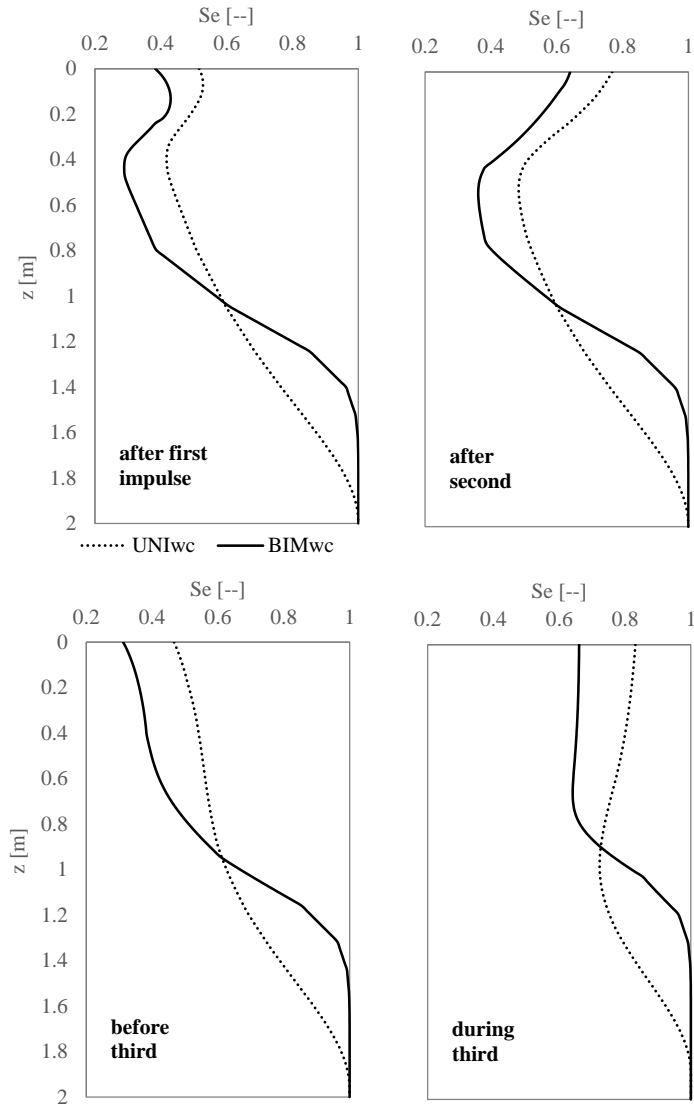


Figure 5.20 Simulated water content profiles for soil 2, Simulation Id5

5.2.4 Transient σ^s and FoS profiles (Soil 2)

Id3 - Steady rainfall – bottom condition 0 kPa (Figure 5.21, Figure 5.22 and Figure 5.23)

In case of a steady upper boundary condition, the same peculiarities found for the unsteady rainfall conditions appear more stressed. The radical inversion of the strength contribution (between UNI_S and BIM_{SS}) is significantly undeniable at surface soil depths (0.5 m). The reasons are essentially the same described in the above sections. An overlapping of the simulated profiles at bottom depths (1.5 m) is identically found during the first 9 hours of the event.

At 0.5 m depth, the FoS profiles display that during the first three hours the SAT_{FOS} predicts more stable conditions than the UnSAT_{FOS} (approximately three times more). The SAT_{FOS} results radically change after the 5th hour when the suction falls to about 3 kPa and a “critical state” is reached; diversely, the UnSAT_{FOS} pattern appears approximately unchanged during the rainfall event.

At 1.5 m depth, the two models profiles are quite similar. The UnSAT_{FOS} predicts the failure occurring before that the SAT_{FOS} with an advance of about 1 hour.

The Figure 5.23 more efficaciously displays the inversion of the stability configuration at upper soil layers.

Id4 - Steady rainfall – bottom condition 20 kPa (Figure 5.24, Figure 5.25 and Figure 5.26)

Compared with the previous case the bottom boundary condition is fixed to 10 kPa and the steady upper condition increased to 5 cm h⁻¹. The above discussed “behavior inversion” described by the UM in this simulation setting occurs at about 3th hour. As a consequence of the high rainfall intensity, the UM at 0.5 m depth early reaches values close to 0 kPa (at about 6th hour). The same occurs at 1.5 m depth where the effect of the new boundary bottom condition is more evident. At the deeper soil layers the “failure delay” described by the UnSAT_{FOS} is approximately of 1 hour.

It is interesting to observe the abruptness (and earliness) of the fall of the stability predicted by the SAT_{FOS} model (2th hour for surface layer whereas at 7th for deeper depths). During the first 10 hours of the rainfall event the mechanical behavior predicted the UnSAT_{FOS} never reaches the failure whereas the stability described by the unimodal saturated approach appears already compromised at about 6th hour (Figure 5.25 and Figure 5.26).

Id5 - Unsteady rainfall – bottom condition 0 kPa (Figure 5.27, Figure 5.28 and Figure 5.29)

A fundamental difference in the σ^s and S_e water content relationship (Figure 5.4) occurs when the moisture content approaches zero between clayey soils (soil 1) and sandy soils (soil 2). For sandy soils (and some silts) σ^s vanishes to zero as the soil dries, whereas for clays (and some silts) σ^s continues to increase approaching a limiting value at the residual water content (Lu et al., 2010). In the suction stress theory the effective water content represents the share of suction that effectively contributes to soil strength. The clayey soil response in terms of σ^s is the opposite for sands. The suction stress concept is aimed to capture the real contribution of suction to the stability of unsaturated natural slopes and it resolves the deficiencies in conventional slope stability analysis to consider in any case (for all soil-types) high effective stress in nearly dry soil where the suction is high. Because of these reasons the differences between σ^s and ψ appear particularly significant (Figure 5.27) at 0.5 m depth, where the soil is highly dry at initial steps of simulations.

The BIM_{SS} pattern resulted among the rainfall impulse remains unchanged at about 5 kPa although the related suction profiles suffer fluctuations (Figure 5.19, solid lines); this is essentially due to “correction” employed by the water content on the related suction (Figure 5.20). It is interesting to observe that the σ^s slightly increases while the moisture content after the third rainfall impulse occurred; this is a consequence of the particular shape of the suction stress characteristic curves (Figure 5.3 and Figure 5.4)

Diversely, the UNI_s profiles exhibit analogously with soil 1 a quite sensitivity to the unsteady rainfall inputs. Reasoning in terms of effective strength an upturning of the two contributions (UNI_s and BIM_{SS}) occurs when the third rainfall is applied.

At 1.5 depth the UNI_s and BIM_{SS} patterns overlap similarly to the UNI_s and BIM_s displayed in Figure 5.19. For low suctions (0.1 ~ 5kPa) the BM exhibits a quasi-saturated state (a slightly increasing of water content falls in a wide suction range: 0.95 – 1 effective water content over a 0.1 ~ 5 kPa in suction); as a consequence of this water retention peculiarity the BIM_{SS} contribution is quite similar to that UNI_s ($S_e * \psi = \sigma^s \Rightarrow 0.95 * 5 \text{ kPa} \approx 5 \text{ kPa}$).

The simulated FoS at 0.5 m depth reveals that the conventional SAT_{FOS} model tends to overestimate (if compared with the $UnSAT_{FOS}$ model) the FoS before the third rainfall impulses. In other words the SAT_{FOS} model appears to be more conservative than the $UnSAT_{FOS}$ model.

After the third rainfall, as above mentioned, the both strength contributions of the two models (UNI_s and BIM_{SS}) tend to overlap and consequently the FoS results too. Failures are not found in this case at shallow soil layers. At 1.5 depth the $UnSAT_{FOS}$ patterns are essentially similar to the SAT_{FOS} results.

The Figure 5.29 does not reveal particular phenomena to be noted. The FoS profiles along the depth exhibit the same characteristics previously highlighted (i.e. more conservative results of SAT_{FOS} during the first two rainfall impulses at the upper and middle soil layers).

Id5bis - *Unsteady rainfall – bottom condition 10 kPa* (Figure 5.30, Figure 5.31 and Figure 5.32)

Suction and moisture content profiles are not depicted. The change of the bottom boundary condition to 10 kPa induces a more sensitivity of the UM to the unsteady boundary upper conditions at the surface soil depths (0.5 m). It is interesting to notice as the redistribution effect induced by the evaporation intensity after the third rainfall impulse is significantly more pronounced than the previous case; instead, the bimodal σ^s profile results approximately the same (thus not affected by the new condition). At 1.5 depth the differences between UNI_s and the BIM_{SS} are essentially attributable to the reasons described at the beginning of this section. The BIM_{SS} contribution (to soil strength) basically appears unchanged ($\approx 5 \text{ kPa}$) if compared to the previous case, it is not affected by the bottom condition change. Diversely, the UNI_s contribution maintains approximately an higher value ($\approx 13 \text{ kPa}$) until it falls to about of 5 kPa during the third rainfall impulse. In this case the “overestimation” of SAT_{FOS} model (if compared with the $UnSAT_{FOS}$)

along the two first rainfall impulses appears at 1.5 depth too and it persists for a longer time than at the upper soil layers.

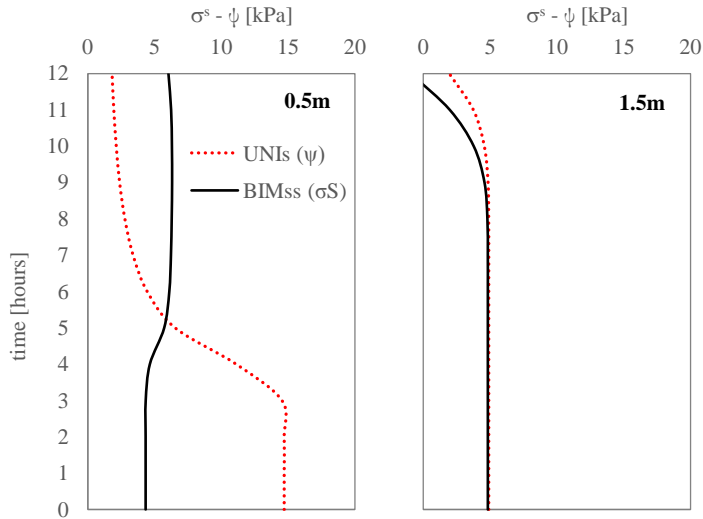


Figure 5.21 Simulated suction and suction stress at two different depths for soil 2, Simulation Id3

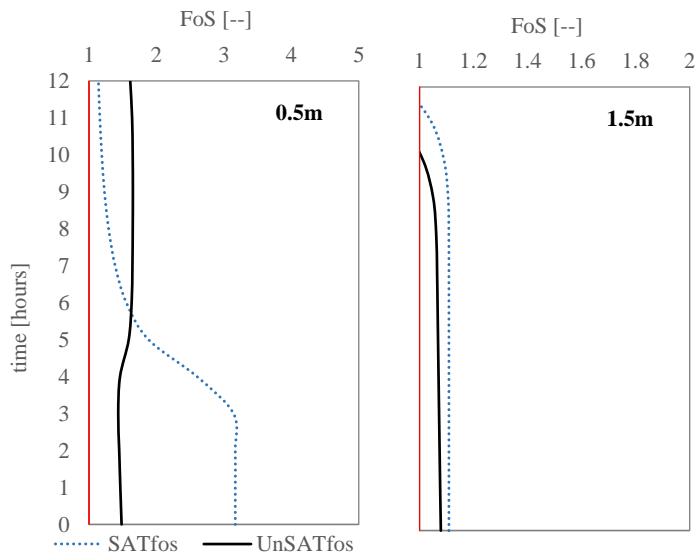


Figure 5.22 Simulated FoS at two different depths for soil 2, Simulation Id3

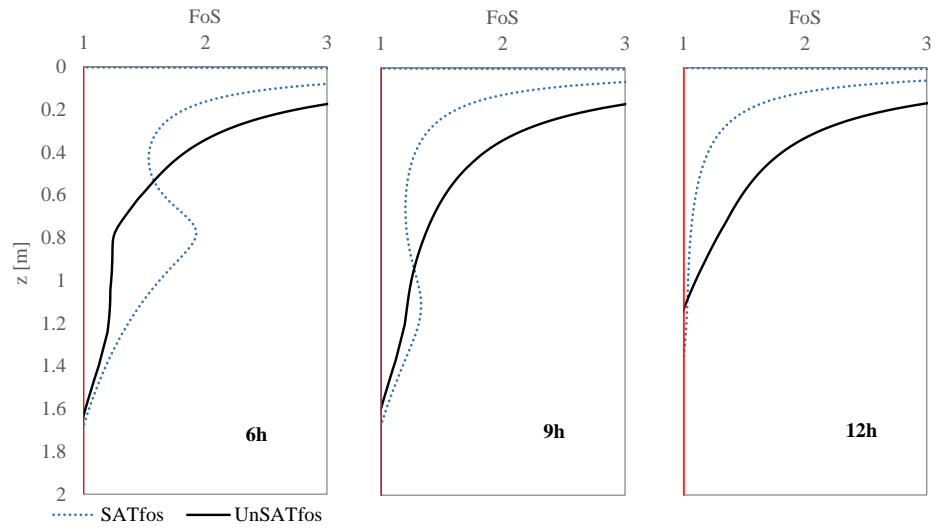


Figure 5.23 Simulated FoS profiles for soil 2, Simulation Id3

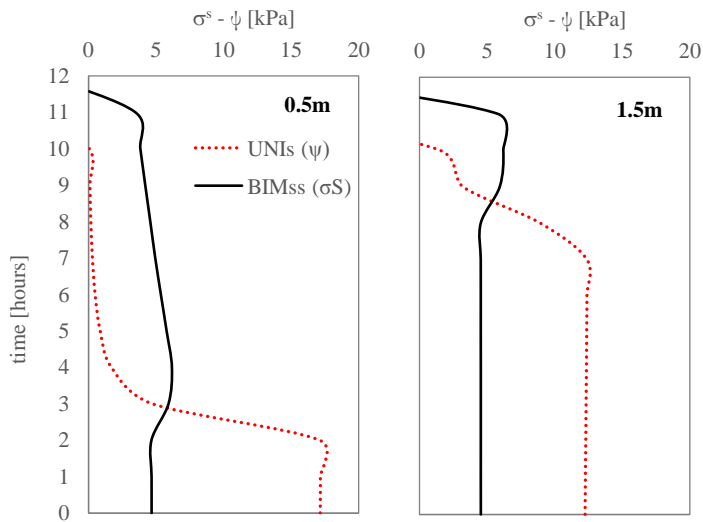


Figure 5.24 Simulated suction and suction stress at two different depths for soil 2, Simulation Id4

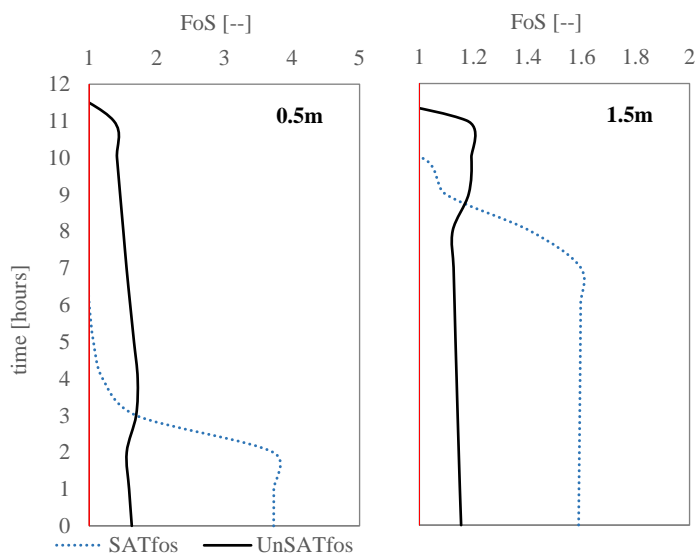


Figure 5.25 Simulated FoS at two different depths for soil 2, Simulation Id4

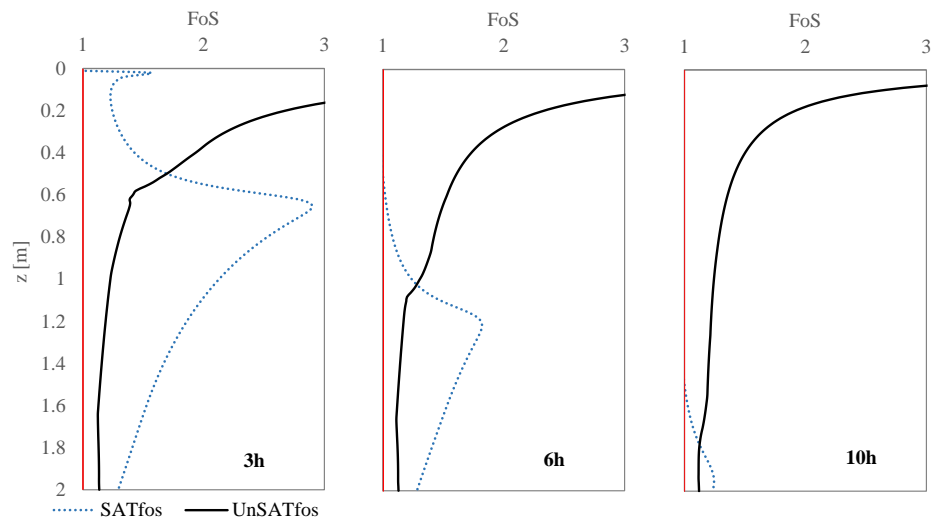


Figure 5.26 Simulated FoS profiles for soil 2, Simulation Id4

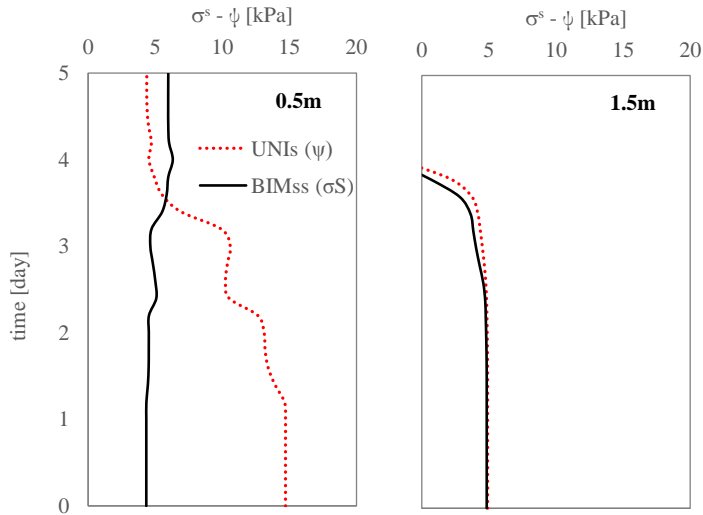


Figure 5.27 Simulated suction and suction stress at two different depths for soil 2, Simulation Id5

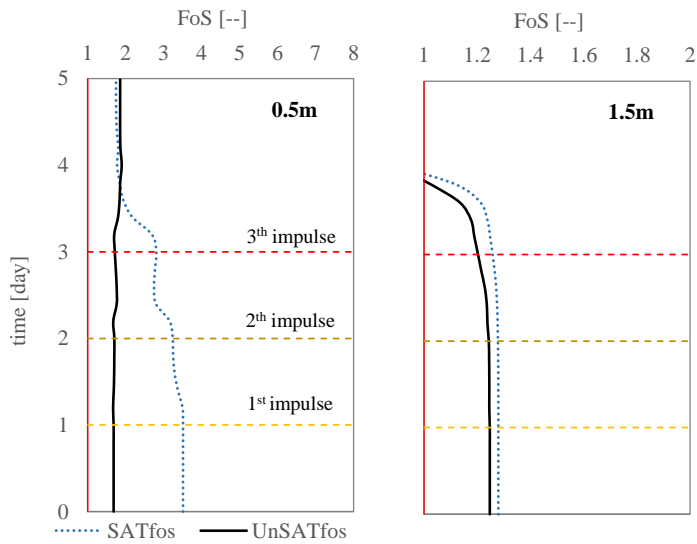


Figure 5.28 Simulated FoS at two different depths for soil 2, Simulation Id5

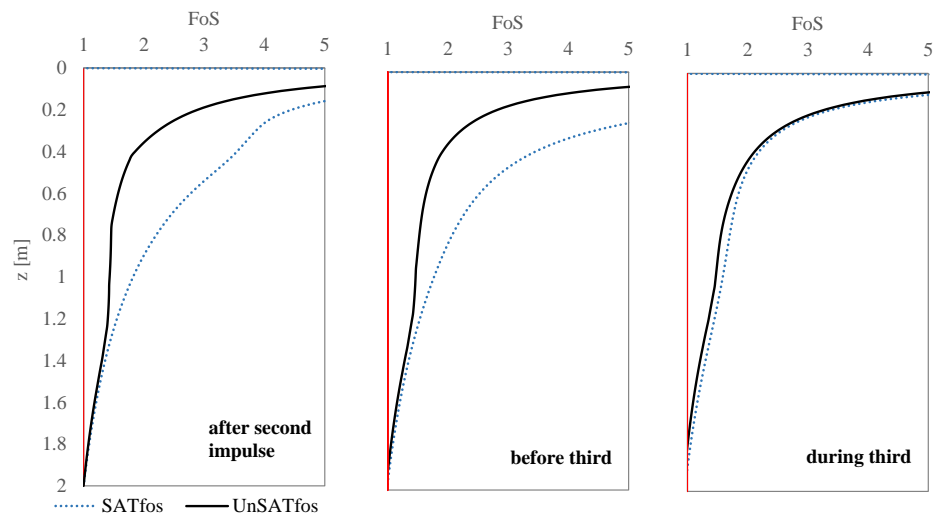


Figure 5.29 Simulated FoS profiles for soil 2, Simulation Id5

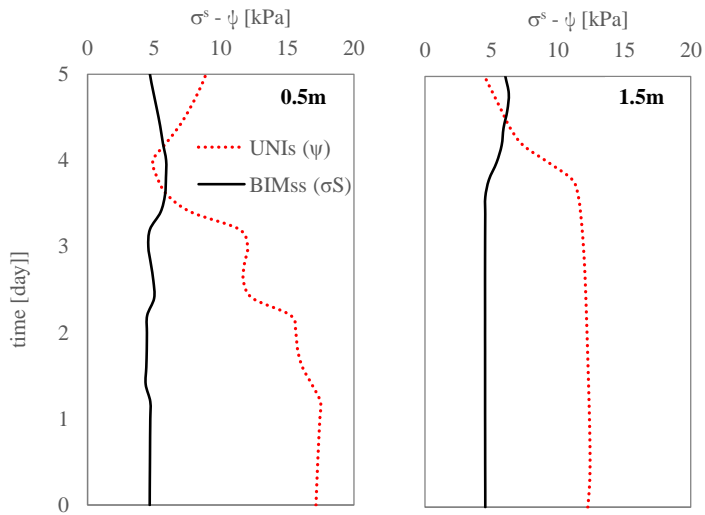


Figure 5.30 Simulated suction and suction stress at two different depths for soil 2, Simulation Id5bis

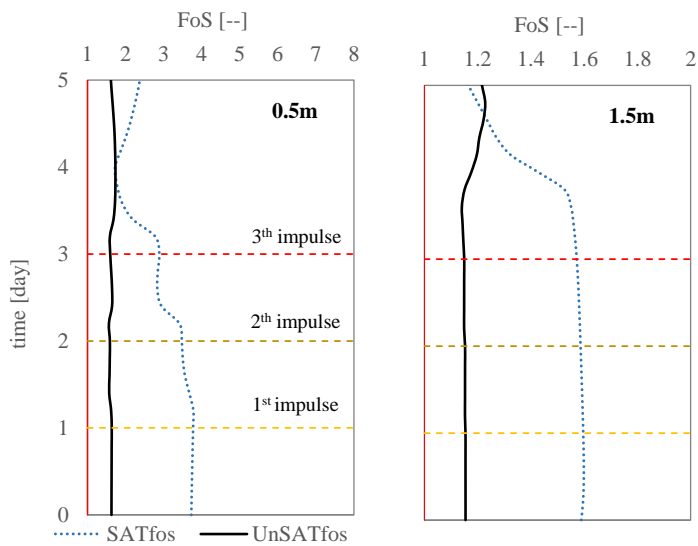


Figure 5.31 Simulated FoS at two different depths for soil 2, Simulation Id5bis

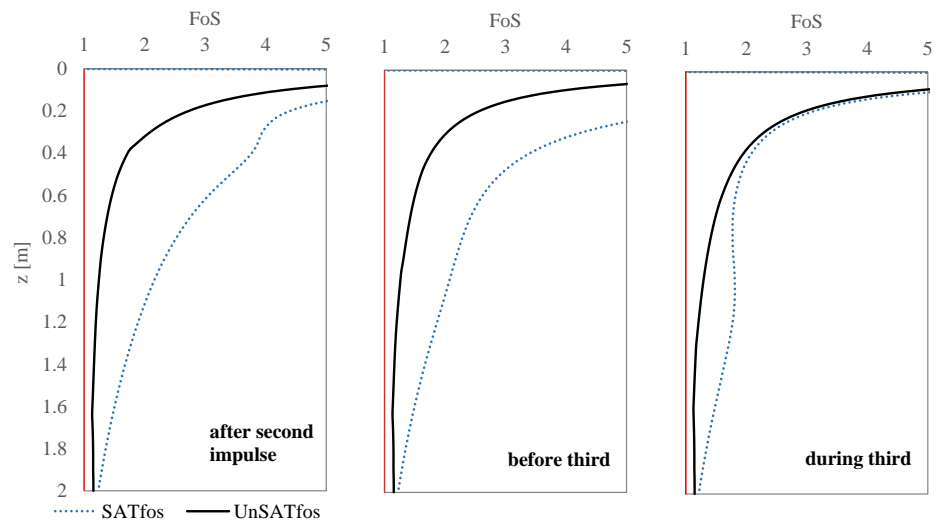


Figure 5.32 Simulated FoS profiles for soil 2, Simulation Id5bis

5.3 FINAL REMARKS

Water retention data of soil 1 and 2 (clayey and sandy soils) have been described with both a unimodal (UM) and a bimodal hydraulic function (BM). For soil 1 the predicted hydraulic conductivity curve obtained by using bimodal water retention function has been resulted significantly different from the conventional unimodal description. Diversely, the discrepancies between the unimodal and bimodal hydraulic conductivity curves of soil 2 are less significant. Several variables may affect the processes of the water movement through the soil. The multitude and variety of these factors (i.e. saturated hydraulic conductivity, boundaries conditions, initial conditions) make particularly difficult to obtain generalized remarks by the performed comparisons. It was observed that the differences between the constitutive hydraulic descriptions may lead to not negligible discrepancies in prediction of the hydraulic processes; this is the case of the soil 1 in which a sharp difference in terms of “infiltration mechanism” has been founded between the two approaches (e.g. sharp wetting front of the BM compared against more distributed downward processes described by the UM have been highlighted).

Same initial conditions in suction reflect in different initial water content profiles; a different initial moisture content controls the magnitude of the discrepancies in terms of delays or advances of the processes described by the UM and BM model. Soil 2 is a striking case of how initial conditions can influence the comparison: initial conditions fixed close or within the domain of the high effective water contents and the low suctions entail delay of the UM predictions compared with BM results; diversely, if the initial conditions fall in a certain range of suction (i.e. 10 kPa ~ 30 kPa - soil 2) a reversed situation can be found, and it may result in delay of BM predictions compared with the UM.

Slope stability analysis have been performed with both an infinite slope stability model (SAT_{FOS}) and a generalized variable-saturated infinite slope stability model ($UnSAT_{FOS}$). The first (SAT_{FOS}) approach uses a van Genuchten-Mualem model to describe the hydraulic properties and the suction (UNI_s) as strength contribution due to the capillary forces. Diversely, the second model ($UnSAT_{FOS}$) uses lognormal bimodal functions to describe the hydraulic behavior of the soil and the suction

stress (BIM_{ss}) to represent the strength contribution in partially saturated conditions.

The differences found between the two above mentioned approaches reflect the different effects on the hydraulic processes descriptions induced by using UM and BM constitutive models. The sharp discrepancy found in soil 1 between the UM and BM wetting profiles reflect in failures staggered in time and in depth: whereas the $UnSAT_{FOS}$ predicts early shallow failures, the SAT_{FOS} model generally gives a more rapid “un-stabilization” at deeper depths. The different way of the two models to quantify the strength contribution related to capillary forces (suction and suction stress) reflects in FoS results obtained for soil 2. The suction stress concept is aimed to capture the real contribution of suction to the stability of unsaturated natural slopes and it tries to resolve the deficiencies in conventional slope stability analysis to consider in any case high effective stress in nearly dry soil where the suction is high. In non-completely dry conditions of soil 2 the $UnSAT_{FOS}$ predicts a low strength contribution, whereas the SAT_{FOS} maintains high value in suction. This may entail non-negligible differences between the stability predictions performed by considering suction stress in bimodal setting rather than a conventional infinite slope model based on suction, especially if the possibility that the failure occurs within the vadose zone can be contemplated (e.g., Wolle and Hachich, 1989; de Campos et al., 1991; Fredlund, 2006; Godt et al., 2007; others).

In many of the performed tests, the use of bimodal constitutive hydraulic functions has led to a prediction of the occurrence of instability significantly delayed in time. This result enlighten the need to include this approach in the practical field applications in order to obtain more reliable predictions of slope instability. This is particularly sensible in case of early warning, in which case it is necessary to have good predictors of the triggering time.



CONCLUSIONS

The topic of this work arises within the broader context of research on the potential effects induced by the heterogeneities on the hydraulic and mechanical behavior of natural unsaturated soils. The presence of heterogeneities complicates the commonly interpretation of hydrological and geotechnical processes. Understanding how to capture them and their time dependent variables, in an accurate quantitative description is a challenging problem. Given these issues, an additional research problem that needs to be addressed is to improve our understanding if the “disturbances” due to heterogeneities can affect the engineering practice, which may relate hydrological predictions, landslide initiation analysis, building up of hazard warning systems.

In order to improve the reliability of hydrological modeling and predictions numerous research studies focused on the formulation of more suitable constitutive hydraulic relationships to describe the hydraulics of hill-slope response under rainfall loading. Contextually, new theoretical solutions have emerged and introduced to treat the slope stability analysis with appropriate shear strength equations specifically developed for unsaturated soils.

Matric suction plays a significant role in determining the stress state of unsaturated soils. It has been widely established that its variation of is very sensitive to the water content. Furthermore, this phenomenological relationship between water (in terms of suction and moisture content) and strength is strongly affected by soil heterogeneities and have potentially effects on how water moves through the soil. Despite their known significance, heterogeneities are poorly considered in slope stability modelling. The most used approaches for the assessment of shallow landslide initiation have no real treatment of heterogeneities.

A large class of heterogeneous soil formations can be described as double-structure porous media. Aggregated soils, widely-graded soils or fractured rocks are typical examples of double-structure soils.

In this study, we faced finally with the above problems. All analyses and applications have been performed on granular-type structured soils. The research assumes that the local scale (of evaluation), also known as Darcy scale, corresponds to the characteristic dimension of

heterogeneities (approachable by Richards' model). To mathematically represent the dual (-structure) implications on the hydraulic soil behavior several bimodal constitutive hydraulic relationships have been presented in literature to replace the conventional sigmoidal/unimodal functions (e.g. van Genuchten model).

In particular, this study mainly concerns the modeling of effects induced by granular-heterogeneities in terms of hydrological and slope stability response. Some recently proposed theories and models have been used and novel analytical and numerical model developed to obtain insights: a) on bimodality effects of the hydraulic properties on shear strength of unsaturated double-structure soils; b) on effects induced on modeling transient water infiltration and slope stability by assuming bimodal constitutive hydraulic models. Both the parts of the work are strongly connected to each other. The validation of the proposed extension of the suction stress theory to the bimodal hydraulic response (described in the first part of the Thesis) allows to consequently employ a generalized variable-saturated infinite slope model and describe transient slope stability processes that may be affected by bimodal behavior. Three were the main achievements.

- a) A new analytical method to assess the effects of the hydraulic properties on soil shear has been developed integrating a bimodal lognormal function proposed by Romano et al. (2011) to describe the hydraulic behavior of unsaturated double-structured soils within the suction stress theory framework of Lu and Likos (2006). A new closed-form expression for suction stress has been proposed and validated. The chosen bimodal lognormal model is firmly grounded on physical principles, since it uses the particle size distribution to describe the soil hydraulic behavior, thus overcoming the limits of the classic empirical functions. The results of the model in terms of suction stress has been compared to that obtained by laboratory measurements on different soils such as sand with gravel or silt and volcanic ash soils (the latter actually coming from literature data). A discrepancy between the model adopted and the experimental data has been observed for materials with high fine content. This should be due to the dependency of the bimodal water retention curve on the void ratio, which has been neglected as a first approximation. The model developed gives an accurate description of the suction

stress characteristic curves at quasi-saturation dominium, dominated by the macrostructure, and over a range of suction up to 1000 kPa, dominated by microstructure.

- b) A new Java code for integrating Richards equations in 1D. In order to explore the effects on modeling transient water infiltration, and slope stability by assuming bimodal constitutive hydraulic models a novel JAVA-code has been developed (Ri.D1). Ri.D1 simulates one-dimensional vertical transient water flow by numerically solving the Richards' equation; unimodal (van Genuchten-Mualem) and bimodal models (Romano-Mualem) have been implemented. The code includes a dedicated module for simulating slope stability analysis. Furthermore, a conventional infinite slope stability method and a generalized factor of safety equation for infinite slope model under variably saturated condition (Godt et al., 2008) have been implemented. The purpose of the implementation was to prepare the tools deemed necessary to cope with the new multimodal theories.
- c) The outcomes of the analysis of the soil with the new theoretical and software tools. The focus of this part was on the differences in simulated flow infiltration and slope stability originating from the choice of a given hydraulic model and contextually from different (saturated and unsaturated) approaches to evaluate the factor of safety.

There are a few disclaimers regarding the applications performed:

1. The structured state of granular-structured soils can be strongly unstable with respect to hydraulic and mechanical forcing; under a given load, aggregates may be deformed and spatially rearranged, macrostructural pores shrink and the bulk soil volume decreases. Soil compaction affects PSD modifying the shape of related hydraulic functions.
2. Analogously, hysteresis can affect the accuracy of unsaturated flow calculations. In this work this aspects have been neglected.
3. The multitude and variety of the variables that may affect the physical processes of water movement through the soil makes impossible a systematic exploration of all the possibilities.

However, it has been seen that the differences explored in the Thesis between the constitutive hydraulic descriptions lead to not negligible discrepancies in the prediction of the hydraulic processes and slope stability. Moreover, significant differences between the conventional “saturated” infinite slope stability model and the variable-saturated approach have been found especially in sandy soils, where the strength contribution in suction may be substantially different from the strength magnitude due to “suction stress”.

Certainly the model implemented needs to be further generalized in order to include other factors controlling hydraulic processes that have been mentioned above, such as soil compaction and hydraulic hysteresis. However, more complicated processes interplays can be the subject of future research.

Future research should focus on: a) further investigation on the evolution of the bimodal water retention and suction stress characteristic curves with mechanical loading in order to find a relationship between soil compaction degrees and bimodal hydro-mechanical response; b) analogous investigations which are expected to enlighten the hydraulic hysteresis implications; c) further validations with ad hoc laboratory measurements of soil shear strength, retention and hydraulic conductivity; d) extension of Ri.D1 model applications to larger scales (i.e. slope or catchment scale), with its possible coupling with lateral flow; e) in reference to the previous objective the numerical model may necessitate improvements in order to ensure controlled computational time effort in wider variety of bimodal setting.

REFERENCES

- Aitchison, G. D. 1961. Relationship of moisture and effective stress functions in unsaturated soils. Proceedings of the Conference on Pore Pressure and Suction in Soils. Butterworths, London, 47-52.
- Al-Sharrad, M. A. (2013). Evolving anisotropy in unsaturated soils: experimental investigation and constitutive modelling (Doctoral dissertation, University of Glasgow).
- Alonso, E. E., Gens, A., & Josa, A. (1990). A constitutive model for partially saturated soils. *Géotechnique*, 40(3), 405-430.
- Alonso, E. E., Pereira, J. M., Vaunat, J., & Olivella, S. (2010). A microstructurally based effective stress for unsaturated soils. *Géotechnique*, 60(12), 913-925.
- Baille, W., Tripathy, S., & Schanz, T. (2014). Effective stress in clays of various mineralogy. *Vadose Zone Journal*, 13(5).
- Basile, A., A. Coppola, R. De Mascellis, G. Mele, and F. Terribile. (2007). A comparative analysis of the pore system in volcanic soils by means of water retention measurements and image analysis. p. 493–513. In O. Arnalds et al. (ed.) *Soils of volcanic regions in Europe*. Springer-Verlag, Berlin.
- Beven, K. J., & Kirkby, M. J. (1979). A physically based, variable contributing area model of basin hydrology/Un modèle à base physique de zone d'appel variable de l'hydrologie du bassin versant. *Hydrological Sciences Journal*, 24(1), 43-69.
- Beven, K., & Germann, P. (1982). Macropores and water flow in soils. *Water resources research*, 18(5), 1311-1325.
- Bilotta, E., L. Cascini, V. Foresta and G. Sorbino. (2005). Geotechnical characterization of pyroclastic soils involved in huge flowslides. *Geotech. Geol. Eng.* 23: 365–402.
- Bird, N.R.A., A.R. Preston, E.W. Randall, W.R. Whalley, A.P. Whitmore. (2005). Measurement of the size distribution of water filled pores at different matric potentials by stray field nuclear magnetic resonance. *European Journal of Soil Science*, 56: 135–143.
- Bishop, A. (1959). The principle of effective stress. *Tek. Ukebl.* 106:859–863.
- Bishop, A. W., & Donald, I. B. (1961, July). The experimental study of partly saturated soil in the triaxial apparatus. In Proceedings of the 5th international conference on soil mechanics and foundation engineering, Paris (Vol. 1, pp. 13-21).

-
- Bishop, A. W., & Blight, G. E. (1963). Some aspects of effective stress in saturated and partly saturated soils. *Geotechnique*, 13(3), 177-197.
- Bloemen, G. W. (1980). Calculation of hydraulic conductivities of soils from texture and organic matter content. *Zeitschrift für Pflanzenernährung und Bodenkunde*, 143(5), 581-605.
- Bogaard, T. A., Greco, R., Olivares, L., & Picarelli, L. (2014). The Round Robin test on landslide hydrological modeling at IWL2013. *Procedia Earth and Planetary Science*, 9, 180-188.
- Brooks, R.H. and A.T. Corey. (1964). Hydraulic properties of porous media. Colorado State University. Fort Collins. Colo. Hydrology Paper No. 3 (March).
- Bruce, R. R., & Luxmoore, R. J. (1986). Water retention: field methods. *Methods of Soil Analysis: Part 1—Physical and Mineralogical Methods*, (methodsofsoilan1), 663-686.
- Brutsaert, W. (1966). Probability laws for pore-size distributions. *Soil Soc. Am. J.* 101, 85-92.
- Buckingham, E. (1907). Studies on the movement of soil moisture.
- Burger, C.A. and C.D. Shackelford. (2001). Evaluating dual porosity of pelletized diatomaceous earth using bimodal soil–water characteristic curve functions. *Can. Geotech. J.* 38: 53–66
- Burland, J. B. (1965). Some aspects of the mechanical behaviour of partly saturated soils. In *Moisture Equilibria and Moisture Changes in Soils Beneath Covered Areas*, A Symposium in Print, Butterworth, Sidney, Australia (pp. 270-278).
- Capparelli, G., & Versace, P. (2014). Analysis of landslide triggering conditions in the Sarno area using a physically based model. *Hydrology and Earth System Sciences*, 18(8), 3225-3237.
- Carminati, A., Kaestner, A., Lehmann, P., & Flühler, H. (2008). Unsaturated water flow across soil aggregate contacts. *Advances in water resources*, 31(9), 1221-1232.
- Casadei, M., Dietrich, W. E., & Miller, N. L. (2003). Testing a model for predicting the timing and location of shallow landslide initiation in soil-mantled landscapes. *Earth Surface Processes and Landforms*, 28(9), 925-950.
- Cascini, L., & Sorbino, G. (2003, May). The contribution of soil suction measurements to the analysis of flowslide triggering. In *Workshop “Flows”* (pp. 77-86).
- Casini, F., P.Minder, and S. M. Springman. (2011). Shear strength of an unsaturated silty sand. In *Unsaturated Soils-Proceedings of the 5th International Conference on Unsaturated Soils*. Barcelona. Spain. Vol. 1. pp. 211-216.

-
- Casini, F., J. Vaunat, E. Romero, and A. Desideri. (2012). Consequences on water retention properties of double porosity features in a compacted silt. *Acta Geotechnica*, 7: 139–150.
- Casulli, V., & Zanolli, P. (2010). A nested Newton-type algorithm for finite volume methods solving Richards' equation in mixed form. *SIAM Journal on Scientific Computing*, 32(4), 2255-2273.
- Chen, C., & Wagenet, R. J. (1992). Simulation of water and chemicals in macropore soils Part 1. Representation of the equivalent macropore influence and its effect on soilwater flow. *Journal of Hydrology*, 130(1), 105-126.
- Chen, C., & Wagenet, R. J. (1992). Simulation of water and chemicals in macropore soils Part 2. Application of linear filter theory. *Journal of hydrology*, 130(1), 127-149.
- Chirico, G.B., H. Medina, and N. Romano. (2007). Uncertainty in predicting soil hydraulic properties at the hillslope scale with indirect methods. *J. Hydrol.* 334: 405–422.
- Cho, S. E., & Lee, S. R. (2002). Evaluation of surficial stability for homogeneous slopes considering rainfall characteristics. *Journal of Geotechnical and Geoenvironmental Engineering*, 128(9), 756-763.
- Coleman, J. D. (1962) Stress/strain relations for partly saturated soils. *Geotechnique*, 12(4), 348-350.
- Colombo, L. (2009). Large shear box for analyzing strength mobilization in unsaturated conditions. Master Thesis. Politecnico di Milano.
- Collins, B. D., & Znidarcic, D. (2004). Stability analyses of rainfall induced landslides. *Journal of Geotechnical and Geoenvironmental Engineering*, 130(4), 362-372.
- Coppola, A., & Greco, R. (1997, September). Preferential flow through swelling and shrinking clay soil columns. In *Proceedings of the International conference on Water management, salinity and pollution control towards sustainable irrigation in the Mediterranean area*. Bari, Italy.
- Coppola, A. (2000). Unimodal and bimodal descriptions of hydraulic properties for aggregated soils. *Soil Science Society of America Journal*, 64(4), 1252-1262.
- Crandall, D., G. Ahmadi, M. Ferer, and D. H. Smith (2009), Distribution and occurrence of localized-bursts in two-phase flow through porous media, *Physica A*, 388, 574 – 584, doi:10.1016/j.physa.2008.11.010.
- Dagan, G., & Bresler, E. (1983). Unsaturated flow in spatially variable fields: 1. Derivation of models of infiltration and redistribution. *Water Resources Research*, 19(2), 413-420.
- Damiano, E. and L. Olivares. (2009). The role of infiltration processes in steep slope stability of pyroclastic granular soils: laboratory and numerical

-
- investigation. *Natural Hazards*. 52: 329–350. doi: 10.1007/s11069-009-9374-3.
- de Campos, T. M. P., M. H. N. Andrade, and E. A. Vargas Jr. (1991). Unsaturated colluvium over rock slide in a forested site in Rio de Janeiro, Brazil, in Proc. 6th Int. Symp. on Landslides, Christchurch New Zealand, pp. 1357–1364, Balkema, Rotterdam, Netherlands.
- De Vita, P., E. Napolitano, J.W. Godt, and R.L. Baum. (2013). Deterministic estimation of hydrological thresholds for shallow landslide initiation and slope stability models: case study from the Somma-Vesuvius area of southern Italy. *Landslides*. 10(6) 713-728.
- Debieche, T. H., Bogaard, T. A., Marc, V., Emblanch, C., Krzeminska, D. M., & Malet, J. P. (2012). Hydrological and hydrochemical processes observed during a large-scale infiltration experiment at the Super-Sauze mudslide (France). *Hydrological Processes*, 26(14), 2157-2170.
- Della Vecchia, G., A.C. Dieudonné, C. Jommi, and R. Charlier. (2014). Accounting for evolving pore size distribution in water retention models for compacted clays. *Int. J. Numer. Anal. Meth. Geomech.* DOI: 10.1002/nag.2326.
- Destouni, G. (1993). Stochastic modelling of solute flux in the unsaturated zone at the field scale. *Journal of hydrology*, 143(1), 45-61.
- Dexter, A.R., and G. Richard. (2009). Tillage of soils in relation to their bimodal pore size distributions. *Soil Tillage Res.* 103:113–118.
- Dunne, T., & Black, R. D. (1970). Partial area contributions to storm runoff in a small New England watershed. *Water resources research*, 6(5), 1296-1311.
- Durner, W. (1992). Predicting the unsaturated hydraulic conductivity using multi-porosity water retention curves. *Indirect Methods for Estimating the Hydraulic Properties of Unsaturated Soils*. University of California, Riverside, CA, USA, 185-202.
- Durner, W. (1994). Hydraulic conductivity estimation for soils with heterogeneous pore structure. *Water Resour. Res.* 30:211–223.
- Escario, V., Juca, J. F. T., & Coppe, M. S. (1989). Strength and deformation of partly saturated soils. Proc. 12th ICSMFE, Rio de Janeiro, 1, 43-46.
- Fannin, R. J., Jaakkola, J., Wilkinson, J. M. T., & Hetherington, E. D. (2000). Hydrologic response of soils to precipitation at Carnation Creek, British Columbia, Canada. *Water Resources Research*, 36(6), 1481-1494.
- Fannin, R. J., Eliadorani, A., & Wilkinson, J. M. T. (2005). Shear strength of cohesionless soils at low stress. *Geotechnique*, 55(6), 467-478.
- Fellenius, W. (1936). Calculation of the stability of earth dams. In *Transactions of the 2nd congress on large dams*, Washington, DC (Vol. 4, pp. 445-463).
- Fetter, C. W., & Fetter, C. W. (2001). *Applied hydrogeology* (Vol. 3, No. 3). New Jersey: Prentice hall.

-
- Fisher, R.V., and H.U.Schminke. (1984). *Pyroclastic Rocks*. Springer-Verlag. Berlin. pp. 472.
- Fredlund, D. G., & Morgenstern, N. R. (1977). Stress state variables for unsaturated soils. *Journal of Geotechnical and Geoenvironmental Engineering*, 103(ASCE 12919).
- Fredlund, D. G., N.R. Morgenstern, and R.A. Widger. (1978). Shear strength of unsaturated soils. *Can. Geotech. J.* 15:313-321.
- Fredlund, D. G., & Rahardjo, H. (1993). *Soil mechanics for unsaturated soils*. John Wiley & Sons.
- Fredlund, D.G. and Xing, A. (1994). Equations for the soil-water characteristic curve. *Can. Geotech. J.*, 31(4): 521–532. doi:10.1139/t94-061.
- Fredlund, D.G. (1995). The scope of unsaturated soil mechanics: an overview. Invited keynote address. In *Proceedings of the First International Conference on Unsaturated Soils*, Paris, France, 6–8 September 1995. Edited by E.E. Alonso and P. Delage. A.A. Balkema, Rotterdam, the Netherlands. Vol. 3, pp. 1155–1177.
- Fredlund, D. G., Xing, A., Fredlund, M. D., & Barbour, S. L. (1996). The relationship of the unsaturated soil shear to the soil-water characteristic curve. *Canadian Geotechnical Journal*, 33(3), 440-448.
- Fredlund, M. D., D. G. Fredlund, and G. W. Wilson. (2000). An equation to represent grain-size distribution. *Canadian Geotechnical Journal*. 37(4), 817-827.
- Gallipoli, D., Gens, A., Sharma, R., & Vaunat, J. (2003). An elasto-plastic model for unsaturated soil incorporating the effects of suction and degree of saturation on mechanical behaviour. *Géotechnique.*, 53(1), 123-136.
- ISO 690
- Gan, J. K. M., Fredlund, D. G., & Rahardjo, H. (1988). Determination of the shear strength parameters of an unsaturated soil using the direct shear test. *Canadian Geotechnical Journal*, 25(3), 500-510.
- Gan, J. K., & Fredlund, D. G. (1996). Shear strength characteristics of two saprolitic soils. *Canadian Geotechnical Journal*, 33(4), 595-609.
- Gerke, H. H., & Genuchten, M. V. (1993). A dual-porosity model for simulating the preferential movement of water and solutes in structured porous media. *Water Resources Research*, 29(2), 305-319.
- Germann, P. F., & Beven, K. (1985). Kinematic wave approximation to infiltration into soils with sorbing macropores. *Water Resources Research*, 21(7), 990-996.
- Godt, J. W., & Coe, J. A. (2007). Alpine debris flows triggered by a 28 July 1999 thunderstorm in the central Front Range, Colorado. *Geomorphology*, 84(1), 80-97.
- Godt, J. W., Baum, R. L., & Lu, N. (2009). Landsliding in partially saturated materials. *Geophysical Research Letters*, 36(2).

-
- Godt, J. W., Şener-Kaya, B., Lu, N., & Baum, R. L. (2012). Stability of infinite slopes under transient partially saturated seepage conditions. *Water Resources Research*, 48(5).
- Gray, W. G., & Hassanizadeh, S. M. (1991). Unsaturated flow theory including interfacial phenomena. *Water Resources Research*, 27(8), 1855-1863.
- Gray, W. G., & Hassanizadeh, S. M. (1991). Paradoxes and realities in unsaturated flow theory. *Water Resources Research*, 27(8), 1847-1854.
- ISO 690
- Greco, R. (2002). Preferential flow in macroporous swelling soil with internal catchment: model development and applications. *Journal of Hydrology*, 269(3), 150-168.
- Greco, R., A. Guida, E. Damiano, and L. Olivares. (2010). Soil water content and suction monitoring in model slopes for shallow flowslides early warning applications. *Phys. Chem. Earth*. 35(3): 127-136.
- Jarvis, N. J., Bergström, L., & Dik, P. E. (1991). Modelling water and solute transport in macroporous soil. II. Chloride breakthrough under non-steady flow. *Journal of Soil Science*, 42(1), 71-81.
- Javaux, M., J. Vanderborght, R. Kasteel, and M. Vanclooster. (2006). Three-dimensional modeling of the scale-and flow rate-dependency of dispersion in a heterogeneous unsaturated sandy monolith. *Vadose Zone Journal*. 5(2), 515-528.
- Jennings, J. E. B., & Burland, J. B. (1962). Limitations to the use of effective stresses in partly saturated soils. *Géotechnique*, 12(2), 125-144.
- Jennings, J. E. 1960. A revised effective stress law for use in the prediction of the behaviour of unsaturated soils. *Proceedings of the Conference on Pore Pressure and Suction in Soils*. Butterworths, London, 26–30.
- Kartal Toker, N., J.T. Germaine, and P.J. Culligan. (2014). Effective Stress and Shear Strength of Moist Uniform Spheres *Vadose Zone Journal*. May 2014. v. 13, , doi:10.2136/vzj2013.07.0129
- Khalili, N., & Khabbaz, M. H. (1998). A unique relationship of chi for the determination of the shear strength of unsaturated soils. *Geotechnique*, 48(5).
- Khalili, N., Geiser, F., & Blight, G. E. (2004). Effective stress in unsaturated soils: review with new evidence. *International Journal of Geomechanics*, 4(2), 115-126.
- Kim, T. H. (2001). Moisture-induced tensile strength and cohesion in sand. Ph.D. thesis. Univ. of Colo. at Boulder. Boulder.
- Kim, B. S., Shibuya, S., Park, S. W., & Kato, S. (2010). Application of suction stress for estimating unsaturated shear strength of soils using direct shear testing under low confining pressure. *Canadian Geotechnical Journal*, 47(9), 955-970.
- Kosugi, K. (1994). Three-parameter log-normal distribution model for soil water retention. *Water Resour. Res.* 30:891–901.

-
- Kosugi, K., J.W. Hopmans, and J.H. Dane. (2002). Parametric models. 739–757. In J.H. Dane and G.C. Topp (ed.) *Methods of soil analysis. Part 4. Physical methods*. SSSA Book Ser. 5. SSSA, Madison, WI.
- Kutilek, M., & Nielsen, D. R. (1994). *Soil hydrology: textbook for students of soil science, agriculture, forestry, geoecology, hydrology, geomorphology and other related disciplines*. Catena Verlag.
- Kutilek, M., and L. Jendele. (2008). The structural porosity in soil hydraulic functions: A review. *Soil Water Res.* 3:S7–S20.
- Hamamoto, S., M.S.A. Perera, A.C. Resurreccion, K. Kawamoto, S. Hasegawa, T. Komatsu, and P. Moldrup. (2009). The solute diffusion coefficient in variably compacted, unsaturated volcanic ash soils. *Vadose Zone J.*, 8: 942–952, doi: 10.2136/vzj2008.0184.
- Hill, M.C., and C.R. Tiedman. (2007). *Effective Groundwater Model Calibration: With Analysis of Data. Sensitivities, Predictions and Uncertainty*, Wiley.
- Hillel, D. (1980). *Fundamentals of soil physics*. Academic Press, Inc.(London) Ltd..
- Horn, R., & Smucker, A. (2005). Structure formation and its consequences for gas and water transport in unsaturated arable and forest soils. *Soil and Tillage Research*, 82(1), 5-14.
- Horton, R. E. (1933). The role of infiltration in the hydrologic cycle. *Eos, Transactions American Geophysical Union*, 14(1), 446-460.
- Houlsby, G. T. (1997). The work input to an unsaturated granular material. *Géotechnique*, 47(1), 193-196.
- Illman, W. A., & Hughson, D. L. (2005). Stochastic simulations of steady state unsaturated flow in a three-layer, heterogeneous, dual continuum model of fractured rock. *Journal of Hydrology*, 307(1), 17-37.
- Indelman, P., Touber-Yasur, I., Yaron, B., & Dagan, G. (1998). Stochastic analysis of water flow and pesticides transport in a field experiment. *Journal of contaminant hydrology*, 32(1), 77-97.
- Iverson, R. M. (2000). Landslide triggering by rain infiltration. *Water resources research*, 36(7), 1897-1910.
- Laloui, L., & Nuth, M. (2009). On the use of the generalised effective stress in the constitutive modelling of unsaturated soils. *Computers and Geotechnics*, 36(1), 20-23.
- Lambe, T. W., & Whitman, R. V. (1969). *Soil Mechanics*, 553 pp.
- Lanni, C., Borga, M., Rigon, R., & Tarolli, P. (2012). Modelling shallow landslide susceptibility by means of a subsurface flow path connectivity index and estimates of soil depth spatial distribution. *Hydrology and Earth System Sciences*, 16(11), 3959-3971.

-
- Lee, I. M., S. G. Sung, and G. C. Cho. (2005). Effect of stress state on the unsaturated shear strength of a weathered granite. *Can. Geotech. J.* 42(2), 624–631.
- Lehmann, P., & Or, D. (2012). Hydromechanical triggering of landslides: From progressive local failures to mass release. *Water Resources Research*, 48(3).
- Lepore, C., E. Arnone, L.V. Noto, G. Sivandran, R.L. Bras RL. (2013). Physically based modeling of rainfall-triggered landslides: a case study in the Luquillo forest, Puerto Rico. *Hydrol Earth Syst Sci* 17:3371–3387.
- Li, X., J. H. Li, and L.M. Zhang. (2014). Predicting bimodal soil–water characteristic curves and permeability functions using physically based parameters. *Computers and Geotechnics*. 57, 85-96.
- Likos, W.J., A.W. Wayllace, J.G. Godt, and N. Lu. (2010). Modified direct shear apparatus for unsaturated sands at low suction and stress. *ASTM Geotech Test. J.* 33(4), 1–13.
- Loret, B., & Khalili, N. (2002). An effective stress elastic–plastic model for unsaturated porous media. *Mechanics of Materials*, 34(2), 97-116.
- Lu, N., and W. J. Likos. (2004). *Unsaturated Soil Mechanics*. 556 pp. John Wiley. New York.
- Lu, N., and W. J. Likos. (2006). Suction stress characteristic curve for unsaturated soil. *J. Geotech. Geoenviron. Eng.* 132(2): 131–142. doi:10.1061/(ASCE)1090-0241(2006)132:2(131).
- Lu, N., & Godt, J. (2008). Infinite slope stability under steady unsaturated seepage conditions. *Water Resources Research*, 44(11).
- Lu, N., Kim, T. H., Sture, S., & Likos, W. J. (2009). Tensile strength of unsaturated sand. *Journal of engineering mechanics*, 135(12), 1410-1419.
- Lu, N., J.W. Godt, and D.T. Wu (2010). A closed-form equation for effective stress in unsaturated soil. *Water Resour. Res.* 46, W05515.
- Lu, N., & Godt, J. W. (2013). *Hillslope hydrology and stability*. Cambridge University Press.
- Lu, N., & Godt, J. W. (2013). *Hillslope hydrology and stability*. Cambridge University Press.
- Mainka, J., M.A. Murad, C. Moyne, and S.A. Lima, (2014). A modified effective stress principle for unsaturated swelling clays derived from microstructure. *Vadose Zone Journal*, 13(5).
- Matyas, E. L., & Radhakrishna, H. S. (1968). Volume change characteristics of partially saturated soils. *Géotechnique*, 18(4), 432-448.
- Miao, L., Z. Yin, S. Liu. (2001). Empirical function representing the shear strength of unsaturated soils. *Geotech. Testing Journal* 24: 220–223.
- Miao, L., Liu, S., & Lai, Y. (2002). Research of soil–water characteristics and shear strength features of Nanyang expansive soil. *Engineering Geology*, 65(4), 261-267.

-
- Michiels, P., Hartmann, R., & De Strooper, E. (1989). Comparisons of the unsaturated hydraulic conductivity of a coarse-textured soil as determined in the field, in the laboratory, and with mathematical models. *Soil Science*, 147(4), 299-304.
- Miyamoto, T., T. Annaka, and J. Chikusi. (2003). Soil aggregate structure effects on dielectric permittivity of an Andisol measured by time domain reflectometry. *Vadose Zone J.* 2: 90–97. doi: 10.2136/vzj2003.9000.
- Miller, E. E., & Miller, R. D. (1956). Physical theory for capillary flow phenomena. *Journal of Applied Physics*, 27(4), 324-332.
- Mitchell, J. K., & Soga, K. (1976). *Fundamentals of soil behavior* (p. 422). New York: Wiley.
- Montgomery, D. R., & Dietrich, W. E. (1994). Landscape dissection and drainage area-slope thresholds. *Process models and theoretical geomorphology*, 221-246.
- Morgenstern, N. R., & Price, V. E. (1965). The analysis of the stability of general slip surfaces. *Geotechnique*, 15(1), 79-93.
- Mualem, Y. (1976). A new model for predicting the hydraulic conductivity of unsaturated porous media. *Water resources research*, 12(3), 513-522.
- Mualem, Y. (1984). A modified dependent domain theory of hysteresis. *Water Resources Research*, 12:513-522.
- Mualem, Y., & Klute, A. (1986). Hydraulic conductivity of unsaturated soils: prediction and formulas. *Methods of soil analysis. Part 1. Physical and mineralogical methods*, 799-823.
- Ng, C.W.W., and Y.W. Pang. (2000). Influence of stress state on soil water characteristics and slope stability. *J. Geotechn. Geoenviron. Eng.* ASCE. 126(2): 157–166.
- Nimmo, J. (2004). Porosity and pore size distribution. *Encyclopedia of Soils in the Environment*, 3, 295-303.
- Nuth, M., & Laloui, L. (2008). Effective stress concept in unsaturated soils: Clarification and validation of a unified framework. *International journal for numerical and analytical methods in Geomechanics*, 32(7), 771-801.
- Öberg, A., and G. Sällfors. (1997). Determination of shear strength parameters of unsaturated silts and sands based on the water retention curve. *Geotech. Test. J.* 20(1): 41–48.
- Olivares, L., and L. Picarelli. (2003). Shallow flowslides triggered by intense rainfalls on natural slopes covered by loose unsaturated pyroclastic soils. *Geotechnique* 53(2):283–288. doi:10.1680/geot.53.2.283.37268
- Oloo, S. Y., & Fredlund, D. G. (1996). A method for determination of ψ_b for statically compacted soils. *Canadian Geotechnical Journal*, 33(2), 272-280.
- Othmer, H., Diekkrüger, B., & Kutilek, M. (1991). Bimodal Porosity And Unsaturated Hydraulic Conductivity. *Soil Science*, 152(3), 139-150.

-
- Papa, M. N., V. Medina, F. Ciervo and Bateman, A. (2013). Derivation of critical rainfall thresholds for shallow landslides as a tool for debris flow early warning systems. *Hydrol Earth Syst Sci*, 17(10), 4095-4107.
- Peters, R., & Klavetter, E. A. (1988). A continuum model for water movement in an unsaturated fractured rock mass. *Water Resources Research*, 24(3), 416-430.
- Picarelli, L., Urciuoli, G., & Russo, C. (2004). Effect of groundwater regime on the behaviour of clayey slopes. *Canadian Geotechnical Journal*, 41(3), 467-484.
- Priesack, E., & Durner, W. (2006). Closed-form expression for the multi-modal unsaturated conductivity function. *Vadose Zone Journal*, 5(1), 121-124.
- Raats, P. A. C. (1984). Tracing parcels of water and solutes in unsaturated zones (pp. 4-16). Springer Berlin Heidelberg.
- Rahardjo, H., Ong, T. H., Rezaur, R. B., & Leong, E. C. (2007). Factors controlling instability of homogeneous soil slopes under rainfall. *Journal of Geotechnical and Geoenvironmental Engineering*, 133(12), 1532-1543.
- Rassam, D. W., & Williams, D. J. (1997). Shear strength of unsaturated gold tailings. In *Proceedings of the eighth Australia-New Zealand conference on geotechnics* (Vol. 1, pp. 329-335).
- Rassam, D.W., and F Cook. (2002). Predicting the shear strength envelope of unsaturated soils. *Geotechn. Test J.* 25(2):215–220.
- Richards, L. A. (1931). Capillary conduction of liquids through porous mediums. *Journal of Applied Physics*, 1(5), 318-333.
- Romano, N., P. Nasta, G. Severino, and J.W. Hopmans. (2011). Using bimodal lognormal function to describe soil Hydraulic properties. *Soil Sci. Soc. Am. J.* 75(2): 468-480.
- Romero, E., & Vaunat, J. (2000). Retention curves of deformable clays. Experimental evidence and theoretical approaches in unsaturated soils. 91-106.
- Romero, E., G. Della Vecchia, C. Jommi. (2011). An insight into the water retention properties of compacted clayey soils. *Geotechnique*. 61(4):313–328.
- Ross, P.J., and R.J. Smettem. (1993). Describing soil hydraulic properties with sums of simple functions. *Soil Sci. Soc. Am. J.* 57:26–29.
- Russo, D. (1984). A geostatistical approach to solute transport in heterogeneous fields and its applications to salinity management. *Water Resources Research*, 20(9), 1260-1270.
- Santini, A., Romano, N., Ciollaro, G., & Comegna, V. (1995). Evaluation Of A Laboratory Inverse Method For Determining Unsaturated Hydraulic Properties Of A Soil Under Different Tillage Practices. *Soil science*, 160(5), 340-351.

-
- Saxton, K. E., Rawls, W., Romberger, J. S., & Papendick, R. I. (1986). Estimating generalized soil-water characteristics from texture. *Soil Science Society of America Journal*, 50(4), 1031-1036.
- Schubert, H. (1984). Capillary forces - modeling and application in particulate technology. *Powder Technol.* 37: 105–116. doi:10.1016/0032-5910(84)80010-8.
- Sheng, D., Fredlund, D. G., & Gens, A. (2008). A new modelling approach for unsaturated soils using independent stress variables. *Canadian Geotechnical Journal*, 45(4), 511-534.
- Sheng, D. C., A. N. Zhou, and D. G. Fredlund. (2011). Shear strength criteria for unsaturated soils. *Geotech. Geologic. Eng.* 29(2): 145–159.
- Sidiropoulos, E., & Yannopoulos, S. (1988). Sensitivity analysis of closed-form analytical hydraulic conductivity models. *Journal of hydrology*, 101(1), 159-172.
- Simoni, S., Zanotti, F., Bertoldi, G., & Rigon, R. (2008). Modelling the probability of occurrence of shallow landslides and channelized debris flows using GEOtop-FS. *Hydrological Processes*, 22(4), 532-545.
- Šimůnek, J., van Genuchten, M. T., & Wendroth, O. (1998). Parameter estimation analysis of the evaporation method for determining soil hydraulic properties. *Soil Science Society of America Journal*, 62(4), 894-905.
- Šimůnek, J., Jarvis, N. J., Van Genuchten, M. T., & Gärdenäs, A. (2003). Review and comparison of models for describing non-equilibrium and preferential flow and transport in the vadose zone. *Journal of Hydrology*, 272(1), 14-35.
- Smettem, K. R. J., Chittleborough, D. J., Richards, B. G., & Leaney, F. W. (1991). The influence of macropores on runoff generation from a hillslope soil with a contrasting textural class. *Journal of Hydrology*, 122(1), 235-251.
- Šimůnek, J., M. Šejna, and M. Th. van Genuchten, The HYDRUS-1D software package for simulating the one-dimensional movement of water, heat, and multiple solutes in variably- saturated media, Version 2.0. IGWMC - TPS - 70, International Ground Water Modeling Center, Colorado School of Mines, Golden, Colorado, 162pp., 1998.
- Smith, R. E., & Diekkrüger, B. (1996). Effective soil water characteristics and ensemble soil water profiles in heterogeneous soils. *Water Resources Research*, 32(7), 1993-2002.
- Song, Y. S. (2014). Suction stress in unsaturated sand at different relative densities. *Engineering Geology* 176 1-10.
- Sorbino, G., and V. Foresta. (2002). Unsaturated hydraulic characteristics of pyroclastic soils. *Proc. 3rd Int. Conf. on Unsaturated Soils*. Vol. 1, Swets and Zeitlinger. Lisse. pp. 405–410.

-
- Sorbino, G., and M.V. Nicotera. (2012). Unsaturated soil mechanics in rainfall-induced flowlandslides, *Engineering Geology*.
<http://dx.doi.org/10.1016/j.enggeo.2012.10.008>
- Spencer, D. W. (1963). The interpretation of grain size distribution curves of clastic sediments. *Journal of Sedimentary Research*, 33(1).
- Springman, S.M., C. Jommi, P. Teyssere. (2003). Instabilities on moraine slopes induced by loss of suction: a case history. *Géotechnique*. 53(1): 3–10.
- Tegnander, C. (2001). Models for ground water flow: A numerical comparison between Richards' model and the fractional flow model. *Transport in Porous Media*, 43(2), 213-224.
- Terzaghi, K. (1943). *Theoretical soil mechanics* (Vol. 18). New York: Wiley.
- Tindall, J. A., Kunkel, J. R., & Anderson, D. E. (1999). Unsaturated zone hydrology for scientists and engineers (p. 624). Upper Saddle River, NJ: Prentice Hall.
- Toker, N. K., Germaine, J. T., & Culligan, P. J. (2014). Effective stress and shear strength of moist uniform spheres. *Vadose Zone Journal*, 13(5).
- Toll, D. G., & Ong, B. H. (2003). Critical-state parameters for an unsaturated residual sandy clay. *Géotechnique*., 53(1), 93-103.
- Touma, J., & Vaucelin, M. (1986). Experimental and numerical analysis of two-phase infiltration in a partially saturated soil. *Transport in Porous Media*, 1(1), 27-55.
- Tuller, M., & Or, D. (2002). Unsaturated hydraulic conductivity of structured porous media. *Vadose Zone Journal*, 1(1), 14-37.
- Van Genuchten, M.T. (1980). A closed form equation for predicting the hydraulic conductivity of unsaturated soils. *Soil Science Society of America Journal*. 44(5): 892–898. doi:10.2136/sssaj1980.03615995004400050002x.
- Van Genuchten, M. T., & Nielsen, D. R. (1985). On describing and predicting the hydraulic properties of unsaturated soils. *Ann. Geophys*, 3(5), 615-628.
- Vanapalli, S. K., D. G. Fredlund, D. E. Pufahl, and A. W. Clifton. (1996). Model for the prediction of shear strength with respect to soil suction. *Can. Geotech. J.* 33(3), 379–392.
- Vanapalli, S.K., D.G. Fredlund, and D.E. Pufahl. (1999). The influence of soil structure and stress history on the soil-water characteristic of a compacted till. *Géotechnique*. 49(2): 143–159.
- Vaunat, J., E. Romero, C. Marchi, C. Jommi. (2002). Modeling the shear strength of unsaturated soils. 3rd Intern. Conf. on Unsaturated Soils, 2: 245–251. Balkema.
- Villarraga, C., D. Ruiz, J. Vaunat, and F. Casini. (2014). Modelling landslides induced by rainfall: a coupled approach. *Procedia Earth and Planetary Science*. 9, 222-228.

-
- Vachaud, G., Vauclin, M., Khanji, D., & Wakil, M. (1973). Effects of air pressure on water flow in an unsaturated stratified vertical column of sand. *Water Resources Research*, 9(1), 160-173.
- Vereecken, H., Maes, J., Feyen, J., & Darius, P. (1989). Estimating the soil moisture retention characteristic from texture, bulk density, and carbon content. *Soil science*, 148(6), 389-403.
- Vogel, T., & Cislérova, M. (1988). On the reliability of unsaturated hydraulic conductivity calculated from the moisture retention curve. *Transport in porous media*, 3(1), 1-15.
- Vogel, T., K. Huang, R. Zhang, and M. Th. van Genuchten, The HYDRUS code for simulating one-dimensional water flow, solute transport, and heat movement in variably-saturated media, Version 5.0, Research Report No 140, U.S. Salinity Laboratory, USDA, ARS, Riverside, CA, 1996.
- Vogel, T., M.Th. van Genuchten, and M. Cislérova. (2001). Effect of the shape of the soil hydraulic functions near saturation on variably-saturated flow predictions. *Adv. Water Resour.* 24:133–144.
- Wheeler, S. J., & Sivakumar, V. (1995). An elasto-plastic critical state framework for unsaturated soil. *Géotechnique*, 45(1), 35-53.
- Wheeler, S. J., Näätänen, A., Karstunen, M., & Lojander, M. (2003). An anisotropic elastoplastic model for soft clays. *Canadian Geotechnical Journal*, 40(2), 403-418.
- Whitaker, S. (1986). Flow in porous media II: The governing equations for immiscible, two-phase flow. *Transport in Porous Media*, 1(2), 105-125.
- Wilson, G. V., Jardine, P. M., & Gwo, J. P. (1992). Modeling the hydraulic properties of a multiregion soil. *Soil Science Society of America Journal*, 56(6), 1731-1737.
- Wolle, C. M., & Hachich, W. (1989). Rain-induced landslides in southeastern Brazil. In *The 12 th International Conference on Soil Mechanics and Foundation Engineering*, Rio de Janeiro, Br, 08/13-18/89 (pp. 1639-1642).
- Xu, Y. F. (2004). Fractal approach to unsaturated shear strength. *Journal of Geotechnical and Geoenvironmental engineering*, 130(3), 264-273.
- Xu, C., and C. Torres-Verdin. (2013). Pore System Characterization and Petrophysical Rock Classification Using a Bimodal Gaussian Density Function. *Math. Geosci.* 45(6): 753-771. doi: 0.1007/s11004-013-9473-2.
- Zhang, L. M., and X. Li. (2010). Microporosity structure of coarse granular soils. *J. Geotech. Geoenviron. Eng.*, 136 (10), 1425e1436.
- Zhao, H.F., L.M. Zhang, and D.S. Chang. (2013). Behavior of coarse widely graded soil under low confining pressures. *J. Geotech. Geoenviron. Eng.* 139(1): 35-48. doi: 10.1061/(ASCE)GT.1943-5606.0000755.